The functional neuroanatomy of episodic retrieval: using neuroimaging to understand the computational processes underlying human memory

By

James E Kragel

Dissertation

Submitted to the Faculty of the

Graduate School of Vanderbilt University

in partial fulfillment of the requirements

for the degree of

DOCTOR OF PHILOSOPHY

in

Neuroscience

August, 2015

Nashville, Tennessee

Approved:

Sean M. Polyn, Ph.D.

Frank Tong, Ph.D.

Thomas J. Palmeri, Ph.D.

René Marois, Ph.D.

For Tara

ACKNOWLEDGMENTS

The work contained within this dissertation would not have been possible without the support of countless individuals. I want to thank my advisor, Dr. Sean M. Polyn, who has guided me throughout the entirety of my graduate career. Dr. Polyn has supported my graduate education and research through grants awarded to him through the National Science Foundation (1157432) as well as a Vanderbilt University Discovery Grant. I would like to thank the other members of my dissertation committee, Drs. Frank Tong, Thomas J. Palmeri, and René Marois for constructive feedback and guidance on my research path. You have all steered me towards an effective and productive approach to memory research.

I would not have developed expertise in the domain of cognitive modeling without influence from the computational modeling environment at Vanderbilt University. Additional thanks to members of the Vanderbilt Computational Memory lab, who contributed useful discussions and feedback on many of the projects contained within. I would especially like to thank Joshua McCluey and Neal Morton for assistance in data collection as well as providing valuable discussions and feedback. I would like to thank Zachary Cohen and Cage Spoden for supporting me in data collection and annotation.

I would like to thank past and present members of the Vanderbilt University Institute for Imaging Science who facilitated the collection of neuroimaging data. I would like to thank Brain Welch and Chris Cannistraci for assistance with scanning equipment and setting up fMRI studies at the 3T. I would also like to thank the MRI technologists who assisted with data collection, including Donna Butler, David Pennel, and Kristen George-Durrett.

Finally, I am grateful to acknowledge the support of my family. Thanks to my parents, Drs. Amy and Peter Kragel for their endless support in all aspects of my life. I would additionally like to thank my brother, Phil, for countless discussions about the nature of the mind and brain. Most importantly, I would like to thank my fiancée, Tara Hartmann, for her love and understanding.

TABLE OF CONTENTS

LIST OF TABLES

LIST OF FIGURES

CHAPTER I

Introduction

The human memory system has the capacity to not only recognize a familiar item in the environment, but also makes possible the ability to re-experience events that occurred in the past (Tulving, 1983). To study this form of episodic memory, aspects of which are unique to the human species (Tulving, 2005), experimentalists have used the free-recall task, in which a list of items is studied and then recalled in any order. This task has led to the discovery of both neurobiological signatures (Polyn et al., 2005; Gelbard-Sagiv et al., 2008) and computational mechanisms (Raaijmakers and Shiffrin, 1981; Howard and Kahana, 2002a) that enable the individuals to search through prior experience and retrieve information in a goal-directed fashion. Neural theories of memory search (Polyn and Kahana, 2008) propose interactions between the medial temporal lobe (MTL) and prefrontal cortex (PFC) are critical to supporting the computational mechanisms described by an influential model of the free-recall task. In this work, I examine interactions between the MTL and distributed cortical systems during memory search. To directly relate the engagement of neural structures to specific cognitive mechanisms, I develop a neuro-cognitive model of free recall, describing the neural underpinnings of episodic retrieval.*

Retrieved-context models of human memory

Computational models of human memory have been developed in order to better understand the cognitive mechanisms that give rise to structure and organization of episodic memory. A family of retrieved-context models have been developed from theories initially formalized by Estes (1959) and Bower (1972), which accommodate observed recall behavior through a mechanism in which associations are forged between items and a slowly drifting contextual representation. While this conception of internal context has influenced many foundational models of episodic memory (e.g.,

---

*Portions of this chapter were published as Using context to search memory: functional roles of the medial temporal lobe and prefrontal cortex. Kragel JE. *Vanderbilt Reviews Neuroscience* 2013 the search of associative memory, Raaijmakers and Shiffrin, 1981), I will focus on models which directly examine the influence of slowly drifting internal context on the organization of memory and recall behavior.

The temporal context model (TCM, Howard and Kahana, 2002a) first tested the ability of a slowly drifting temporal context to account for observed behavioral phenomena in the domain of free recall. This model describes memory search through the interaction of two neural network layers. Activation within a feature-based item layer, **f**, represents individual items in memory. Memory processes are mediated through interactions between the representations of individual items and activation within the context layer, **c**. When an item is studied, two processes occur. First, item information within the feature layer is integrated into the contextual representation, reflecting the influence of the studied item on the current internal state. Next, encoding takes place in the form of a Hebbian learning process: the associative weights connecting the item and context layers are updated based on their activation. These associative connections enable two critical operations to occur during retrieval. In order for an item to be recalled, a state of context can serve as input to the item layer. This drives activation of item features, enabling an individual item to be retrieved from memory. The next retrieval process is namesake of this family of models: context retrieval. It is assumed that when an item is recalled from memory, the state of context in which it was previously encoded is also retrieved. This general structure enables retrieved-context models to account for the temporal organization of memory search across different variants of the free-recall task.

While not a complete model of the free-recall task per se, TCM was capable of accounting for two major behavioral effects: recency and contiguity. Recency, the advantage in recall for items studied near the end of a list, is observed as a result due to the similarity of contextual states at the end of the study period and the beginning of memory search. As this contextual state serves as a cue for the memory system, items studied near the end of the list are likely to be retrieved at the beginning of list learning (Howard and Kahana, 2002a). Temporal contiguity refers to the tendency for items studied nearby in time to be successively recalled (Kahana et al., 2008). Contextual retrieval is the fundamental mechanism that enables TCM to account for the contiguity effect. When an item is retrieved, the contextual retrieval process reactivates patterns of activity within the context layer that are associated to a specific point in time during the study episode. As this contextual information is input to the associative machinery that drives the retrieval of individual items, items from nearby points in time are likely to be retrieved.

A number of generalized version of TCM have been constructed in order to provide a more complete description of behavior in the free-recall task. Sederberg et al. (2008) developed TCM-A, a model of free recall that incorporates decision processes described by a set of leaky accumulators (Usher and McClelland, 2001). According to this model, when the context-based representation cues individual list items during memory search, evidence accumulates at a rate determined by the associations between items and states of context. Lateral inhibition between items provides competition between individual items during recall. These processes enable TCM to predict response latencies during recall, as well as determining when recall terminates. This model additionally demonstrated that context-based models can account for a number of behavioral effects that arise when the memory system is perturbed (e.g., by the presentation of distracting information) during, or following the encoding of study items. Distractors are represented by activation of item features that when integrated, cause context to drift at a rate indicative of the amount of distraction. These mechanisms allowed this variant of TCM to account for decreased recency following end-of-list distraction (Glanzer and Cunitz, 1966), as well as preserved recency when distraction is pervasive throughout the study list (Bjork and Whitten, 1974). While these additions enabled retrieved-context models to account for the effects of distraction, the Context Maintenance and Retrieval (CMR) model (Polyn et al., 2009a) incorporated a number of additional computational mechanisms in order to further account for the organization of human memory. By incorporating non-temporal information into representation of internal context, this model could account for clustering of retrieved information according to its source. In addition, by allowing items to support the retrieval of semantically similar items through pre-experimental context-to-item associations, semantic clustering (i.e., consecutive recall of semantically related words) in recall sequences (Bousfield, 1953; Howard and Kahana, 2002b) can be predicted.

Retrieved-context models can serve as a tool to interpret the neural substrates of episodic memory retrieval. These computational models propose a set of cognitive operations that are sufficient to account for the organization of human memory, with the implicit assumption that engagement of such processes are reflected in the complex dynamics of the human brain. Neuroimaging studies investigating the neural basis of memory search (Andreasen et al., 1995; Gelbard-Sagiv et al., 2008; Long et al., 2010; Shapira-Lichter et al., 2012) provide a description of the neural systems that are essential to free recall. A major challenge to understanding the neural basis of memory search is relating the dynamics of brain systems to specific cognitive operations. By incorporating patterns of neural activity that are recorded as individuals encode and retrieve memories, links can be drawn between observed cortical dynamics and specific cognitive processes. If retrieved-context theory provides an accurate description of the human memory system, recruitment of specific brain regions should prove informative to the computational model, enabling better prediction of recall behavior. In the following section, I provide a brief overview of specialized cortical systems that mediate episodic memory retrieval, and may embody the cognitive mechanisms described by retrieved-context models of human memory.

Functional neuroanatomy of episodic retrieval

Studies of cognitive neuroscience have consistently implicated both the prefrontal cortex (PFC) and the medial temporal lobe (MTL) as being crucial for memory (Simons and Spiers, 2003). I begin by reviewing their relative contributions to episodic retrieval, with a specific focus on the functional properites that enable these regions to mediate self-guided memory search. Then, I provide an overview of large-scale cortical networks anchored within the MTL and PFC, and describe neural mechanisms supported by these networks that may facilitate retrieval during the free-recall task.

Medial temporal lobe

The human MTL lobe contains of the hippocampus, as well as the parahippocampal gyrus, which comprises the entorhinal, perirhinal and parahippocampal cortices. The hippocampus receives the majority of its inputs from the entorhinal cortex, allowing it to rapidly bind inputs from multiple sensory regions in the formation of episodic memories (McClelland et al., 1995; Eichenbaum, 2004). Functional neuroimaging studies have identified distinct contributions of subregions of the parahippocampal gryus to episodic memory, with context-based representations specific to the parahippocampal cortex and item-based processing in the perirhinal cortex (Diana et al., 2007). In addition to forming associations between items and the contexts in which they occur, the hippocampus has been shown to play a specific role in the recollection of episodic details (Eldridge et al., 2000). Computational models of the MTL system describe a pattern completion process by which the hippocampus can reinstate the details of past experience (Norman and O'Reilly, 2003). Given a partial input, recurrent connections between ensembles of hippocampal neurons complete patterns of activity based on prior activation. Polyn and Kahana (2008) describe a similar role for the hippocampus during recall, using a context-based representations serve as input to the hippocampal system, driving reactivation of item information through hippocampal associations.

The MTL may also contain cortical structures that represent an integrated context representation and provide temporal structure to episodic memory (Howard et al., 2005). Given the persistent activity observed within the entorhinal cortex (Egorov et al., 2002), its afferent sensory inputs, and extensive reciprocal connections to the hippocampus, activity in this parahippocampal region is well suited to mediate a contextual representation (Suzuki, 1996; Burwell et al., 2004). Studies examining working memory in humans have identified a dissociation between the maintenance of novel information, supported through MTL function, and the maintenance of familiar information, supported in part by increased prefrontal activation (Stern et al., 2001). Similar work has identified that successful encoding of novel visual information is supported by the parahippocampal gyrus (Schon et al., 2004), which can be reduced through the disruption of persistent firing through application of the muscarinic cholinergic antagonist, scopolamine (Schoffelen et al., 2005). These studies implicate the parahippocampal region in supporting the maintenance of an integrated representation of the recent past. If these parahippocampal regions serve as input to the hippocampus during recall, they may drive the of associative retrieval of item-based representations in cortex.

The most compelling evidence for a temporal context representation supported through activity within the MTL comes from recent electrophysiological studies of the human MTL. Work by Manning et al. (2011) found direct support for contextual reinstatement, evidenced by the reactivation of oscillatory patterns of brain activity recorded in local field potentials during free recall. In their analysis, they identified a slowly changing, autocorrelated signal while patients studied specific items- a potential contextual representation. Consistent with the process of context reinstatement, patterns of activity recorded from temporal lobe electrodes, including the hippocampus, returned to prior states just prior to the recall of individual items. Recordings from within the MTL have also revealed autocorrelated patterns of neuronal firing, which return to prior states during performance of a continuous recognition task (Howard et al., 2012). These studies build on a growing body of evidence from rodent (Fortin et al., 2002; Manns et al., 2007), nonhuman primates (Naya and Suzuki, 2011), and humans (Jenkins and Ranganath, 2010; Tubridy and Davachi, 2011) for the maintenance of temporal context within the MTL.

Prefrontal cortex

Theories of PFC function describe multiple cognitive operations that are supported by specific prefrontal subregions during episodic retrieval. Evidence from functional neuroimaging suggests subdivisions within VLPFC support distinct control processes (Badre and Wagner, 2004). The anterior VLPFC supports controlled retrieval processes (Wagner et al., 2001; Badre and Wagner, 2005, 2007); co-activation of this region with the hippocampus is commonly observed during episodic retrieval (Simons and Spiers, 2003). In contrast to the anterior VLPFC, activation of the mid-VLPFC has been associated with selection of task-relevant information in memory (Badre and Wagner, 2005), especially under circumstances in which irrelevant information interferes with current mnemonic representations (Kuhl et al., 2012). These cognitive mechanisms describe how the PFC can interact with the MTL system to facilitate the retrieval of task-relevant information.

The dorsolateral PFC (DLPFC) has been proposed to act as central locus for context (Braver et al., 2001), reflecting the integrated representation that maintains information relevant to upcoming task demands. Neuropsychological evidence for context-like representations in the PFC has been observed in deficits of source memory (Baldo et al., 2002; Duarte et al., 2005), and recency judgments (Milner et al., 1991; Shimamura et al., 1990) in patients with frontal lesion pathology. Recent neuroimaging work investigating the role of DLPFC provides a potential mechanistic role in organizing currently active representations held in working memory (Blumenfeld and Ranganath, 2006). Increased activity within DLPFC has also been linked to relational memory (Blumenfeld and Ranganath, 2007; Murray and Ranganath, 2007), and semantic clustering (Long et al., 2010). These findings support a role for the DLPFC in the encoding of associations between information across time. In addition to supporting relational encoding of items, neuroimaging studies of lateral prefrontal cortex function associate it with temporal context encoding. Lesions to PFC often cause deficits in recency discrimination (Milner et al., 1991; McAndrews and Milner, 1991; Duarte et al., 2009). Functional neuroimaging work by Jenkins and Ranganath (2010); Tubridy and Davachi (2011) further demonstrate and MTL contributions to the encoding of temporal-order memory. It has been proposed that lateral PFC may serve as the seat of context, as described by retrieved-context models of human memory (Polyn and Kahana, 2008). In this framework, the maintenance and manipulation of context-based representation in the PFC dictates the accessibility of information in memory, which is accessed through interactions with the MTL.

Large-scale brain networks

While distinct regions within the PFC and MTL act as cortical modules that mediate specific cognitive operations during retrieval, recent evidence suggests cognitive processing is not solely reflected in the recruitment of individual brain areas, but also through the interactions between distributed cortical nodes that support large-scale networks (Bressler and Menon, 2010). A large-scale brain network is a collection of interconnected brain structures that interact to mediate specific cognitive operations (Bullmore and Sporns, 2009). These networks are composed brain regions that regularly show common activation or deactivation in response to a specific cognitive state. Under this conceptual framework of brain function, the cognitive operations that are critical to memory search are not mediated by the activation of individual cortical modules alone, but rather through interactions between episodic machinery within the MTL and disparate cortical networks. Two core large-scale neural networks are likely to support cognitive operations that are critical to memory search: the external attention system (EAS) and the default mode network (DMN).

Perhaps the most commonly characterized large-scale brain network is the DMN, which has been related to internally-directed cognitive operations (Buckner et al., 2008). This network was initially characterized due to its high metabolic demands (Raichle et al., 2001), and deactivation in the presence of externally focused cognitive tasks (Fox et al., 2006). Multiple functional and anatomical methods have been used to identify the structure of the DMN, including examining intrinsic connectivity of fMRI signal, and functional studies of task-based deactivation (Shulman et al., 1997; Greicius et al., 2003). The DMN spans many regions of association cortex, including ventral medial prefrontal cortex, dorsal medial prefrontal cortex, posterior cingulate and retrosplenial cortices, the inferior parietal lobe, lateral temporal cortex, and the hippocampal formation, including entorhinal and parahippocampal cortices Buckner et al. (2008).

Inspection of the functional properties of the regions within the DMN has identified multiple subsystems within the greater network (Andrews-Hanna et al., 2010b). A midline core, which exhibits instrinsic connectivity with the full extent of the DMN, is recruited when individuals make self-relevant decisions. In contrast, episodic simulations tasks, that require the construction of mental images or scenarios from memory, are heavily dependent on the MTL (Andrews-Hanna et al., 2010b; Schacter et al., 2007; Addis et al., 2007). Studies of the DMN support a framework wherein interactions between these subsystems may enable self-relevant processing supported by the medial prefrontal subsystem to facilitate the use of memory-guided mental simulations. Recruitment of subregions of the DMN have been observed across multiple studies of autobiographical memory (Svoboda et al., 2006), suggesting that interactions within the DMN are essential to effective memory search and retrieval.

Models of DMN function suggest deactivation of this network is essential to maintaining cognitive control (Anticevic et al., 2012), as activation of this network leads to decrements in behavioral performance, potentially due to interference from mind wandering (Andrews-Hanna et al., 2010b) and other self-referential processing (Buckner et al., 2008) associated with activation of this network. In contrast to the theory that the DMN acts in opposition to goal-directed cognition, recent investigations of episodic memory suggest that activation within this network is not inherently disruptive to cognitively demanding tasks. Recruitment of the DMN, in addition to regions of the posterior MTL complex, including parahippocampal cortex and nearby retrosplenial cortex, is associated with successful memory for the contextual details encompassing an event (Diana et al., 2007; Davachi, 2006; Spaniol et al., 2009; Vilberg and Rugg, 2008). Studies specifically link the recruitment of specific nodes within this network, namely parahippocampal and retrosplenial cortices, to the recollection of contextual details that compose episodic memories (Yonelinas et al., 2005; Johnson et al., 2009; Daselaar et al., 2006). It has been proposed that these cortical regions belong to another core large-scale cortical network: the posterior medial (PM) network (Ranganath and Ritchey, 2012). Based on anatomical (Kondo et al., 2005) and functional (Kahn et al., 2008) connectivity, this network has been shown to span parahippocampal cortex, retrosplenial cortex, the mamillary bodies, the subiculum, and extends to regions within the DMN. Characterizing the cognitive mechanisms mediated through interactions between the PM network and the rest of the DMN remain critical to understanding the role these networks play in human memory.

The EAS is a functional network responsible for high-level cognitive functions, particularly cognitive control operations and working memory functions. This network can be decomposed into multiple subnetworks, as individual cortical regions within this network show selective responses to specific cognitive challenges. The broader system commonly dissociates into two lateralized frontoparietal control networks (FPCN) (Smith et al., 2009), which are commonly recruited based on specific cognitive demands (e.g., language based processing commonly activates the left-lateralized network). These networks, which include regions of lateral prefrontal cortex and parietal cortex near the intraparietal sulcus, have also been implicated in many facets of cognitive control, including dynamic adaptation to task demands (Dosenbach et al., 2006), with dynamic connectivity with disparate cortical systems enabling the brain to respond to specific task demands (Cole et al., 2013). Another subnetwork of the EAS is the salience network (Seeley et al., 2007), which partially overlaps with the ventral attention network (VAN, Fox et al., 2006; Yeo et al., 2011), that is anchored within anterior insular regions and dorsal anterior cingulate cortex. Network analysis suggests that this network plays a causal role in the direction of attention to internal and external information, by shifting relative activation of the DMN and FPC networks (Sridharan et al., 2008). Interactions between the control-related subnetworks of the EAS and MTL systems are likely to play a key role in the control of self-guided memory search.

Overview

In this dissertation, I present a series of studies that examine the neuroanatomical and computational processes that enable the human memory system to target and retrieve information from memory in the absence of an external memory cue. The studies fall along two individual lines of work. In the first two chapters of this dissertation, I use fMRI to investigate the neuroanatomical correlates of free recall (Chapter II), and determine whether the neural substrates that support the recollection of episodic details and processing of item familiarity are instantiated during free recall (Chapter III). In the next two studies (Chapters IV and V) I develop neuro-cognitive models of human memory, that test specific predictions regarding the capacity of neural mechanisms to reflect computational operations as formalized by retrieved-context models of human memory.

The first study, described in Chapter II, examines the functional properties of large-scale cortical networks when items are spontaneously retrieved from memory. The recollection of prior experience has been associated with the activation of a cortico-hippocampal network that is spatially consistent with the DMN (Vincent et al., 2006; Hayama et al., 2012). If the same recollective processes are responsible for supporting the recall of list items on the free-recall task, the activation of this network should be requisite for recall performance. Theories of cortical organization propose that the DMN acts in direct opposition to the EAS (Fox et al., 2005), with the two systems supporting internally and externally directed cognition, respectively. Given the internal focus of attention during free recall, cortical dynamics between these two networks should antagonistic during memory search. This prediction was tested by performing independent component analysis (ICA) to estimate the activation of large-scale cortical networks during the free-recall task. As predicted, we observed recruitment of a sub-network of the PM network, a sub-network of the DMN, during memory search. While measures of intrinsic correlations between the DMN and EAS reflected antagonism between these two systems, we unexpectedly observed transient cooperative dynamics between a dorsal attention network (DAN) and the PM network. In characterizing these network interactions during recall, we identified potential neural mechanisms that may reflect the reinstatement of contextual information during recall, as well as top-down processes that interact with retrieved contextual information to guide memory search.

In Chapter III, I test the prediction that activation of the MTL and frontoparietal networks observed during free recall reflects the cognitive operations of episodic recollection (remembering specific contextual details linked to a memory) and top-down processing related to the familiarity of a presented memory probe (i.e., a stimulus that has either been recently presented or is a novel lure). Functional neuroimaging studies of episodic memory have identified a critical role of the hippocampus (Diana et al., 2007), as well as cortico-hippocampal networks (Hayama et al., 2012) in recollection. Signals within prefrontal and dorsal parietal cortex have reflect the perceived familiarity of a presented stimulus (Wagner et al., 2005; Hutchinson et al., 2012; Sestieri et al., 2014a), without indicating the presence of contextual details during retrieval. Retrieved-context models emphasize the process role of contextual retrieval in guiding memory search (Howard and Kahana, 2002a; Polyn et al., 2009a), suggesting the process of episodic recollection would be critical to the free-recall task. Several models of recall additionally propose a judgment of familiarity as a component of the free-recall task (Raaijmakers and Shiffrin, 1980; Lohnas et al., in press). Based on this modeling work, I predicted the neural substrates that mediate recollection and familiarity during recognition-based tests of memory would be commonly engaged during the free-recall task. By comparing patterns of neural activity while subjects perform free-recall and source recognition tasks, I tested this hypothesis. Using univariate techniques, we observed common activation in the MTL during the retrieval of episodic details as well as free recall. Prefrontal and posterior parietal cortex were also linked to both item familiarity and free recall. Using multivariate techniques, we observed that patterns of activity during free-recall reflected the detection of familiar item information, but not the retrieval of contextual, source details. These findings suggest that while similar cognitive operations are engaged during recognition and recall tasks, free recall may not be dependent upon the same neural mechanism that drive the episodic recollection of prior experience.

While the first two chapters characterize the neural correlates of free recall, they do not relate the functional properties of the brain to computational processes that have been proposed to give rise to observed human behavior. In Chapter IV, I test hypotheses that activation of specific subregions within the MTL reflects specific computational processes described by retrieved-context theories of human memory. I developed a neuro-cognitive model of free recall based on the CMR model (Polyn et al., 2009a), that allowed activity recorded from the MTL to influence the strength of cognitive processes within the model. Two model variants tested whether activation of structures within the MTL reflected the process of temporal reinstatement, which accounts for the temporal organization of memory search, or retrieval success, which indicates successful retrieval of item information. Based on electrophysiological evidence in rodents (Manns et al., 2007) and humans (Manning et al., 2011; Howard et al., 2012), I predicted activation of the hippocampus during recall would be indicative of temporal reinstatement. We demonstrated that computational models incorporating neural signal from the hippocampus and posterior MTL could predict the temporal organization of recall sequences better than a neurally naive baseline model. These findings provide direct evidence for proposals that the MTL plays a direct role in reinstating temporal information thats guides memory search (Polyn and Kahana, 2008).

In the final study of this dissertation, detailed in Chapter V, I used the neuro-cognitive model of free recall developed in Chapter IV in order to better understand the neural processes that determine how memory search is initiated. In order to study the control processes that may be reflected in the engagement of large-scale networks, I developed a variant of the free-recall task designed to pit the cognitive operations of active maintenance and memory retrieval against one another, by challenging the memory system with a distracting math task. We observed functional reorganization of large-scale network activity (estimated using ICA), indicated by increased functional connectivity between the DMN and two additional networks: the VAN and a left-lateralized FPCN. I developed two variants of neurally informed models. In one family of models, large-scale network activity during the delay influenced the degree to which recently learned information in memory was disrupted. In the absence of disruption, the model predicts the maintenance of contextual information occurs, allowing recently learned information to persist in the face of distraction. Activation of the DAN signaled context disruption, predicting decreased accessibility of recently learned information. The other model variant used large-scale network activity estimated during the delay to influence the amount of contextual reinstatement that occurred prior to recall initiation. When FPCN activity during the math-filled delay influenced the engagement of this process in the computational model, we observed better predictions of when individuals would initiate recall by retrieving an item from the beginning of the list. These findings demonstate neural and computational mechanisms by which frontoaparietal networks interact with the MTL to shape the contents of memory.

Together, these studies explore the neural mechanisms that are responsible for the reinstatement of contextual information during the free-recall task. Using combined neuroimaging and computational modeling approaches, this work provides insights into the functional organization and computational mechanisms of the human memory system.

CHAPTER II

Functional interactions between large-scale networks during memory search[1]

Abstract

Neuroimaging studies have identified two major large-scale brain networks, the default mode network (DMN) and the dorsal attention network (DAN), which are engaged for internally and externally directed cognitive tasks respectively, and which show anticorrelated activity during cognitively demanding tests and at rest. We identified these brain networks using independent component analysis (ICA) of functional magnetic resonance imaging data, and examined their interactions during the free-recall task, a self-initiated memory search task in which retrieval is performed in the absence of external cues. Despite the internally directed nature of the task, the DAN showed transient engagement in the seconds leading up to successful retrieval. ICA revealed a fractionation of the DMN into 3 components. A posteromedial network increased engagement during memory search, while the two others showed suppressed activity during memory search. Cooperative interactions between this posteromedial network, a right-lateralized frontoparietal control network, and a medial prefrontal network were maintained during memory search. The DAN demonstrated heterogeneous task-dependent shifts in functional coupling with various subnetworks within the DMN. This functional reorganization suggests a broader role of the DAN in the absence of externally directed cognition, and highlights the contribution of the posteromedial network to episodic retrieval.

Introduction

In studies of the human memory system, when a specific external cue successfully prompts memory retrieval, functional magnetic resonance imaging (fMRI) techniques reliably identify a core network of brain regions spanning the hippocampal formation, posterior cingulate cortex, posterior parietal

---

[1] James E. Kragel and Sean M. Polyn. Functional Interactions Between Large-Scale Networks During Memory Search. *Cerebral Cortex*, 25(3):667–679, March 2015.

cortex, and medial prefrontal cortex (Shannon and Buckner, 2004; Vincent et al., 2006; Spaniol et al., 2009). These regions belong to a brain network known as the *default mode network* (DMN). They show spontaneous correlation during resting states (Raichle et al., 2001), and exhibit increased activity during self-referential tasks (Buckner and Carroll, 2007; Andrews-Hanna et al., 2010b; Qin and Northoff, 2011), suggesting that these regions play a critical role in internally directed cognitive processes.

In contrast to the DMN, Corbetta and Shulman (Corbetta and Shulman, 2002) described the *dorsal attention network* (DAN), which is implicated in attentional orienting to external stimuli, and consists of dorsal parietal cortex including the intraparietal sulcus, and dorsal prefrontal cortex, including the putative frontal eye fields. These two networks are consistently anticorrelated during cognitive tasks requiring external attention (Fox et al., 2005). A study by Sestieri et al. (Sestieri et al., 2011) illustrates this anticorrelation across tasks: While a perceptual search task engaged the DAN and suppressed the DMN, an episodic retrieval task engaged the DMN and suppressed the DAN. Guerin et al. (Guerin et al., 2012) explicitly varied the attentional and memorial difficulty of the test stimuli in a recognition paradigm, showing that even within-task, these networks exhibit competitive interactions, particularly within lateral parietal cortex. These findings support a bipartite view of cortical organization, in which distinct large-scale networks support internally and externally based cognitive processes (Fox et al., 2005; Binder et al., 1999; Greicius et al., 2003; Frank et al., 2005).

Recent human neuroimaging results challenge this bipartite organizational scheme, suggesting that the exclusively competitive nature of these networks is an artifact of the particular cognitive tasks used to examine their dynamics. In particular, when an external cue is used to prompt recollection of source details of a particular experience, DAN and DMN show cooperative interactions in the form of positive functional coupling (Simons et al., 2007; Fornito et al., 2012). Spreng et al. (Spreng et al., 2010) compared the dynamics of these networks during an autobiographical planning task and a visuospatial planning task, and found a functional reorganization between the two tasks. They identified a frontoparietal control network that coupled with DMN when the task involved self-referential information, and coupled with DAN when the task involved visual information. While the autobiographical planning task of Spreng et al. (Spreng et al., 2010) is both goal-driven and internally directed, it yields subjective behavioral responses (regarding the fidelity and quality of the generated plans), limiting one's ability to link the neural dynamics of the DAN and DMN to the behavioral dynamics of memory retrieval.

Free recall is an excellent paradigm for examining the nature of DAN and DMN interactions during internally directed cognitive processes. This task is goal-driven, internally directed, and yields well-characterized behavioral responses regarding the particular contents of remembered experience. Participants study a series of items, and then are asked to vocally report those items in any order, without the aid of an external cue. A recent study by Shapira-Lichter et al. (Shapira-Lichter et al., 2012) found a competitive interaction between DAN and DMN brain regions during free recall, supporting the bipartite view of cortical organization. While DAN regions showed strong activity early in the free-recall period which declined over the course of memory search, DMN regions were deactivated early in the period, showing a gradual recovery over the course of the search. Notably, Shapira-Lichter et al. (Shapira-Lichter et al., 2012) did not observe recruitment of the same frontoparietal control network that coupled with the DMN in the autobiographical planning task reported by Spreng et al. (Spreng et al., 2010), suggesting that internally directed memory search may require a distinct network organization from internally directed planning.

We used a combination of network-based (using independent component analysis) and region-based analysis to examine the dynamics of these large-scale functional networks as participants searched their memory during a free-recall task. We observe a functional reorganization of the DMN during the recall period itself, with increased functional coupling between a posteromedial network, a right-lateralized frontoparietal control network, and a medial prefrontal network demonstrating spatial correspondence with the DMN. Our results suggest that memory retrieval in free recall involves increased coupling of attentional and memorial networks, reflecting reorganization of intrinsic connectivity.

Materials and Methods

Participants

We tested 20 (12 female) native English speakers between 18 and 35 years of age, after obtaining consent in accordance with procedures approved by the Vanderbilt University Institutional Review Board. Participants received payment of $20/hour for their participation, with up to an additional $10 earned dependent upon performance in the task.

Experimental Procedure

Participants ran in a variant of the free-recall paradigm, in which they studied a sequence of 12 lists (spanning two separate sessions), each of which contained 24 study items. Stimuli were presented with a computer running *PyEPL* (Geller et al., 2007). After each study list, participants performed either a free-recall test or a source recognition test. Each session included 3 free recall lists and 3 source recognition lists; the conditions were pseudo-randomly ordered within each session. Here, we focus exclusively on the free-recall trials, depicted in a schematic representation in Figure 1A.

Each word was studied with a semantic orienting task (either a size judgment or an animacy judgment) requiring a keypress response from the participant. Prior to stimulus presentation, a cue appeared on the screen for 0.7 sec in order to indicate which orienting task would apply to the upcoming stimulus. After presentation of the task cue, we displayed a fixation cross for an interval of 0.3 ± 0.1 sec, followed by presentation of a study item for 2.5 sec, during which the participant made their judgment. An inter-stimulus fixation interval between 0.5 and 5 sec in duration followed each study item. We optimized the order of tasks and the durations of the inter-stimulus intervals to increase efficiency in estimation of the hemodynamic response to each task (Dale, 1999), with the constraints that a task was not repeated more than 6 consecutive times, and that half of the items on a given list were studied in each of the two tasks.

After the final study item was presented on a given list, participants were given 75 sec to freely recall as many items as they could remember from the most recent list, in any order. We recorded vocal responses using a scanner-safe voice recording system (Resonance Technologies, Inc.). Custom software (Cusack et al., 2005) and the "Noise Removal" tool in Audacity removed audio noise from the scanner from audio recordings. We scored vocalized responses offline using *PyParse* (Solway et al., 2010) and *Penn TotalRecall*.

Following the recall portion of the task, participants performed one of three control tasks: a speech control task, an eyes-open task, and an eyes-closed task. During the speech control task, words were presented in the same format as in the encoding period. Items presented during the speech task were presented for a duration of 2 sec, with an inter-stimulus interval of 4 sec. Participants were presented a total of 3 items per list, for a total of 18 speech trials. The eyes-open, and eyes-closed tasks consisted of presentation of the auditory cues "open" and "close", which instructed the participant to either attend to the fixation cross, or close their eyes, respectively. Auditory cues were presented with an ISI of ten seconds, with a total of 6 cues per functional run.

Each of the 20 participants performed two sessions of the free-recall paradigm in the 3T Phillips MRI scanner at the Vanderbilt University Institute of Imaging Science. Prior to imaging sessions, participants performed two behavioral sessions for familiarization with the task, to ensure consistent behavioral performance during scanning.

Image acquisition

Functional images were collected using an interleaved EPI pulse sequence (TR = 2000 msec, TE=30 msec, voxel size=3.0x3.0x3.6 mm, flip angle = 75^o, FOV=192 mm). During the functional EPI scans, 30 oblique slices were collected over the whole brain, oriented parallel to the AC-PC plane. Whole brain MP-RAGE structural scans were collected (TR = 2500 msec, TE=4.38 msec, voxel size= 1.0x1.0x1.0mm, flip angle = 8^o, FOV=256 mm).

Image processing

Preprocessing

The first four volumes of each functional run were removed to allow for equilibration of scanner signal. Preprocessing of fMRI data was performed using routines as implemented by the SPM8 software package. All volumes from the twelve functional runs were realigned to the first functional volume of the first run, correcting for head motion. A mean functional image was generated from the realigned time-series and co-registered to the T1-weighted whole brain anatomical scan. These T1-weighted anatomical images were then segmented into gray matter, white matter, and cerebrospinal fluid, and normalized to a template in Montreal Neurological Institute (MNI) stereotactic space using the unified segmentation approach as implemented in the *New Segment* tool in SPM8 (Ashburner and Friston, 2005). Images were resampled to 3-mm isotropic voxels and spatially smoothed with a 8-mm FWHM Gaussian kernel.

Independent Component Analysis

ICA was used to identify spatially distinct neural networks contributing to fMRI signal during the free recall task, without assumption of a temporal model of hemodynamic activity. Independent networks were identified using the Group ICA of fMRI Toolbox (Calhoun et al., 2001). To reduce data complexity, principle component analysis was applied to each individual participants data. The number of independent sources was estimated to be 28 using the minimum description length criterion (Li et al., 2007). Next, the resultant timeseries were concatenated across participants, and independent component analysis was conducted using the Infomax algorithm. Time courses and spatial maps resulting from the ICA solution were back-projected for each individual participant. Timeseries amplitude was converted to percent signal for comparison across participants. Spatial loading of components was examined using a random effects model, by performing one-sample t–tests on the component maps, accounting for multiple comparisons (family-wise error corrected, $p < 0.05$). Group component maps constructed in this manner were used in post hoc region-based analyses.

Rejection of non-neural components

Use of ICA as an analytic tool has the benefit of identifying sources of noise in the BOLD timeseries. We employed an automated artifact removal method based on both anatomical and spatial constraints in the components (Sui et al., 2009). This method uses two criteria for component rejection based upon anatomical and geometric properties of the spatial maps. The grey matter and ventricular cerebrospinal fluid probabilistic atlases provided by SPM8 were correlated with the spatial map of each component, yielding two correlation values c_{GM} and c_{CSF}. Components of interest should be localized to grey matter, and as such, any components with $|c_{CSF}| > |c_{GM}|$ were rejected. The second criteria ensured the components were spatially clustered, as expected of physiological sources measured with fMRI. For each component map, we computed the focusing degree, defined as the ratio between the spatial entropy and the degree of clustering, the proportion of above threshold ($|t(19)| > 6.51$) voxels within a $100mm^3$ cluster (see: Formisano et al. (Formisano et al., 2002) for more details). The focusing degree was compared to a dynamically determined threshold, and components below the threshold were identified as artifacts.

Component selection and general linear modeling

A single general linear model (GLM) was constructed for the selection of ICs of interest, as well as subsequent post-hoc analyses (e.g., psychophysiological interaction analysis). As described in Experimental Procedure, a single functional run can be decomposed into three periods: encoding, retrieval, and control tasks. As the present analyses focus on network dynamics during the free-recall task, any functional run in which a participant performed the source recognition task was omitted from further analysis. Three conditions of interest were incorporated into the model: transient recall events, a sustained event covering the duration of the entire recall period, and speech control events. Nine additional covariates were included within the model: encoding events, eyes-open events, eyes-closed events, and six motion parameters computed during image realignment. Regressors of interest were constructed by convolving a basis function at the time of an individual event onset, with the canonical hemodynamic response function and is temporal derivative as implemented in SPM8.

Transient recall events and speech events were modeled with Dirac delta functions, with a stimulus duration of 0 sec, and onset at the initiation of the vocal response. The sustained recall condition was modeled with a duration of 75 sec (the duration of the recall period) and onset coincident with presentation of the initiation cue. Encoding events were modeled with a duration of

3 sec, with onsets placed coincident with presentation of the task cue. Eyes-open and eyes-closed events were modeled with a duration of 10 sec, allowing for the construction of alternating block regressors.

The regression analysis produced estimated β-coefficients for transient recall (β_{Rt}), sustained recall (β_{Rs}), and speech (β_{Sp}) events for each participant. A linear contrast of transient and speech-related activity ($\beta_{Rt} - \beta_{Sp}$) was constructed to identify recall-related neural signals unrelated to speech production. A second-level "random-effects" analysis was performed using a one-sample t-test to identify recall-related components across the group of participants, treating participant as a random factor.

Components (ICs) were considered task relevant if they exhibited either a significantly non-zero β_{Rt} or β_{Rs} at a threshold of $p < 0.05$ (Bonferroni corrected for the total number of non-noise components). It should be noted that this contrast identifies task-relevant activity versus the implicit baseline in the described GLM, which is comprised of passive fixation across the session, including inter-trial intervals during encoding, as well as periods of rest between task periods (encoding, retrieval, and control tasks).

The study period included two distinct encoding tasks, which have previously been shown to influence neural activity both during the encoding and retrieval of items associated with each respective task (Polyn et al., 2012). We implemented an additional regression analysis, constructing separate transient recall regressors for the *size task* and *animacy task* separately. To ensure that the identified components reflected task-general activity, a conjunction analysis was implemented: any transient component must be significantly non-zero regardless of encoding task ($\beta_{Rt,size} > 0 \cap \beta_{Rt,animacy} > 0$).

To examine variability in the response of functional networks showing task-related profiles, we constructed a finite impulse response (FIR) model, using the same GLM as described above. The FIR basis set modeled activity ranging from six seconds pre-vocalization to twenty seconds post-vocalization. The FIR window length was determined post-hoc in order to maximize the efficiency in estimating the response at each timepoint, given the distribution of individual recall times (Öztekin et al., 2010). While the overlap in responses does introduce collinearity into the GLM and reduces overall power, it allows for the separation of neural activation that occurs leading up to, and concurrent with, individual retrieval events. Activity leading up to individual recall events is of interest, given prior studies demonstrating retrieval-related processing preceding individual recalls (Polyn et al., 2005; Gelbard-Sagiv et al., 2008).

Minimizing motion-related signal

Overt speech production, as required by the free-recall and speech control tasks examined here, has been shown to increase head motion relative to covert speech (Barch et al., 1999). We implemented a number of measures in order to ensure the neural dynamics characterized in this study were not unduly influenced by motion-induced artifact. To minimize head motion in the scanner, padding was placed within the head coil around the participant's head, and the participant was given specific instructions to remain as still as possible while speaking.

Motion-related artifacts tend to have characteristic spatial profiles, with artifactual signal appearing near the edge of the skull, and at the boundaries of different tissue classes (Barch et al., 1999). Additionally, the inferior region of the brain is noticeably susceptible to magnetic field change caused by speaking, due to proximity to the mouth and throat (Birn et al., 1998). The ICA-based artifact rejection technique described above identifies ICs that were likely to have been artifactual in origin, and removes these components from the set of analyzed components (Beckmann et al., 2000; Sui et al., 2009).

In addition, we inspected incremental head motion during scanning, to ensure that no within-scan movement exceeded half the voxel size ($> 1.5mm$). Additionally, we ensured no within-scan rotation exceeded 1.5 degrees. Choice of these thresholds was determined based on visual inspection of the raw fMRI and participant motion timeseries. Even minimal head motion can produce a characteristic striped artifact when using interleaved slice acquisition. We visually inspected the global fMRI signal over the course of the experimental session to identify such artifacts. If a participant exhibited such an artifact during a given scan (regardless if it was coincident with subject motion), an additional binary regressor was added to that participant's GLM to remove the effects of artifactual variances on the regression analyses. A total of three participants exceeded this within-scan movement threshold. The total number of TRs recorded during within-scan motion, or additional artifact was minimal (range of 1–3 TRs). Similar procedures have been developed in dealing with high-movement clinical populations (Mazaika et al., 2009).

To ensure that the identified components reflected cognitive rather than motion-related signal, we included estimated motion parameters as a covariate of interest in all GLM-based analyses. Finally, prior work has shown that certain motion-induced artifacts arising from overt speech production are variable in terms of their spatial location across participants (Barch et al., 1999). The group-based analyses employed here will tend to minimize the influence of these artifacts.

Network Correspondence Analysis

To identify the correspondence between the observed ICs and large-scale networks that have been observed in low-frequency spontaneous fluctuations in BOLD signal, we performed a correlation-based correspondence analysis. For each IC, we computed the Pearson product-moment correlation between the group-averaged spatial map (thresholded at $|t| > 3$) and masks corresponding to seven (binary) cortical network maps constructed by Yeo et al. (Yeo et al., 2011). Voxels contained in the intersection of the two images were included in the computation. It should be noted that the resisting state network templates are restricted to the cortical mantle, and deep brain structures such as the hippocampus and basal ganglia are excluded. Networks templates included in this analysis include the dorsal attention, ventral attention, default mode, frontoparietal control, somatomotor, visual, and limbic networks (see Yeo et al. (2011) for details).

Network Interaction Analysis

Spontaneous (task-unrelated) network interactions

We implemented a partial correlation analysis, after accounting for variability in the BOLD response due to recall-related activity, to estimate spontaneous (i.e., task-unrelated) functional connectivity of pairs of regions. First, we applied a low-pass filter ($f < 0.08$ Hz) to each of the component timeseries engaged during the free-recall task. For each pairwise combination of the components of interest, functional coupling was estimated as the partial correlation of the noise-corrected component timeseries, while controlling for the effects of the remaining three component timeseries, as well as the task regressors constructed in the basic general linear model. This procedure allowed for the isolation of interactions that were specific to each network pair, and could not be explained by a common response to the task.

Task-related network interactions

To analyze changes in coupling between the functional networks identified using ICA, we implemented a correlational psychophysiological interaction (cPPI) analysis (Fornito et al., 2012). It should be emphasized that this analysis examines the effective connectivity between the identified ICs, and tests for a changes in coupling resulting from specific events during the cognitive task. By focusing on the coupling of networks, rather than specific regions of interest, analyses of this nature have provided insight into the organization and interactions of large-scale functional networks (Sridharan et al., 2008; St. Jacques et al., 2011).

This analysis identifies components whose covariation changes as a function of task state, by modeling main effects of the psychological task, physiological signal, and their interaction. It controls for any correlations that may arise from either spontaneous or independent coactivation effects by including timeseries representing both the component of interest, as well as the predicted activity associated with the free-recall task. The remaining interaction term provides a measure of task-related changes in functional coupling between the timeseries of interest. For each of the component timeseries of interest, we computed the interaction effect using a deconvolution technique (Gitelman et al., 2003). For each pairwise combination of the networks of interest we calculated the partial correlation between the interaction effects, while controlling for component timeseries and modeled task effects. Given violations of normality in observed measures of functional coupling, we implemented nonparametric tests in the form of Wilcoxon signed-rank and rank-sum tests to determine significant interactions across participants.

Regions of interest analyses

We constructed regions of interest (ROIs) by identifying, within each component map, clusters composed of contiguous voxels within *a priori* anatomical regions of interest using the Automated Anatomical Labeling toolbox (Tzourio-Mazoyer et al., 2002). Anatomical regions of interest included association cortex within the prefrontal cortex, parietal cortex, and medial temporal lobe (i.e., we excluded the occipital lobe, lateral temporal cortex, pre- and postcentral gyri, and the cerebellum). Anatomical information concerning the constructed ROIs can be found in Supplementary Materials. We extracted the average signal within each cluster, and modeled the signal using a univariate linear regression as previously described (see: Component identification and general linear modeling). This analysis yielded estimates for a sustained recall-related component (β_{Rs}), a transient recall-related component (β_{Rt}), and speech-related (β_{Sp}) network activity, for each ROI. Statistical testing of ROI timeseries was implemented under the same framework as the component identification analysis, with Bonferroni correction calculated based on the total number of ROIs.

Results

Behavioral results

Overall, the proportion of items recalled by participants was 0.42 (SEM 0.03). Figure 1B shows the serial position curve observed when probability of recall was calculated as a function of list position. We observed a primacy effect (increased recall for serial positions 1–3 relative to serial positions 4–21 [$t(19) = 5.31$, $p < 0.0001$]), and a recency effect (increased recall for serial positions 22–24 relative to serial positions 4–21 [$t(19) = 5.91$, $p < 0.0001$]). Figure 1C characterizes the timing of participants' recall responses; as the recall period progresses, the number of recalls made increased in a negatively accelerating manner, with a mean inter-response time (IRT) of 5.09 sec (SEM 1.21 sec). A more thorough description of the behavioral effects observed in this experiment can be found in a prior publication examining patterns of task-related activity in these data (Polyn et al., 2012).

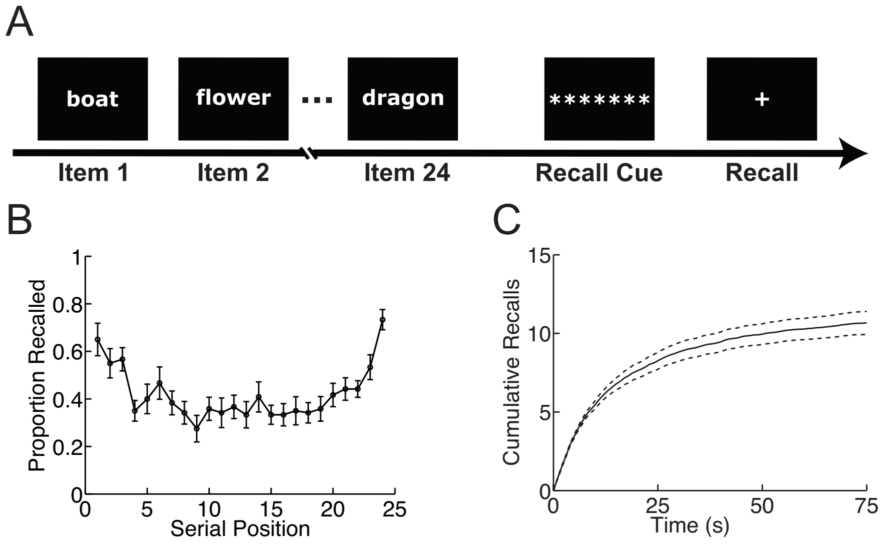

Figure 1. **(A)** Schematic representation of a free-recall trial used in the experiment. During the encoding period, participants were presented with a list of 24 items. Each encoding period was followed by a recall cue of 300 msec duration, followed by a 75 second recall period. **(B)** Mean recall (± 1 SEM) performance as a function of serial position. **(C)** Cumulative distribution plot of recalls made across the recall period. Dotted lines represent SEM.

Speech-induced head motion

We characterized speech-induced head motion with a one-way repeated measures ANOVAs, with the computed incremental motion parameters as the dependent variable, task (e.g., encoding, recall, and speech) as the independent variable, and subject as an additional factor. Despite subject motion increasing numerically during the speech and control tasks, as shown in Table 1, this increase was not statistically significant for any of the comparisons (all $p > 0.05$). Nevertheless, we include estimates of subject motion as covariates in the following regression-based analyses to ensure the observed patterns of activity are not unduly influenced by non-neural signal sources.

Imaging results

Functional networks engaged during recall

The free-recall paradigm presents a challenge to standard analysis techniques, in that the timing of the responses are determined by the behavior of the subject (Öztekin et al., 2010), and the timing of hemodynamic response relative to the behavioral response is unknown. Spatial ICA (Calhoun

Table 1. Differences in head motion across task conditions.

		Encoding	Recall	Speech
Translations (mm)	X	0.013 (0.11)	0.0089 (0.15)	0.006 (0.18)
	Y	0.033 (0.11)	0.045 (0.16)	0.069 (0.18)
	Z	0.019 (0.24)	-0.084 (0.38)	-0.024 (0.36)
Rotations (degrees)	Roll	0.059 (0.29)	0.17 (0.45)	0.039 (0.52)
	Pitch	0.012 (0.11)	-0.0057 (0.18)	-0.031 (0.19)
	Yaw	0.0099 (0.14)	-0.025 (0.19)	-0.023 (0.22)

Note: Differences in head motion are compared across three separate task conditions. Across-subject incremental averages are reported, with the standard deviation in parentheses.

et al., 2001) provides a data-driven technique that characterizes the temporal dynamics and spatial distribution of functional networks, and has been shown to identify functional networks that are present during both task-related cognition and rest (Smith et al., 2009). We applied this technique to the neural signal recorded during free recall periods, and identified a set of components related to memory search. To this end, we constructed two sets of regression coefficients, one designed to identify sustained component activity related to memory search (a block regressor rising for the entire free-recall period and flat otherwise), and one designed to identify transient component activity related to memory search (delta functions corresponding to the individual recall vocalizations). Both sets of coefficients were convolved with a standard hemodynamic response function. This analysis identified one independent component (IC) exhibiting a sustained positive response during memory search, seven ICs showing a sustained negative response, four ICs exhibiting transient positive responses, and one IC showing a transient negative response, from among the full set of components. Here, we describe the five positive-going components (sustained and transient), in the next section we describe the negative-going components.

We assign a descriptive name to each of these five networks, based on the most prominent brain regions identified within it. A full accounting of the regions associated with each network is provided in Supplementary Table 2. IC_6 (posteromedial, "PM") included bilateral medial temporal lobe structures (including hippocampus), retrosplenial cortex, and ventromedial prefrontal cortex. This network was identified as having a sustained response during free recall, using the above mentioned regression analysis (β_{Rs} significantly greater than zero; $t(19) = 4.38$, $p < 0.008$). Previous studies examined a network with similar structure that was shown to activate during declarative (Vincent et al., 2006) and autobiographical (St. Jacques et al., 2011) memory tasks. A subset of these regions are part of the default mode network (DMN), which shows increased activation when mental images are constructed from mnemonic representations (Hasselmo et al., 2007; Andrews-Hanna et al., 2010b).

The first transiently responding network (significantly non-zero β_{Rt} across subjects; $t(19) = 3.94$, $p < 0.02$) was IC_7 (dorsal frontoparietal, "DFP"), which contained bilateral prefrontal cortex (including bilateral dorsolateral prefrontal cortex, and left lateralized rostrolateral prefrontal cortex), bilateral supramarginal gyrus, and precuneus. Previous studies have implicated a similar network in top-down cognitive control processes (Vincent et al., 2008; Badre and Wagner, 2007). The second transiently responding network (positive β_{Rt}; $t(19) = 11.88$, $p < 0.0001$) was IC_{12} (temporo-insular, "TI"), which covered the superior temporal gyrus, Heschl's gyrus, middle temporal gyrus, insula, and anterior cingulate cortex. Previous studies have implicated similar regions in tasks involving speech execution, verbal feedback (Christoffels et al., 2007) and auditory perception, specifically speech processing (Binder et al., 2000). The third transient network (positive β_{Rt}; $t(19) = 4.39$, $p < 0.008$) was IC_{13} (cerebellar,"CER"), which spans the cerebellum and portions of dorsolateral prefrontal cortex. The final transient network (positive β_{Rt}; $t(19) = 13.17$, $p < 0.0001$) was IC_{24} (somatomotor, "SM"), which included bilateral somatomotor cortex, striatum, and superior cerebellum. Previous studies have implicated a similar network during execution of overt speech (Huang et al., 2001; van de Ven et al., 2009).

For each of the transiently responding components, we contrasted activity during recall events to activity during a speech production task, to determine whether fluctuations in activity were better thought of as speech-related or recall-related. The DFP and CER networks showed a reliably smaller response during the speech control task as compared to recall events (DFP/IC_7: $t(19) = 6.24$, $p < 0.0001$; CER/IC_{13}: $t(19) = 3.92$, $p < 0.009$). In addition to being reliably activated during recall, the SM network was reliably activated during speech production ($t(19) = 7.45$, $p < 4.27x10^{-6}$), and recall-related activity was not reliably stronger than speech ($t(19) = -1.32$, $p > .99$).

Functional networks disengaged during recall

A single component (IC_{20}) consisting mainly of ventromedial prefrontal cortex ("VP"), transiently decreased activity during recall events relative to baseline (negative β_{Rt}; $t(19) = -6.56$, $p < 0.0001$). Six networks exhibited sustained deactivation across the recall period, including two of the four networks exhibiting transient positive responses relative to recall events: DFP/IC_7 (negative β_{Rs}; $t(19) = -8.83$, $p < 0.0001$), TI/IC_{12} (negative β_{Rs}; $t(19) = -6.57$, $p < 0.0001$).

This analysis identified three other components exhibiting sustained deactivation across recall. The first deactivated component (negative β_{Rs}; $t(19) = -3.62$, $p < 0.05$) was IC_{14} (right frontoparietal, "RFP"). Two additional networks exhibited deactivation: IC_{23} (posterior cingulate, "PC") showed sustained decreases during memory search (negative β_{Rs}; $t(19) = -7.01$, $p < 0.0001$), as well as IC_{26} (medial prefrontal, "MP": negative β_{Rs}; $t(19) = -5.83$, $p < 0.0001$). Figure 2 depicts the spatial distribution (top row) and temporal dynamics (bottom row) of the ICs exhibiting sustained increases in activity during memory search. These temporal profiles are averaged across all recall periods for all subjects, and provide a coarse view of when during the recall period the corresponding network shows maximal activity.

Network Correspondence Analysis

Given the known correspondence between large-scale functional networks identified using intrinsic measures of functional coupling during rest and task-based activation patterns (Smith et al., 2009), we next sought to identify the degree to which the identified ICs correspond to resting-state networks. Yeo et al. (Yeo et al., 2011) published spatial templates of seven large-scale functional networks identified during resting periods with fMRI, allowing us to quantify the correspondence between these networks and our ICs, using a Pearson product-moment correlation statistic.

A number of ICs showed a one-to-one correspondence with resting state networks. Three components showed a strong correspondence with the DMN, including PM/IC_6 ($r = 0.20$, $p <$

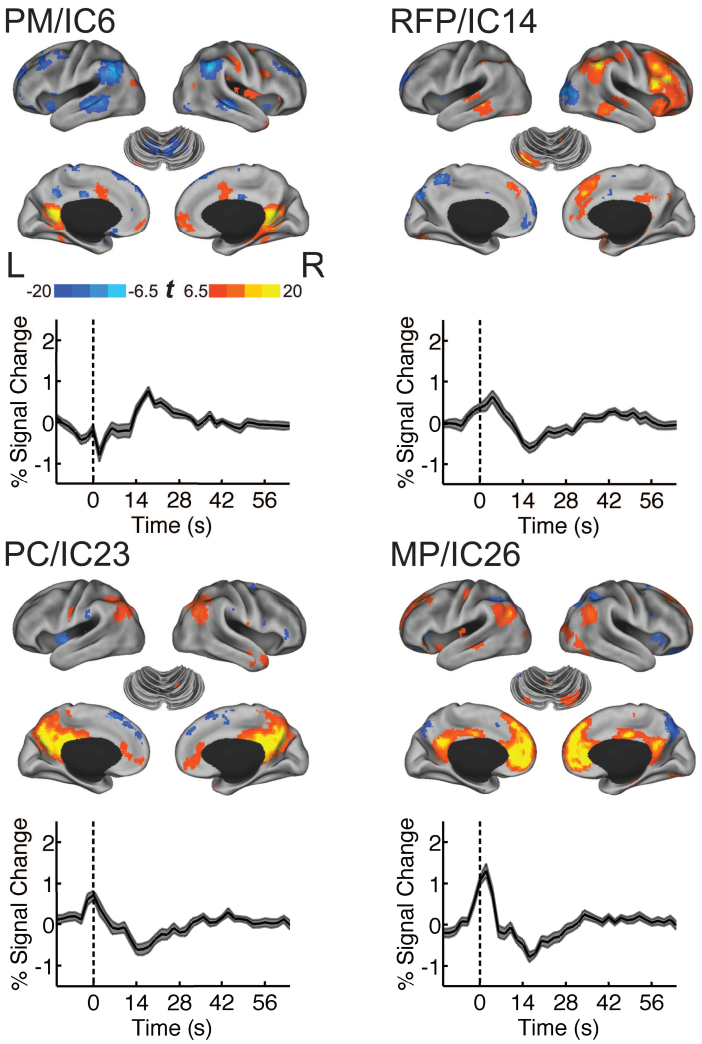

Figure 2. Large-scale functional networks exhibiting sustained changes in activity during self-initiated memory search. Component *t* maps are projected onto the inflation population average landmark surface (PALS) using CARET software (Van Essen et al., 2001). The mean component time series across the recall period, averaged across subjects, is depicted below each component map. The beginning of the recall period is marked at timepoint 0, indicated with the dashed vertical line. Shaded regions represent ±1 SEM.

0.0001), PC/IC_{23} ($r = 0.29$, $p < 0.0001$), and MP/IC_{26} ($r = 0.45$, $p < 0.0001$). We observed a high degree of spatial correspondence between SM/IC_{24} and the somatomotor network ($r = 0.48$, $p < 0.0001$). RFP/IC_{14} exhibited a high degree of spatial correspondence with the frontoparietal control network ($r = 0.28$, $p < 0.0001$). DFP/IC_7 was the sole component identified with spatial similarity to the DAN ($r = 0.28$, $p < 0.0001$).

Of the task-relevant ICs, three did not demonstrate a clear one-to-one mapping with the resting state networks. VP/IC_{20} demonstrated moderate correspondence between both the DMN ($r = 0.22$, $p < 0.0001$) and the limbic network ($r = 0.37$, $p < 0.0001$). Despite the lack of a one-to-one mapping, a Hotelling-Williams test revealed significantly greater correlation between VP/IC_{20} and the limbic network than the DMN ($t(12981) = 8.21$, $p < 0.0001$). TI/IC_{12} showed functional correspondence to both the somatomotor network ($r = 0.30$, $p < 0.0001$) as well as the ventral attention network ($r = 0.22$, $p < 0.0001$). The magnitude of the correlation between TI/IC_{12} and the somatomotor network was greater than its correlation with the ventral attention network ($t(12981) = 5.51$, $p < 0.0001$). CER/IC_{13} showed functional correspondence to both the visual network ($r = 0.12$, $p < 0.0001$) as well as the ventral attention network ($r = 0.12$, $p < 0.0001$). These correlation values were not significantly different from one another ($t(12981) = 0.06$, $p > 0.47$).

Recall-locked analysis reveals a cascade of engagement

In order to examine the dynamics of these components in the time surrounding each recall event, we constructed a finite impulse response (FIR) model for each component exhibiting transient activation during memory search, relative to the onset of the vocal response for each recall event. Figure 3 depicts the average response within multiple large-scale networks, from six seconds before to twenty seconds after vocalization onset. These event-averaged responses confirm the transient nature of the DFP, TI, CER, SM, and VP responses.

Furthermore, the FIR analysis reveals that these networks are engaged in a cascade relative to the recall onset. The temporal ordering of engagement was not specified or predicted by the

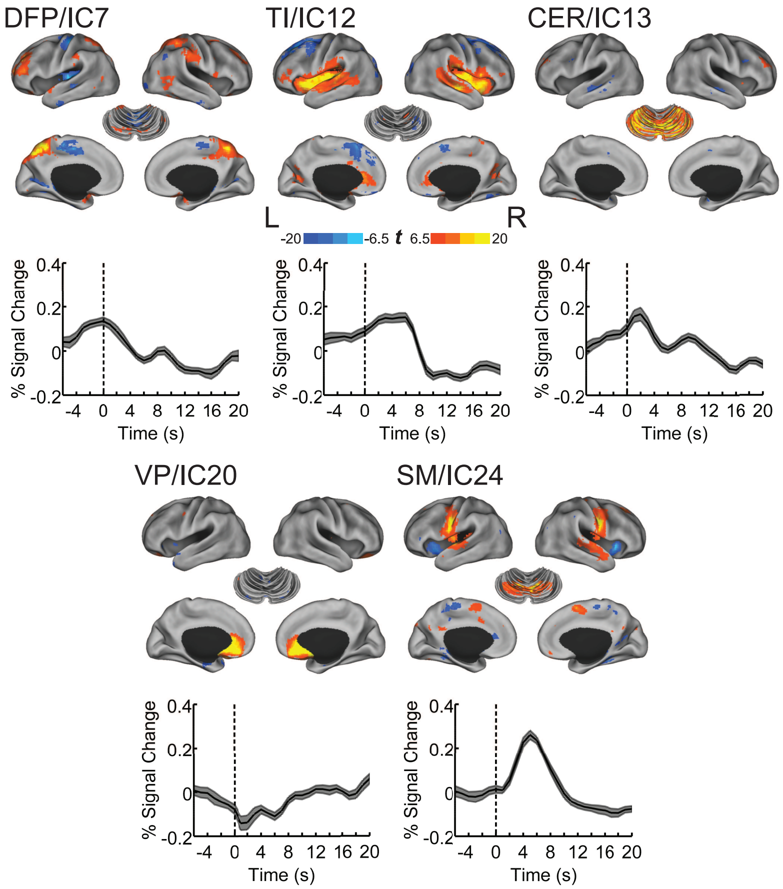

Figure 3. Large-scale functional networks exhibiting transient changes in activity locked to individual recall events. The top row depicts component *t* maps projected onto the inflation population average landmark surface (PALS) using CARET software (Van Essen et al., 2001). The time-course of each component relative to the onset of recall vocalization (dashed vertical line), estimated using a finite impulse response model applied to the component time-series is depicted below each respective component map. Shaded regions represent ±1 SEM.

regression analysis used to identify the components. We characterized the temporal order of engagement statistically by comparing, for pairs of components, the latency of the peak response across participants. The earliest peak was in the DFP/IC_7 network, which led the SM/IC_{24} network ($t(19) = 3.66$, $p < 0.002$). The peak response within the SM network reliably lagged the CER/IC_{13} network ($t(19) = 3.27$, $p < 0.004$). A summary of the statistically reliable peak latency differences is provided in Table 2. While variability in the hemodynamic response limits one's ability to resolve the relative timing of neural activity using fMRI, this variability is greater across subjects than across cortical regions (Handwerker et al., 2004). Given the magnitude of the observed differences in peak latencies between components, these findings potentially reflect differences in the onset of neural activity. Regardless, confirmatory findings using modalities with superior temporal resolution (e.g., electrocorticography) are necessary to validate temporal or causal dependency between these networks.

Table 2. Differences in event-averaged signal peak across components.

	DFP/IC_7	TI/IC_{12}	CER/IC_{13}	SM/IC_{24}
DFP/IC_7		-3.1 ± 0.02	-1.65 ± 0.14	$-4.8 \pm 1.31^{\dagger}$
TI/IC_{12}			1.45 ± 1.53	-1.7 ± 0.01
CER/IC_{13}				$-3.15 \pm 0.01^{\dagger}$

Note: Mean differences (± standard error) for each component pair are shown. $\dagger, p < 0.05$, Bonferroni-corrected for multiple comparisons.

Large-scale network interactions during memory search

Network analysis of neural activity suggests that the brain is organized into competitive, large-scale functional brain networks (Fox et al., 2005). A classic example is the trade-off between the DMN, which engages during self-referential activity and disengages during attentional shifts to salient external stimuli (Andrews-Hanna et al., 2010a), and attentional networks that show the converse pattern (Fox et al., 2006; Dosenbach et al., 2006). Computational models of human memory (Polyn and Kahana, 2008) suggest that frontal and MTL regions should cooperate during self-initiated retrieval, but are presently too abstract to predict the nuanced temporal dynamics of this interaction.

In the present work, we implemented a partial correlation analysis to characterize the pairwise interactions of the five networks comprised of cortical regions commonly associated with either the DAN, DMN, or FPC networks (as identified in our network correspondence analysis). This analysis identifies correlations in spontaneous network activity, after accounting for variance correlated with the task structure (as modeled in the GLM). Spontaneous (i.e., not explicitly related to task regressors, which include regressors for recall events) interactions exhibited themselves both in terms of competition (a negative correlation in spontaneous activity) and cooperation (a positive correlation in spontaneous activity). All spontaneous network interactions are depicted in Figure 4A. The PM/IC_6 network exhibited a competitive interaction with the DFP/IC_7 network ($Z = -3.70$, $p < 0.002$), and a cooperative interaction with the MP/IC_{26} ($Z = 3.88$, $p < 0.02$) network. Additionally, low-frequency spontaneous fluctuations in the DFP/IC_7 network negatively coupled with those in the RFP/IC_{14} network ($Z = -3.73$, $p < 0.002$).

To test the degree to which memory search influences the functional coupling between the identified large-scale networks, we implemented a PPI analysis examining differences in functional coupling sustained throughout the recall period. As depicted in Figure 4B, the PM/IC_6 network exhibited sustained increases in functional coupling across the recall period with both the RFP/IC_{13} ($Z = 3.35$, $p < 0.004$) and the MP/IC_{26} ($Z = 3.81$, $p < 0.001$). The DFP/IC_7 network exhibited sustained increases in functional coupling with PC/IC_{23} ($Z = 3.40$, $p < 0.007$). We observed significant coupling between MP/IC_{26} (which demonstrates spatial correspondence with the DMN), and both DFP/IC_7 ($Z = 3.40$, $p < 0.007$) and RFP/IC_{13} ($Z = 3.02$, $p < 0.03$).

In addition to differences in functional coupling sustained throughout the recall period, we examined the degree to which functional connectivity between large-scale networks shifted during successful recall events by implementing an additional PPI analysis, constructing the interaction term based on the transient recall regressor. As shown in 4C, of all network interactions, only the DFP/IC_7 and PC/IC_{23} demonstrated significant coupling ($Z = -3.14$, $p < 0.017$). To ensure that observed differences in network interactions are not attributable to response production alone, an additional PPI analysis was implemented by examining the interaction between large-scale network activity during the speech production task. Anticorrelation between the DFP/IC_7 and PC/IC_{23} was stronger during recall than the speech control task ($Z = -3.15$, $p < 0.016$).

A number of network pairs demonstrated an increase in functional coupling during the recall period, as compared to spontaneous coupling: PM/IC_6 and DFP/IC_7 ($Z = 3.72$, $p < 0.002$), DFP/IC_7 and RFP/IC_{14} ($Z = 4.26$, $p < 0.0002$), DFP/IC_7 and MP/IC_{26} ($Z = 4.04$, $p < 0.0005$), and PC/IC_{23} and MP/IC_{26} ($Z = 3.45$, $p < 0.006$) networks. Only the DFP/IC_7 and PC/IC_{23} networks demonstrated stronger anticorrelation during the recall period ($Z = -4.36$, $p < 0.0001$).

Discussion

We identified the contributions of multiple large-scale functional networks during self-initiated memory search, by applying independent component analysis (ICA) to fMRI while subjects performed a free-recall task. Multiple regression techniques were used to characterize how fluctuations in each component related to recall performance, and we observed unique recall-related signatures in several networks associated with the default mode network (DMN), dorsal attention network (DAN), and frontoparietal control (FPC) network. These findings provide insight into the role of these networks during an internally directed memory search task, and provide novel constraints for theories of the role of these networks in cognition.

Fractionation of the DMN during memory search

We identified three networks that demonstrated spatial correspondence with the DMN; however, only the PM/IC_6 network increased in engagement during memory search. In contrast, PC/IC_{23} and MP/IC_{26} demonstrated decreased activity sustained throughout the recall period. Cooperative interactions between PM/IC_6 and RFP/IC_{14} and PC/IC_{23} increased during memory search, replicating prior work showing increased coupling between FPC networks and the DMN during internally directed cognitive tasks (Spreng et al., 2010; Fornito et al., 2012). This functional organization during memory search highlights the flexibility of large-scale networks (Fornito et al., 2012). Additionally, networks that are commonly observed to be anticorrelated using measures of intrinsic functional

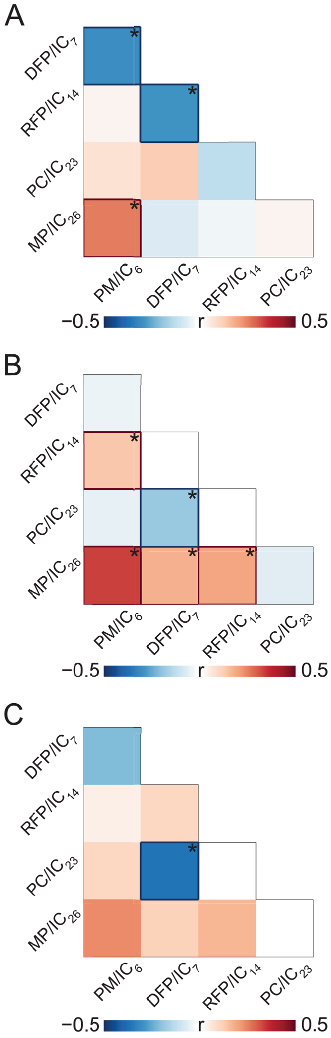

Figure 4. Interactions between functional networks. Distributions of **(A)** spontaneous, **(B)** sustained recall-related and **(C)** transient recall-related connectivity. Significant cooperative interactions ($p < 0.05$, Bonferroni corrected) are outlined in red, with significant competitive interactions outlined in blue.

coupling may demonstrate cooperative interactions during specific tasks, such as memory retrieval.

Recent studies examining the functional organization of the DMN have identified fractionation of this large-scale network during both memory search (Sestieri et al., 2011) and internally directed paradigms (Andrews-Hanna et al., 2010a). In an attempt to dissociate regions of the DMN that provide a specifically mnemonic function, Shapira-Lichter et al. (Shapira-Lichter et al., 2013) compared decreases in activity during various internally directed search tasks, in which subjects performed either semantic, episodic, or phonemic fluency tasks. Consistent with findings from the present data, regions within the DMN demonstrated selectivity for both of the episodic and semantic tasks. Findings of heterogeneous contributions of the DMN suggest that a bipartite (e.g., Fox et al., 2005; Golland et al., 2007) view of cortical organization is an oversimplification. The posteromedial network, while commonly coactivated with the DMN, is functionally distinct from this larger network during the free-recall task.

Retrosplenial and parahippocampal cortices have been proposed by Ranganath and Ritchey (Ranganath and Ritchey, 2012) to form the core of a posteromedial system that is recruited during episodic simulation (Hasselmo et al., 2007) and spatial navigation (Burgess et al., 2007), and which represents information pertinent to temporal and other causal relationships within a certain context. While the current study cannot speak to the specific function of the observed PM network outside of engagement during the free-recall task, activity within this network may reflect the integration of retrieved contextual information, which can be used to guide memory search (Howard and Kahana, 2002a; Polyn et al., 2009a). Intracranial recordings within the temporal lobes have identified the reactivation of patterns of activity that may represent contextual information (Manning et al., 2011). Future work will determine whether the topographic patterns of neural activity in the functional networks investigated here show dynamics characteristic of modern computational models of memory (Polyn and Kahana, 2008; Polyn and Sederberg, 2014).

DAN engagement during internally-directed memory search

A single functional network demonstrated a significant degree of spatial correspondence with the DAN, DFP/IC_7. Consistent with theories of competitive interactions between the DAN and DMN Fox et al. (2005), the anticorrelation between this network and PC/IC_{23} became more pronounced during successful retrieval. Despite anticorrelation between these two networks that have been proposed to mediate internally and externally directed information Corbetta et al. (2008); Vincent et al. (2008); Spreng et al. (2010), this transient engagement of this DFP/IC_7 may suggest a more general cognitive mechanism supported by this network.

While the network correspondence analysis revealed similarity between the DFP/IC_7 network and the DAN, differences exist between the cortical regions comprising these networks. First, the medial bank of the intraparietal sulcus is absent within DFP/IC_7, with posterior parietal cortex activity occurring near the mid-line. Additionally, while DFP/IC_7 contains spatial overlap with the DAN in the putative frontal eye fields, prefrontal activation within DFP/IC_7 extends well into anterior prefrontal cortex, in cortical regions commonly implicated in frontoparietal control networks. We speculate that differences in the observed network activity reflect task demands. Given the internal, rather than external, demands of the free-recall task, the observed absence of activity within visual cortex is consistent with these theories. The shift towards more pervasive prefrontal activity within this network may reflect additional executive control processes required to maintain internal representations during retrieval. Recruitment of this network may reflect top-down modulation of internal representations, concurrently supported through activity within anterior prefrontal cortex.

It has been hypothesized that the DMN and DAN represent to major divisions of functional processing in cortex, with both networks supporting endogenous and exogenous specific processing, respectively. We observe competitive interactions between the DFP/IC_7 and PC/IC_{23}, sustained throughout the recall period. The strength of this anticorrelation additional increases during the successful retrieval of individual items, when there are increased demands for action-based processing involved in the planning and execution of speech production. It should be noted that these interactions are likely to result from mnemonic or internal directed focus of the retrieval task, given the absent of a similar effect during the speech control task. These findings are consistent with reduced functional connectivity between the dorsal posterior cingulate cortex (a central hub in the DMN), and frontoparietal networks (Leech et al., 2012). Despite these findings, the present data suggest that different subnetworks within the DMN are flexibly engaged according to task demands. Positive coupling between the DFP/IC_7 and MP/IC_{26} is indicative that anticorrelation functional networks associated with the DMN and DAN is reflective of specific task demands, rather than an intrinsic property of functional organization.

FPC coupling with the DMN during retrieval

Recent studies have identified cooperative functional interactions between FPC networks and the DMN during internally directed tasks (Fornito et al., 2012), and the DAN during externally directed tasks (Spreng et al., 2010). These findings suggest a role for these networks in regulating the amount of internally and externally directed information used to guide behavior. Given the goal-directed nature of FR, the failure to observe increased activity within FPC networks is surprising. However, external stimuli often play an important role in the internally directed tasks used in prior studies, either indicating when subjects are required to make a response, or providing a cue stimulus to guide memory search. It is possible that FPC recruitment reflects cognitive control mechanisms required to mediate between external cue stimuli processed by the DAN, and internal/memorial representations of the DMN. Under such a framework, there would be no need for the FPC network to mediate DAN/DMN interactions in free recall, given the absence of task-relevant perceptual information during the recall period.

While we did not observe engagement of FPC networks during free-recall, the RPF/IC_{14} network functionally coupled with both the PM/IC_6 and MP/IC_{23} networks during memory search. These findings support theories of functional organization that propose goal-directed internally mediated cognition is supported through the integration of information between the DMN and FPC networks. We demonstrate a novel contribution of the PM/IC_6 network during the free-recall task, which functionally couples with DMN and FPC networks. Future studies can be used to infer the role of this network during memory search, possibly arbitrating between the retrieval of contextual information (Burgess et al., 2001), and the reconstruction of the encoding context under which the items were studied (Schacter et al., 2007). It will be critical to determine the degree to which recruitment of this network mediates retrieval during the FR task, or if it is epiphenomenal in nature.

Large-scale networks influence posterior parietal cortex activity during retrieval

The organization of resting state networks within posterior parietal cortex (PPC) has influenced theories of PPC function (Vincent et al., 2006, 2008). Specifically, functional coupling between inferior PPC and the medial temporal lobe has led to the development of theories purporting a variety of mnemonic roles for the angular gyrus. In the present data, the overall BOLD response in this region is dominated by two networks within the DMN, PC/IC_{23} and MP/IC_{26}, resulting in sustained decreases in activity during memory search. Furthermore, both IC and ROI based analyses failed to demonstrate transient increases in activity. These findings provide constraints for theories of the role of parietal cortex in memory retrieval.

Amongst theories of PPC function, the *Attention to Memory (AtoM)* account (Cabeza et al., 2008; Ciaramelli et al., 2008; Cabeza et al., 2011) explains retrieval-related activation within parietal cortex as a result of dissociable attention-based functions within dorsal and ventral parietal cortex. Activity within dorsal parietal cortex (ranging from the lateral bank of the intraparietal sulcus to superior parietal cortex) is proposed to support top-down attention engaged during memory search. By this framework, inferior parietal activity is thought to reflect bottom-up capture of attention by the recovery of mnemonically salient information. Under the assumptions of the *AtoM* model, the free-recall tasks should recruit dorsal parietal cortex during memory search (e.g., sustained during IRTs within the recall period), and ventral parietal cortex during the detection of retrieved content. Consistent with the *AtoM* model, regions within anterior inferior parietal cortex, within the supramarginal gyrus, exhibited transient increases in activity during successful recall, as compared to a speech control task. Conflicting with the *AtoM* account, we observed a different pattern of activity within posterior parietal cortex near the angular gyrus, which failed to demonstrate transient, detection-related activity. To account for this pattern of activity, we turn to alternative models of parietal lobe functions during episodic retrieval.

The output buffer hypothesis (Wagner et al., 2005) describes the role of the inferior parietal cortex (i.e., the angular gyrus) as supporting the online maintenance of recollected information. Expanding upon this theory, Vilberg and Rugg (Vilberg and Rugg, 2008) propose that the angular gyrus serves as the neural locus for the episodic buffer, supporting the online maintenance of multimodal representation of retrieved episodic information. This theory is supported by sustained activation in angular gyrus when retrieved content must be maintained over a delay (Vilberg and Rugg, 2012). The role of the angular gyrus may be akin to dorsal frontoparietal networks that support the maintenance of online information in working memory (Curtis and D'Esposito, 2003). Recent multivariate neuroimaging studies provide evidence suggesting that these networks play a role in the support of, but not the representation of information within working memory (Riggall and Postle, 2012). All functional networks including the angular gyrus demonstrate sustained deactivation during memory search; however, DMN networks (but not the PM network) exhibited marked increase in activity leading up to the recall period, consistent with the role of this network in maintenance of episodic content. While this interpretation is based upon reverse inference (under the assumption that increased angular gyrus activation reflects the maintenance of retrieved episodic information), this finding could be used to theoretically constrain mechanistic models of memory search.

Conclusions

In sum, we identified multiple large-scale functional networks that show modulation in activity during self-initiated memory search. We build upon recent neuroimaging findings implicating a role of the DMN and DAN in free recall (Shapira-Lichter et al., 2012, 2013). We extend these findings through the application of ICA, which fractionated the DMN into three components. While two of these components exhibited sustained decreases in activity during memory search, a network centered in posteromedial cortex exhibited sustained increases in activity. These findings highlight the heterogeneity of large-scale functional networks, capable of flexibly being recruited to accomplish task-specific goals. Despite their intrinsically competitive nature, the PM network and the DFP network exhibited task-dependent functional coupling to mediate retrieval during self-initiated memory search. Our findings propose a challenge to models suggesting an exclusively competitive nature between neural systems supporting episodic retrieval and external attention, and demonstrate the nuanced contributions of multiple large-scale networks modulated by the free recall task.

CHAPTER III

Decoding episodic retrieval processes: frontoparietal and medial temporal lobe contributions to free recall[2]

Abstract

Neuroimaging studies of recognition memory have identified distinct patterns of cortical activity associated with two sets of cognitive processes: Recollective processes supporting retrieval of information specifying a probe item's original source are associated with activation of the hippocampus, ventral posterior parietal cortex, and medial prefrontal cortex. Familiarity processes supporting the correct identification of previously studied probes (in the absence of a recollective response) are associated with activity in anterior medial temporal lobe (MTL), and lateral prefrontal and dorsal posterior parietal regions. Here, we address an open question in the cognitive neuroscientific literature: To what extent are these same neurocognitive processes engaged during an internally directed memory search task like free recall? We recorded functional magnetic resonance imaging (fMRI) activity while participants performed a series of free recall and source recognition trials, and used a combination of univariate and multivariate analysis techniques to compare neural activation profiles across the two tasks. Univariate analyses showed that posterior MTL regions were commonly associated with recollective processes during source recognition, and with free-recall responses. Prefrontal and posterior parietal regions were commonly associated with familiarity processes and free-recall responses, whereas anterior MTL regions were only associated with familiarity processes during recognition. In contrast with the univariate results, free-recall activity patterns characterized using multivariate pattern analysis did not reliably match the neural patterns associated with recollective processes. However, these free-recall patterns did reliably match patterns associated with familiarity processes, supporting theories of memory in which common cognitive mechanisms

---

[2] James E. Kragel and Sean M. Polyn. Decoding episodic retrieval processes: frontoparietal and medial temporal lobe contributions to free recall. *Submitted for publication*, 2015.

support both item recognition and free recall.

Introduction

In recognition tasks, two processes have been posited to support the correct determination that a particular memory probe was previously studied: episodic recollection, and item familiarity (Yonelinas, 2002). Episodic recollection provides conscious access to contextual information associated with prior experience; if a probe in a recognition memory task triggers retrieval of contextual information consistent with the target list, the participant can confidently endorse it as studied. In the absence of detailed contextual information, the item may still trigger a sense of familiarity allowing the participant to correctly identify it as something that was previously encountered. Recently, a number of behavioral studies have implicated both of these processes in free recall (McCabe et al., 2010; Mickes et al., 2013; Sadeh et al., 2014), demonstrating that while some free-recall responses are accompanied by specific contextual details, others responses lack this detail, but the participant still knows that the reported item is from the target list. While a great many neuroimaging studies have examined the neural circuitry associated with each of these processes in recognition tasks (e.g., Kahn et al. 2004; Johnson et al. 2009), only a handful of studies have characterized the neural circuitry engaged during free recall, and none of these have directly contrasted neural engagement between recall and recognition tasks. As such, there is a gap in our understanding of the neural basis of human memory: To what extent are the same neural processes engaged during recognition and free recall?

A large number of neuroimaging studies have used event-related fMRI to understand the mechanisms supporting episodic retrieval in the presence of a salient memory probe (for reviews, see Skinner and Fernandes 2007; Vilberg and Rugg 2008; Spaniol et al. 2009; Mitchell and Johnson 2009). In these studies, researchers have developed a number of standard contrasts to disentangle the neural signatures of different cognitive processes during recognition memory tasks (for a review, see Diana et al. 2007). In recognition experiments where the participant is explicitly asked to remember some source characteristic of a probe item, recollective processes have been identified by contrasting neural activity on trials where source was correctly recalled (often called *Source Hits*) with trials where the item was recognized as studied, but the source was incorrectly reported (often called *No Source Hits*). This contrast may identify cognitive processes involved in the retrieval of contextual information from the study event (Johnson et al., 2009; Danker and Anderson, 2010). As mentioned, these processes are central to cognitive models of recognition (Yonelinas, 2002), but are also fundamental to models of free recall (Howard and Kahana, 2002a; Sederberg et al., 2008; Polyn et al., 2009a), in which the contextual information retrieved during a particular recall event helps to guide the subsequent memory search. These models suggest that the cortical regions mediating episodic recollection should be commonly recruited across recognition and recall tasks.

In order to identify familiarity-related neural processes, researchers have contrasted activity for trials where the item was successfully recognized without recollection (the *No Source Hits* described above), with trials on which a novel lure was successfully detected (*Correct Rejections*, e.g., Wheeler and Buckner 2004). While this comparison should identify neural signals related to a mnemonic familiarity signal, other processes recruited during recognition may be reflected in this contrast (Wagner et al., 2005). For example, processes involved in determining whether the probe item was from the targeted temporal context (i.e., the study list) may also be identified (Mandler, 1980). In free recall, similar processes may be engaged to determine whether a remembered item is from the appropriate temporal context (Lohnas et al., in press). To the extent that both recognition and free-recall tasks rely on a verification process determining whether the retrieved information is from the appropriate temporal context, these networks should show common recruitment across tasks.

By comparing recollective and familiarity contrasts to one another, researchers have revealed a number of functional dissociations across multiple cortical systems, which have been taken as evidence that distinct neural mechanisms contribute to these processes during recognition tasks (Brown and Aggleton, 2001; Diana et al., 2007; Eichenbaum et al., 2007; Ranganath and Ritchey, 2012). The hippocampus (Eldridge et al., 2000; Ranganath et al., 2004) as well as cortico-hippocampal networks spanning prefrontal and posterior parietal cortex (Vilberg and Rugg, 2008;

Hayama et al., 2012; Okada et al., 2012) have been shown to be active selectively during episodic recollection. Familiarity, on the other hand, selectively engages the anterior MTL (Henson et al., 2003; Daselaar et al., 2006; Hayes et al., 2011). Additional dissociations have been observed across frontal and parietal cortices, with activity in the lateral intraparietal sulcus increasing with the perceived familiarity of a stimulus (Wagner et al., 2005; Cabeza et al., 2008; Hutchinson et al., 2012; Sestieri et al., 2014b), and activity in the angular gyrus reflecting recollection of prior experiential details (Hutchinson et al., 2012; Vilberg and Rugg, 2012).

Given its comprehensive spatial coverage of the brain, fMRI is well suited to characterize whether the processing mechanisms engaged during free recall are shared with, or distinct from, those engaged for recollection and familiarity (Mather et al., 2013). A similar approach was taken in recent work demonstrating shared engagement of neural circuits across both visual search and memory search tasks (Cabeza et al., 2011), and across recognition and cued-recall tasks (Hayama et al., 2012; Okada et al., 2012). While a number of recent studies have characterized the neural correlates of internally directed search during free recall (Long et al., 2010; Shapira-Lichter et al., 2012, 2013; Kragel and Polyn, 2015; Kragel et al., 2015), there have been no studies directly comparing free recall with recognition.

In much of the prior work comparing neural engagement across different tasks, univariate statistics have been employed to determine whether the same cortical regions reliably increase (or decrease) in activation for each of the tasks. While these conjunctive analyses provide a starting point for cross-task comparisons of neural engagement, they do not address whether the broader pattern of engagement and disengagement across multiple brain regions is preserved across tasks. Multivariate pattern analysis (MVPA; Norman et al. 2006) can be used to characterize the topography of neural responses both within and across brain regions, allowing one to ask whether the global pattern of brain response is similar for two independent contrasts, allowing one to make a stronger form of inference regarding the significance of overlapping activation (Peelen and Downing, 2007). MVPA has been used to compare topographic patterns of neural activity across experimental conditions in a number of cognitive domains, including task performance (Esterman et al., 2009), and subjective remembering (Rissman et al., 2010). Recent demonstrations of between-subject decoding show that MVPA can be used to determine whether patterns of neural activity (and the cognitive processes presumed to be reflected therein) are common across individuals (Haxby et al., 2011; Clithero et al., 2011).

In the present study, we employed a within-subject fMRI design to determine whether the cognitive processes supporting the retrieval of item and contextual information during a source recognition task also support retrieval during a free-recall task. During recognition, we identified neural activity associated with (1) the recollection of source information and (2) the recognition of a studied item in the absence of source retrieval. Using univariate convergence and multivariate decoding analyses, we compared this recognition-related brain activity to the brain activity recorded during free recall.

Materials and Methods

Participants

Twenty right-handed, native English speakers (12 female) with a mean age of 22.5 years ($SD = 3.8$ years) from the Vanderbilt University community participated in the study. Participants were compensated $20/hour, with the potential to earn up to $10 contingent on task performance. Informed consent was obtained in accordance with the Vanderbilt University Institutional Review Board.

Behavioral Methods

The experiment consisted of twelve fMRI runs across two sessions, with each run containing three phases of interest: study, retrieval, and control tasks (Fig. 5). During the study period, participants studied lists of 24 items. After each study list, participants performed either a free-recall test or a source recognition test. Each session included 3 free recall lists and 3 source recognition lists; the conditions were pseudorandomly ordered within each session. Stimulus presentation and recording of responses was implemented on a laptop using *PyEPL* (Geller et al., 2007).

During the study period, each presented word was studied with one of two semantic orienting

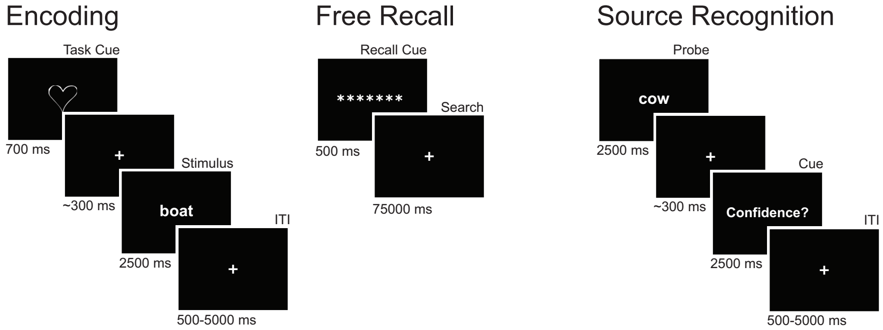

Figure 5. Experimental paradigm. A sample encoding trial is depicted in the left column, showing the task cue for the animacy judgment, followed by a sample stimulus. The middle column depicts the recall cue, which was paired with an auditory tone, that initiated the recall period. A sample source recognition trial is depicted in the right column, in which the subject must first judge whether the probe was encoded under the size task, animacy task, or was a novel lure. Following this period, subjects were cued to make a confidence rating of their previous response. ITI, inter-trial interval.

tasks. Within each list, participants were required to judge either the animacy or size of a stimulus presented on the screen (see Polyn et al. 2012 for details). Before each study item, a cue appeared on the screen for 700 ms in order to indicate which orienting task would apply to the upcoming stimulus. Presentation of a fixation cross followed the task cue for a duration of 300 ± 100 ms, followed by presentation of a study item for 2500 ms. A fixation cross was displayed following the presentation of each studied item for a duration ranging between 500 ms and 5000 ms. The order of encoding tasks was pseudorandomly determined, with the constraint that no task judgment was repeated more than 6 consecutive times, and each task was used for half of the items studied on each list.

During the source recognition portion of the task, participants were presented with lists of 32 stimuli, containing 16 targets (drawn evenly from both encoding tasks on the prior study list) and 16 novel lures. Probe stimuli were presented for a duration of 2500 ms, and participants indicated whether the probe stimulus was encoded using the size task, animacy task, or was a novel item. Following the presentation of a fixation cross (300 ± 100 ms), a cue was presented to indicate to the participant to make a confidence judgment on a 3 point scale. Presentation of this cue lasted for a duration of 2500 ms, followed by an inter trial interval of 500 ms to 5000 ms. All responses made during the encoding and source recognition period were made with the either the first, second, or third digits of the right hand, on a response pad. Button to response mappings were counter-balanced across trials, to control for confounding factors in response times.

During the beginning of the recall period, a recall cue was presented in the form of a row of asterisks displayed for a duration of 500 ms, concurrent with the presentation of an audio tone (800 Hz). Following presentation of the recall cue, participants recalled items studied on the previous list, in any order. Another tone and row of asterisks indicated the end of the 75 s recall period. Vocal responses were recorded using a scanner-safe microphone (Resonance Technologies, Inc.) and scored using *PyParse* (Solway et al., 2010) and *Penn TotalRecall* (http://memory.psych.upenn.edu/TotalRecall).

Following the retrieval phase of the task (either recognition or recall phases), subjects performed a speech control task. Words were presented in the same format as in the encoding period, for a duration of 2 s, followed by an inter-stimulus interval of 4 s. Participants read the presented word aloud, and responses were annotated following the procedures used in the recall period. Each participant performed 18 speech control trials, across the study.

fMRI Methods

Data collection and preprocessing

Images were collected on an Intera Achieva 3T system (Philips Medical System, Best, the Netherlands) at the Vanderbilt University Institute for Imaging Science. An MP-RAGE sequence was used to collect whole-brain structural scans (TR = 2500 msec, TE=4.38 msec, voxel size= 1.0x1.0x1.0mm, flip angle = 8^o, FOV=256 mm). Functional data were collected using an EPI pulse sequence (TR = 2000 msec, TE=30 msec, voxel size=3.0x3.0x3.6 mm, flip angle = 75^o, FOV=192 mm).

Data were processed using SPM8 (Wellcome, Department of Cognitive Neurology, http://www.fil.ion.ucl.ac.uk). Prior to preprocessing of functional images, the first four volumes of each run were discarded to allow for equilibration of scanner signal. Functional images were realigned to the first scan of each run, correcting for head motion. Mean functional images from each run were coregistered to structural images, allowing normalization to Montreal Neurological Institute

(MNI) stereotactic space using the unified segmentation based approach (Ashburner and Friston, 2005). Functional data were resampled to 3-mm cubic voxels and spatially smoothed with an 8-mm FWHM Gaussian kernel.

General linear modeling

The general linear model (GLM), as implemented in SPM8, was utilized to determine whether cortical regions associated with the processes of recollection or familiarity were engaged during memory retrieval in the free recall task. A single GLM was constructed, containing individual regressors to model recognition and recall trials. Trial types of interest during the source recognition task included retrieval of source information (Source Hits), item recognition in the absence of source recollection (No Source Hits), and identification of novel lures (Correct Rejections). Trials in which participants failed to detect novel lures (False Alarms) were additionally modeled; however, they were not used in second-level analyses. Two trial types of interest were used to identify changes in BOLD response associated with recall-related processing. One regressor was used to estimate transient, retrieval-related activity during recall period (Recalls), with an additional regressor used to estimate changes in the BOLD signal during the speech control task (Speech). Additional regressors were included to model neural activity during the encoding period. The neural response on each event of interest was modeled as a delta function coincident with the onset of each event (either stimulus presentation, or the onset of vocalization). The BOLD response for each event was modeled by convolving each series of delta functions with the canonical hemodynamic response function and its temporal derivative. A block regressor, of 75 s in duration, was included to model sustained differences in activity across the recall period. Six covariates were included in first-level models, corresponding to motion parameters corresponding to estimate movement in x, y, and z dimensions, as well as rotation, pitch, and yaw. An autoregressive AR(1) model was implemented to account for temporal autocorrelations in observed BOLD timeseries. Prior to parameter estimation, BOLD timeseries were high-pass filtered with a cutoff at 128 s in order to remove low-frequency components in the timeseries.

Following first level estimation of β coefficients, linear contrasts of interest were computed for each subject, resulting in a single image per trial type, per subject. Second level analyses were conducted using paired t-tests for each contrast of interest, corresponding to source recollection (Source Hits vs. No Source Hits), item familiarity (No Source Hits vs. Correct Rejections), and item recall (Recalls vs. Speech). Effects were considered significant if they survived an uncorrected voxelwise threshold of $p < 0.001$ and an extent threshold, k, of at least 38 voxels. This cluster extent threshold was determined based on Monte-Carlo analysis of statistical maps, using 3dclustsim in AFNI (http://afni.nimh.nih.gov/pub/dist/doc/program_help/3dClustSim.html) and resulted in a cluster-level $\alpha = 0.05$, corrected for multiple comparisons across the whole brain. Statistical maps depicting the overlap between processes of interest were constructed by inclusively masking the item recall t-map with either the recollection or familiarity-based maps.

Multivariate pattern analyses

Two separate applications of MVPA were implemented, using patterns of activity across either the whole brain, or within functionally defined regions of interest (ROIs), defined by the overlapping neural regions identified in the previously described univariate convergence analysis. Regardless of the features used for analysis, each subject's mean response for conditions of interest (i.e., the contrast images resulting from the first level analysis) were converted into z-scores (i.e., standardized across voxels), and used as features for classifier training and evaluation. We then used LIBSVM software, implemented in MATLAB (http://www.csie.ntu.edu.tw/~cjlin/libsvm) to implement a linear support vector machine (SVM). Parameterization of the SVMs was determined using a 2-fold, nested cross-validation approach (Pereira et al., 2009; Mumford et al., 2012), determining the value of the regularization parameter, C, of each classifier. Following parameterization, a leave-one-out cross-validation approach was used to evaluate classifier performance, training on patterns of neural activity from all but one subject, and evaluating classifier performance on the remaining subject's patterns.

Significance of classifier performance was determined using a one-tailed binomial test (Pereira et al., 2009), determining the probability that the observed predictions were generated by chance (assuming the probability of predicting either class was 0.5). While this statistical models assumes that test cases are independent of one another, and can lead to false positive under circumstances where this is not the case (Stelzer et al., 2013), folds of our cross validation procedure are implemented across subject, and as such are unlikely to be dependent upon one another. Whole-brain classification results were considered significant at $p < 0.05$, uncorrected, while models using functionally defined ROIs for feature selection were considered significant after surviving a threshold of $p < 0.05$, Bonferroni corrected for the number of ROIs in each test.

In addition to these classifier-based analyses, follow-up multivariate analysis was implemented on functionally defined ROIs using a pattern similarity approach (Kriegeskorte et al., 2008). The similarity of each subjects estimated activation between item recall (Recalls vs. Speech) and both source recollection (Source Hits vs. No Source Hits) and item familiarity (No Source Hits vs. Correct Rejections) was computed using Pearsons linear correlation coefficient. Correlation coefficients were normalized using a Fisher transformation, and significant group effects were tested using a one-sample t test, with a statistical threshold $p < 0.05$, Bonferroni corrected for the number of functional ROIs.

Results

Behavioral results

Source recognition

During the recognition test, subjects were sensitive to the mnemonic status of the probe, with a d$'$ of 3.44 ± 0.18 ($mean \pm SEM$). Table 3 describes the observed relationship between confidence ratings and recognition performance, showing higher confidence for correct source judgments than incorrect judgments. Hit rates for trials endorsed with low confidence were significantly lower than trials endorsed with medium ($t_{17} = -2.84$, $p = 0.011$) and high ($t_{17} = -3.60$, $p = 0.002$) confidence. Correct rejection rates also varied depending upon the associated confidence response, with paired t-tests revealing significant differences in correct rejection rate between low and

Table 3. Response proportions and response times (RT, in msec) during the source recognition task.

		Proportion (*SEM*)			RT (*SEM*)		
Response	Confidence	Size	Animacy	Novel	Size	Animacy	Novel
Size	Low	1.13 (1.64)	6.65 (6.83)	1.56 (2.47)	1569 (230)	1546 (384)	1768 (377)
	Medium	13.26 (8.31)	14.78 (9.21)	1.51 (3.96)	1534 (313)	1616 (316)	1740 (238)
	High	68.97 (15.23)	6.92 (8.81)	0.52 (0.79)	1338 (313)	1482 (325)	1487 (458)
Animacy	Low	3.96 (3.58)	3.74 (5.73)	1.20 (2.30)	1579 (350)	1711 (347)	1625 (426)
	Medium	4.86 (4.60)	13.02 (7.39)	0.21 (0.54)	1630 (372)	1633 (350)	1882 (247)
	High	2.56 (2.29)	46.38 (15.97)	0.42 (0.71)	1596 (370)	1359 (332)	1155 (224)
Novel	Low	2.66 (3.19)	2.71 (3.58)	1.98 (4.30)	1415 (419)	1423 (452)	1334 (403)
	Medium	0.81 (1.54)	1.70 (1.90)	10.21 (14.68)	1681 (381)	1703 (336)	1276 (359)
	High	1.26 (2.08)	3.19 (3.10)	81.15 (22.36)	1148 (443)	1193 (376)	1015 (277)

medium ($t_{11} = -5.93$, $p = 0.0001$), low and high ($t_{13} = -8.05$, $p < 0.0001$), and medium and high ($t_{15} = -2.25$, $p = 0.039$) confidence judgments.

Subjects performed above chance levels on source judgments of items endorsed as old, with a proportion correct of 0.73 ± 0.02 ($t_{19} = 9.99$, $p < 0.0001$). Hit rates on source correct trials were greater than on trials in which subjects failed to recover the source of the encoded item ($t_{19} = 12.89$, $p < 0.0001$), demonstrating that retrieval of source information influenced both recognition and confidence judgments. Furthermore, source judgments were more accurate during high relative to medium confidence decisions ($t_{19} = 9.51$, $p < 0.0001$). Low-confidence decisions were associated with impaired source recognition when compared with medium ($t_{17} = -5.68$, $p < 0.0001$) and high ($t_{17} = -13.44$, $p < 0.0001$) confidence responses.

Free recall

On average, subjects recalled $42 \pm 0.03\%$ ($mean \pm SEM$) of the studied items. Primacy and recency effects were observed as an advantage in recall for the first three ($t_{19} = 5.31, p < 0.0001$) and last three ($t_{19} = 5.91, p < 0.0001$) serial positions. Additional behavioral analysis of the recall data collected in this experiment is described in previous work (Polyn et al., 2012).

fMRI results

Univariate analyses

In order to investigate whether the neural substrates that support item familiarity and source recollection during recognition tasks are recruited during free recall, we employed a series of GLM-based analyses that allowed us to make forward inferences (Henson, 2006) regarding the cognitive processes that support episodic retrieval. First, we determined which regions were associated with item familiarity in the absence of source recollection (i.e., No Source Hits vs. Correct Rejections). Next, we identified regions where activity was associated with source recollection (i.e., Source Hits vs. No Source Hits). Finally, we implemented a convergence analysis to ask whether any regions related to item familiarity or source recollection were also engaged for retrieval during free recall. For this, we identified regions associated with correct retrievals during memory search (i.e., Recalls vs. Speech).

Figure 6a depicts cortical regions that were sensitive to item familiarity. Increased activity during the detection of previously studied items, in the absence of a correct source judgment, was observed within widespread cortical regions, including lateral and medial parietal cortex, fronto-opercular cortex, and dorsal anterior cingulate. Detection of novel items was accompanied by increased activity within bilateral anterior MTL regions, including hippocampus, amygdala, and surrounding rhinal cortex. Additional regions identified by this contrast include mid-occipital gyrus, and lateral temporal regions, as described in Table 4.

Next, we conducted a univariate analysis to identify cortical regions that were sensitive to source recollection during the recognition task. As shown in Figure 6b, this contrast identified activation within bilateral hippocampal regions that was sensitive to the retrieval of source information. Relative to correct source judgments, incorrect source judgments demonstrated greater levels of activity within dorsal anterior cingulate regions and multiple left-lateralized prefrontal regions, spanning both dorsal and ventral prefrontal cortex (see Table 5 for details).

Finally, we used a convergence analysis to determine whether cortical regions associated with either source recollection or item familiarity (in the absence of the retrieval of criterial source

Table 4. Item familiarity sensitive regions.

Contrast	Gyrus (Hemisphere)	BA	*k*	Coordinates (x,y,z)	*t*
No Source Hit > Correct Rejection	Precuneus (L)	7	1472	-6,-70,43	11.81
	Inferior Parietal Lobule (L)	40		-45,-31,40	5.72
	Claustrum (L)		2662	-30,23,-5	11.62
	Medial Frontal Gyrus (L)	6		-6,23,43	10.81
	Middle Frontal Gyrus (L)	9		-48,23,28	10.07
	Superior Frontal Gyrus (R)	6		24,14,64	4.90
	Superior Frontal Gyrus (L)	6		-27,2,70	4.18
	Insula (R)		145	36,23,-5	7.99
	Caudate (R)		51	12,5,-2	6.95
	Thalamus (L)		225	-9,-13,1	6.79
	Posterior Cingulate (L)	23	88	-6,-34,25	6.34
	Inferior Parietal Lobule (R)	40	194	36,-46,46	5.80
	Middle Frontal Gyrus (R)	6	48	27,-1,52	5.06
	Middle Frontal Gyrus (R)	9	102	42,29,28	4.60
Correct Rejection > No Source Hit	Fusiform Gyrus (R)	37	7372	45,-43,-17	10.34
	Parahippocampal Gyrus (L)	19		-42,-43,-8	8.89
	Cuneus (L)	30		-27,-76,10	7.86
	Parahippocampal Gyrus (L)			-21,-4,-23	7.64
	Insula (R)	13		36,-1,13	7.60
	Superior Temporal Gyrus (L)	22		-54,-10,4	7.34
	Caudate (L)			-18,20,10	7.30
	Parahippocampal Gyrus (R)	34		24,-1,-20	6.91
	Middle Temporal Gyrus (R)	21		60,-7,-23	6.80
	Postcentral Gyrus (R)	3	1190	33,-25,46	6.67
	Sub-Gyral (L)	7		-21,-40,58	6.08
	Middle Frontal Gyrus (R)	8	45	30,35,37	5.10

Note: BA = Brodmann area; L = left; R = right. *k* = cluster extent, in voxels. Brodmann areas and anatomical locations are approximate. Coordinates are given in MNI space.

Table 5. Source recollection sensitive regions.

Contrast	Gyrus (Hemisphere)	BA	*k*	Coordinates (x,y,z)	*t*
Source Hit > No Source Hit	Insula (L)	13	220	-30,2,19	6.22
	Parahippocampal Gyrus (L)	37	182	-33,-46,-8	6.21
	Lentiform Nucleus (R)		257	27,2,1	6.13
	Postcentral Gyrus (R)	3		33,-25,46	5.19
	Caudate (L)		65	-18,26,10	5.77
	Subcallosal Gyrus (R)	34	583	18,8,-20	5.68
	Fusiform Gyrus (R)	20		33,-37,-17	5.39
	Parahippocampal Gyrus (L)			-27,-16,-17	5.01
	Superior Occipital Gyrus (R)	19	145	36,-79,34	5.32
	Middle Temporal Gyrus (R)	39		48,-55,7	4.55
	Paracentral Lobule (L)	7	40	-18,-40,55	4.70
No Source Hit > Source Hit	Cingulate Gyrus (R)	32	496	3,29,31	6.49
	Superior Frontal Gyrus (R)	6		24,17,67	5.18
	Sub-Gyral (L)	6		-24,11,52	4.62
	Middle Frontal Gyrus (L)	9	53	-36,26,25	5.64
	Precentral Gyrus (L)	44	266	-45,20,1	5.41
	Middle Frontal Gyrus (L)	9		-54,11,37	4.47

Note: BA = Brodmann area; L = left; R = right. *k* = cluster extent, in voxels. Brodmann areas and anatomical locations are approximate. Coordinates are given in MNI space.

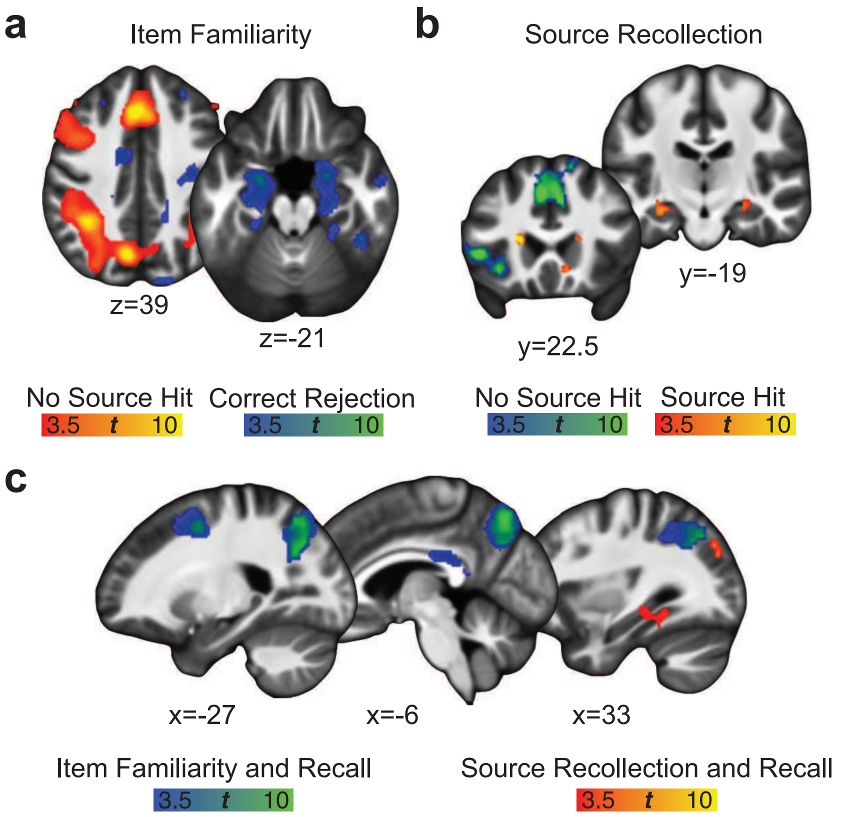

Figure 6. Overlapping neural substrates during source recognition and free recall. Differences in activity between (a) hits in the absence of source recollection and correct rejections, and (b) hits with and without source recollection. (c) Convergence analysis of free recall and source recognition effects. The statistical map for Recall $>$ Speech is displayed, in regions exhibiting either item recognition or source recollection effects. Statistical maps are rendered on the group-mean T1 anatomical image, with a cluster-wise threshold of $p < 0.05$ corrected for the whole brain volume. Slices are labeled with their corresponding MNI coordinates.

information) during the source recognition task overlapped with retrieval-sensitive regions identified during the free-recall task. Using strict individual thresholds of $p < 0.001$, we ensured that the observed cortical regions demonstrate both effects. We observed overlapping activity for free recall and source recollection effects within the right posterior hippocampus and adjacent parahippocampal cortex. Overlapping item familiarity and free-recall activity was observed in multiple prefrontal and parietal regions as shown in Figure 6c (see Table 6 for details). We did not observe overlapping free recall and item familiarity related activity within the MTL.

Table 6. Regions demonstrating overlapping source recollection and item familiarity effects during free recall.

Contrast	Gyrus (Hemisphere)	BA	*k*	Coordinates (x,y,z)	*t*
Recall & Source Recollection	Middle Occipital Gyrus (R)	19	55	33,-79,28	9.49
	Anterior Cingulate (R)	25	90	9,20,-11	7.69
	Fusiform Gyrus (L)	37	38	-45,-43,-20	6.49
	Parahippocampal Gyrus (R)	19	70	42,-49,-8	6.40
Recall & Item Familiarity	Precuneus (R)	7	1195	18,-67,49	10.00
	Precuneus (L)	7		-24,-70,49	9.12
	Inferior Parietal Lobule (L)	40		-45,-28,46	8.45
	Precuneus (R)	19	178	30,-70,40	9.04
	Inferior Parietal Lobule (R)	40		45,-34,46	3.88
	Middle Frontal Gyrus (L)	6	426	-24,-1,46	8.00
	Middle Frontal Gyrus (L)	9		-54,23,34	4.59
	Posterior Cingulate (R)	23	83	6,-31,22	6.08
	Middle Frontal Gyrus (R)	9	74	45,32,19	5.65
	Middle Frontal Gyrus (R)	6	41	27,2,49	5.52

Note: BA = Brodmann area; L = left; R = right. *k* = cluster extent, in voxels. Brodmann areas and anatomical locations are approximate. *t*-values are reported for each peak from the item recall (Recalls vs. Speech) contrast. Coordinates are given in MNI space.

Multivariate decoding reveals cognitive processes engaged during free recall

The preceding GLM-based analyses identified shared neural substrates of item familiarity and source recollection that were engaged during the free recall task. To formally test the degree to which patterns of neural activity evoked during free recall match those present during source recollection or item recognition, we employed a multivariate decoding analysis. We created two classifiers, one trained to differentiate between patterns of neural activity associated with source recollection (i.e., distinguishing Source Hits vs. No Source Hits), and another trained to discriminate between whole-brain patterns of activity associated with item familiarity (i.e., No Source Hits vs. Correct Rejections). First, we used a cross-validation technique to evaluate whether each classifier was able to reliably distinguish the two classes of training patterns, on an across-subject basis. Then, we presented each trained classifier with the patterns of activity associated with item retrieval during free recall. As such, the source recollection classifier was used to estimate whether these free-recall patterns were more similar to successful, or unsuccessful source retrieval. Similarly, the item familiarity classifier was used to estimate whether the free-recall patterns were more similar to detection of a studied item, or detection of a lure item.

The across-subject cross-validation test revealed that the item-familiarity classifier reliably able to distinguish successful recognition of a target (without source recollection) from successful rejection of a novel lure ($accuracy = 0.93$, $p < 0.0001$, 95% CI [0.88 0.96]). These high levels of performance were obtained for both classes: item recognition without source details ($sensitivity = 0.95$, $p < 0.0001$, 95% CI [0.87 0.99]) and detection of novel lures ($sensitivity = 0.90$, $p < 0.0001$, 95% CI [0.81 0.95]). Figure 7a shows the average linear SVM weights across the twenty cross-validation folds, with increased activation of left dorsolateral prefrontal cortex, precuneus, and lateral parietal cortex reflecting detection of a previously encountered memory probe, while increased activity in visual and anterior MTL regions was associated with probe novelty, consistent with the univariate findings depicted in Figure 6a.

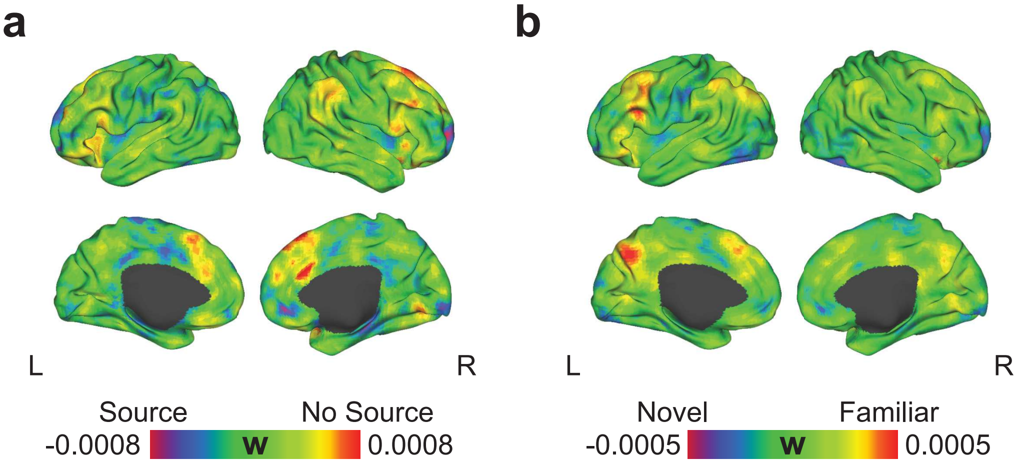

Figure 7. Patterns of neural activity reflect retrieval processes. Support vector machine weights discriminating (a) item novelty and (b) source recollection during the source recognition task. For visualization, images were transformed to Colin atlas space and rendered onto inflated cortical surfaces (Van Essen, 2002). L, left; R right.

In order to determine whether retrieval during the free-recall task recruits the same cognitive processes reflected in the item familiarity contrast, we used the trained item familiarity classifier to decode patterns of activity associated with free recall. When patterns of whole-brain activity from the free-recall task were used as inputs to the item familiarity classifier, the classifier reliably identified these patterns as reflecting correct old ($P(No\ Source\ Hit) = 0.85$, $p = 0.0002$, 95% CI [0.76 0.91]) rather than novel ($P(Correct\ Rejection) = 0.15$, $p = 0.99$, 95% CI [0.09 0.24]) judgments. In other words, the global topographic pattern of activity associated with free recall of a studied item is quite similar to the pattern of activity associated with successful detection of a studied item in our recognition task. Thus, the neural substrates associated with familiarity-based item recognition are also associated with successful retrieval during memory search.

We carried out a follow-up analysis to examine whether the similarity between neural patterns in item familiarity and free recall was observed in each of the functionally defined regions of interest (ROIs) identified in the univariate conjunction analysis described above. For this analysis, the clusters described in Table 6 were used to select features for a set of regional multivariate decoding analyses. Of these 6 clusters, only two allowed a classifier to successfully discriminate No Source Hits from Correct Rejections for the across-subject cross-validation: one cluster in left-lateralized posterior parietal cortex ($accuracy = 0.70$, $p = 0.0023$, 95% CI [0.53 0.83]), and another in left prefrontal cortex ($accuracy = 0.78$, $p < 0.0001$, 95% CI [0.62 0.89]). As with the whole-brain analysis, each of these trained classifiers reliably classified the free-recall patterns as similar to the patterns corresponding to correct item recognition in the absence of source retrieval (left posterior parietal cortex: $P(No\ Source\ Hit) = 0.9$, $p < 0.0001$, 95% CI [0.68 0.99]; left prefrontal cortex: $P(No\ Source\ Hit) = 0.95$, $p < 0.0001$, 95% CI [0.75 0.99]). The item familiarity classifiers constructed from the other 4 ROIs did not perform above chance ($ps > 0.24$).

A separate classification analysis was carried out to examine patterns of neural activity associated with the recollection of source information during recognition. A whole-brain source recollection classifier was able to reliably predict whether patterns of activity reflected the presence or absence of source details during the recognition task ($accuracy = 0.80$, $p < 0.0001$, 95% CI [0.74 0.85]), on an across-subject cross-validation test. Overall classifier performance was above chance for both correct source judgments ($sensitivity = 0.90$, $p < 0.0001$, 95% CI [0.81 0.95]) and incorrect source judgments ($sensitivity = 0.70$, $p = 0.021$, 95% CI [0.60 0.78]). Figure 7b shows the weights from this classifier, identifying regions that contribute to the classification. Consistent with the observed univariate effects, increased activity within the MTL, including right posterior hippocampus and ventromedial prefrontal cortex, informed the classifier of the recollection of source details. In contrast, increased activity within ventrolateral prefrontal cortex, dorsal anterior cingulate, and ventral parietal cortex, signaled item recognition in the absence of source recollection.

In contrast with our item familiarity analysis, when the trained source recollection classifier was presented with free-recall activity patterns, it did not reliably classify them as similar to the set of correct source recall patterns, or the set of incorrect source recall patterns ($P(Source\ Hit) = 0.4$, $p = 0.75$, 95% CI [0.31 0.50]) or item familiarity ($P(No\ Source\ Hit) = 0.6$, $p = 0.13$, 95% CI [0.50 0.69]). These results suggest that at the level of the whole-brain, distinct neural circuits are engaged for successful retrieval during free recall, and for source recollection during a recognition task.

This result stands in contrast to our observation of overlapping neural engagement in these two tasks in our univariate conjunction analysis (Figure 6c), and suggests that despite this common engagement, there is mismatch between the broader topographic patterns associated with these two processes. In order to determine whether any of the subregions identified with the univariate convergence analysis exhibited distributed representations that matched across tasks, we constructed 4 additional classifiers from the clusters specified in Table 6. However, none of these 4 classifiers were reliably able to distinguish patterns corresponding to correct source retrieval from those corresponding to incorrect source retrieval, in the across-subject cross-validation analysis ($ps > 0.54$). This suggests that there was substantial variability in patterns of activity related to source recollection across subjects. Given the failure of the regional classifiers, we carried out a representational similarity analysis to determine whether there was any evidence for similarity between the free-recall patterns and source recollection patterns. We computed the similarity (Pearson's linear correlation coefficient) between the patterns of activity estimated from the source recollection and item recall contrasts, within each ROI. None of the regions exhibited consistent patterns of activity across free recall and source recognition ($rs < 0.047$, $ps > 0.20$). These findings further confirm that while some cortical regions demonstrate shared recruitment across source recognition and free-recall tasks

(Figure 6c), the patterns of activity within these regions are different for the two tasks.

Discussion

We used fMRI to determine whether free recall and source recognition tasks rely on common neurocognitive mechanisms, specifically testing whether item familiarity and source recollection processes commonly associated with recognition-based tasks are recruited during free recall. Within the MTL, univariate tests revealed overlapping free recall and source recollection engagement in the right posterior hippocampus and parahippocampal cortex. More broadly, there was overlap between free recall and familiarity effects within prefrontal and parietal cortex, including precuneus, the lateral bank of the intraparietal sulcus, dorsolateral prefrontal cortex, and fronto-opercular regions. The results of this univariate conjunction analysis suggest that both familiarity and recollective processes are engaged during free recall. However, this analysis is sensitive only to overlapping activation between the tasks. In order to determine whether the broader pattern of neural activity elicited by recollective and familiarity-based processes matched that seen during free recall, we carried out a multivariate pattern classification analysis.

The multivariate analysis demonstrated that whole-brain activity could be used to discriminate correct from incorrect source retrieval, and correct recognition (in the absence of source retrieval) from correct detection of a novel lure. Inspection of the classifier weights confirmed that the recollection discrimination was influenced by activity within the hippocampus and regions comprising the putative recollection network (Hayama et al., 2012). The familiarity discrimination was influenced by activity in a distributed frontoparietal network, encompassing posterior parietal cortex and multiple prefrontal regions (Figure 7a). These trained classifiers were then presented with images drawn from the free recall period. While the recollective classifier was agnostic as to whether the free-recall patterns were more similar to successful or unsuccessful source recollection, the familiarity classifier reliably classified the free-recall patterns as similar to brain patterns in which probe items were correctly identified as studied (in the absence of source recollection). This suggests that the neural substrates supporting familiarity-based retrieval are also recruited during successful retrieval in free recall.

In a number of recent behavioral studies, researchers have examined the potential for familiarity-based processing during memory search in free recall. During the recall period, participants in these experiments indicated for each recall event whether they explicitly remembered studying the reported item (indicating retrieval of contextual information), or whether they simply knew it was from the study list (indicating that the judgment was made in the absence of recollective information; McCabe et al., 2010; Mickes et al., 2013; Sadeh et al., 2014). Participants endorse many recalled items as simply "known," suggesting that item familiarity-related processes may be engaged during free recall. While these studies do not reveal the specific processes engaged in common across recall and recognition, decades of theoretical work in psychology and cognitive neuroscience present a number of possibilities, as we will review below.

A number of theories of MTL organization propose that anterior MTL is centrally involved in processing stimulus familiarity (Norman and O'Reilly, 2003; Diana et al., 2007; Ranganath, 2010; Yonelinas et al., 2010). These theories are supported by neuroimaging work showing that this region is more active for novel lures than for studied items during a recognition test (Henson et al., 2003; Daselaar et al., 2006; Tendolkar et al., 2008; Hayes et al., 2011), a finding replicated in the current study. Convergent evidence showing novelty signals in the anterior MTL of rodents (Brown and Aggleton, 2001), and non-human primates (Brown and Xiang, 1998) supports these theories. Consistent with these prior studies, we observed a signal in anterior MTL indicating stimulus novelty (i.e., greater for novel lures than studied items) during the source recognition task. However, this region did not show differential activity between successful retrieval in free recall and our speech control task. Rather, our analyses indicated that it was regions outside the MTL that showed similar activation profiles between the two tasks.

Specifically, we found that frontal and parietal regions showed similar activation patterns between the item familiarity contrast and the free-recall contrast, suggesting that similar cognitive processes are engaged in both tasks. These regions have been implicated in a number of cognitive functions that could be engaged during free recall, such as the accumulation of mnemonic information (Wagner et al., 2005), monitoring of retrieved information (Dobbins et al., 2004; Rugg, 2004), and biasing of attention to internal representations (Cabeza et al., 2008). A recent study by Hutchinson et al. (2015) suggests that during uncertain mnemonic decisions, dorsal parietal cortex resolves mnemonic uncertainty via enhanced functional coupling with visual word-form regions involved in representing the mnemonic probe. Given recent evidence that activation of networks anchored in dorsal parietal cortex exhibit increased functional connectivity with posterior midline structures, including the hippocampus and retrosplenial complex during free recall (Shirer et al., 2012; Kragel and Polyn, 2015), it is possible that interactions between these regions reflect attentional processes that influence an internally-generated retrieval cue within the MTL.

In addition to dorsal parietal cortex, we observed overlapping activity patterns across tasks within bilateral regions of the inferior parietal lobe, along the lateral bank of the intraparietal sulcus. Posterior parietal cortex has been hypothesized to be involved in the accumulation of mnemonic evidence required to make a judgment of oldness Wagner et al. (2005); Donaldson et al. (2010). Activity within lateral intraparietal sulcus seems to be sensitive to gradations in item memory strength Hutchinson et al. (2012, 2015). Additionally, lesions within the vicinity of this region have been shown to impair the sense of vividness, or perceived oldness, of mnemonic information (Hower et al., 2014). This type of judgment process appears in a number of theories of recall (Anderson and Bower, 1972; Mandler, 1980; Brainerd et al., 2002), wherein judgments of familiarity are a critical component of both recall and recognition based tasks. A recent model of free recall suggests that a similar process is necessary to decide whether a remembered item comes from the appropriate context (Lohnas et al., in press). These observations raise the intriguing possibility that neural circuitry in lateral parietal cortex subserves evidence accumulation for perceived oldness of active mnemonic representations in a task-general fashion. Neurally constrained computational models of retrieval behavior (e.g., Kragel et al., 2015; Turner et al., in press) provide an ideal framework for future work assessing whether activity in this region is consistent with this computational mechanism.

The evidence regarding functional overlap between source recollection and free recall was mixed. We observed a region within the posterior MTL (spanning right hippocampus and parahippocampal cortex) that was identified in both source recollection and free-recall contrasts. This overlapping activity is consistent with the idea that activity within the MTL reflects the reinstatement of contextual information during free recall (Manning et al., 2011; Kragel et al., 2015) as well as during recognition (Howard et al., 2012; Hsieh et al., 2014). The Complementary Learning Systems model (McClelland et al., 1995; Norman and O'Reilly, 2003) provides a potential computational mechanism for these regions, in the form of pattern completion. Hasselmo and Wyble (1997) describe a computational model of the hippocampal system that utilizes a similar mechanism and accounts for both recognition and recall performance in humans, as well as the effects of neuropharmacological disruption of the system. According to this model, the hippocampus allows for both the retrieval of contextual details during recognition, and the retrieval of items given contextual input received via afferent projections from the parahippocampal gyrus during recall. In the Remember/Know free-recall paradigm reported by Mickes et al. (2013), "remember" responses could indicate hippocampally mediated retrieval of contextual information, and "know" responses could indicate that only item-specific information was retrieved (supporting the knowledge that the item was studied, but not providing any extra details regarding the prior occurrence).

Our finding that distributed patterns of neural activity associated with source recollection did not match those associated with free recall may appear somewhat counterintuitive, given overwhelming evidence that the recollection of episodic information (i.e., contextual retrieval) guides free-recall behavior from both computational (Howard and Kahana, 2002a; Sederberg et al., 2008; Polyn et al., 2009a) and neuroimaging (Manning et al., 2011; Shapira-Lichter et al., 2012; Howard et al., 2012; Kragel et al., 2015) perspectives. There are a number of differences between the tasks that may account for these distinct patterns of functional engagement. One obvious difference regards the nature of the retrieval cue, which is externally presented during recognition, but is internally generated during free recall. Recollection during free recall may predominantly require interactions between the default mode network (Buckner et al., 2008), specifically the posterior medial network (Ranganath and Ritchey, 2012), and the hippocampus. However, recollection during source recognition is more likely to be driven by interactions between representations of the memory probe within perceptual regions and the hippocampus.

A second relevant difference between the two tasks regards the nature of the information being retrieved during source recognition and free recall. In the case of source recollection, the participant must retrieve episodic details specifying the encoding task used to process the studied word, whereas in free recall, the participant simply reports the words themselves. While prior work suggests that source details are retrieved during free recall (Polyn et al., 2009a,b, 2012), they are not as important for performance as the successful utilization and retrieval of temporal context, which ensures that the responses all come from the target list (Howard and Kahana, 2002a; Lohnas et al., in press). In contrast, the determination that an item is familiar is more likely to involve retrieval of temporal context; in the absence of source recollection, retrieved temporal information will indicate whether the probe item came from the temporal context of the most recent list.

Conclusion

Using a within-subject design, we demonstrated that neural substrates of source recollection and item familiarity are engaged during performance of the free-recall task. Successful retrieval of an item during free recall engaged posterior MTL regions that were also engaged for source retrieval, as well as posterior parietal and lateral prefrontal regions associated with successful item recognition in the absence of source recollection. In contrast to these univariate findings, multivariate decoding analyses suggest that familiarity-related processes, but not source recollective processes, were engaged during free recall. These results may be challenging for neurocognitive theories proposing that free recall is supported by the same recollective processes underlying item recognition, but that only recognition is supported by familiarity processes (Yonelinas, 2002; Quamme, 2004; Wixted and Squire, 2010). Finally, the observation that prefrontal and posterior parietal regions showed shared engagement for free recall and for the determination of item familiarity may help us understand the cognitive role of these structures across memory tasks.

CHAPTER IV

Neural activity in the medial temporal lobe reveals the fidelity of mental time travel[3]

Abstract

Neural circuitry in the medial temporal lobe (MTL) is critically involved in mental time travel, which involves the vivid retrieval of the details of past experience. Neuroscientific theories propose that the MTL supports memory of the past by retrieving previously encoded episodic information, as well as by reactivating a temporal code specifying the position of a particular event within an episode. However, the neural computations supporting these abilities are underspecified. To test hypotheses regarding the computational mechanisms supported by different MTL subregions during mental time travel, we developed a computational model that linked a blood oxygenation level-dependent signal to cognitive operations, allowing us to predict human performance in a memory search task. Activity in the posterior MTL, including parahippocampal cortex, reflected how strongly one reactivates the temporal context of a retrieved memory, allowing the model to predict whether the next memory will correspond to a nearby moment in the study episode. A signal in the anterior MTL, including perirhinal cortex, indicated the successful retrieval of list items, without providing information regarding temporal organization. A hippocampal signal reflected both processes, consistent with theories that this region binds item and context information together to form episodic memories. These findings provide evidence for modern theories that describe complementary roles of the hippocampus and surrounding parahippocampal and perirhinal cortices during the retrieval of episodic memories, shaping how humans revisit the past.

Introduction

The capabilities of the human memory system rival any internet search engine in terms of the flexibility and specificity of search. With a moment of thought, one can search through memories of

---

[3] James E. Kragel, Neal W Morton, and Sean M. Polyn. Neural Activity in the Medial Temporal Lobe Reveals the Fidelity of Mental Time Travel. *The Journal of Neuroscience*, 35(7):2914–2926, February 2015.

the recent or distant past, retrieving a particular memory from many thousands. The memories one retrieves during search vary in fidelity. When a memory emerges rich in detail regarding the time and place of its original occurrence, the strong subjective sense that one is revisiting past experience inspired Endel Tulving to call this phenomenon *mental time travel* (Tulving, 1993).

Brain structures in the medial temporal lobe (MTL) are critically involved in the retrieval of memories of one's past experience, i.e., episodic memories (Milner et al., 1998). Distinct subregions of MTL cortex have distinct functional properties. Perirhinal cortex, which is located on the anterior portion of the parahippocampal gyrus (PHG), becomes active during retrieval of objects and their features (Davachi et al., 2003; Haskins et al., 2008; Staresina and Davachi, 2010). In contrast, parahippocampal cortex, on the posterior extent of the PHG, is engaged during processing of scene context (Hayes et al., 2007; Litman et al., 2009), spatial attributes (Burgess et al., 2002), and nonspatial contextual attributes (Aminoff et al., 2007; Bar et al., 2008). Activity in this region is also sensitive to the temporal context in which a visual scene is presented (Turk-Browne et al., 2012). One view of MTL function (Diana et al., 2007) describes parahippocampal cortex as encoding and retrieving contextual information, while perirhinal cortex mediates item-specific processing (c.f., Davachi, 2006; Mayes et al., 2007; Wixted and Squire, 2011). Both item and contextual information are thought to converge in hippocampus, allowing this region to represent objects in a specific temporal sequence (Hsieh et al., 2014), and support temporal memory (Ezzyat and Davachi, 2014).

While these theories outline the functional properties of the MTL, they do not specify the cognitive operations underlying neural signals from these brain regions, nor do they describe how these signals relate to memory search. Retrieved-context models (Howard and Kahana, 2002a; Polyn and Kahana, 2008) describe memory search in terms of two interacting cognitive processes: temporal reinstatement and item retrieval. Temporal reinstatement underlies mental time travel: When a particular studied item is remembered, the memory system reactivates a temporal code specifying when the study event occurred relative to other events in the episode. Reactivation of a high-fidelity code makes memories that were formed near that point in time more accessible. The temporal reinstatement operation is followed by a recall competition, to determine which memories will be retrieved. A successful competition yields a remembered item, while a failed competition leads to termination of memory search.

To test whether subregions of the MTL are involved in these cognitive operations, we developed a set of neurally informed models of memory search. These models were designed to predict the sequence of recalls made by a participant in a free recall task, while neural signal was measured using functional MRI. In the temporal reinstatement (TR) model, neural signal at the time of a recall event controls the fidelity with which the temporal code associated with the retrieved memory is reactivated. In the retrieval success (RS) model, neural signal controls the balance between success and failure in the recall competition. In this approach, the computational model bridges between neural signal and human behavior, providing a framework to test hypotheses regarding the computational mechanisms supported by specific MTL structures.

Materials and Methods

Participants and Behavioral Task

Twenty native English speakers (thirteen female) between 18 and 35 years of age participated in the study after giving informed consent, in accordance with the procedures approved by the Vanderbilt University Institutional Review Board. Participants received compensation of twenty dollars per hour, with the opportunity to earn up to ten additional dollars based upon task performance.

Each participant performed 12 trials, spread across 2 scanning sessions, with 6 trials per session. On each trial, a list of 24 words was presented serially. On half of the trials, list learning was followed by a free-recall test. On the remainder of trials, a source recognition task was used to test memory. Order of the trials was deteremined pseudo-randomly, within each session. In the present work, we examine only the free-recall trials. As each word was presented, the participant performed an orienting task, in which they made a button press indicating either the size or animacy of the word, using an MRI compatible response box. A prior study characterizing task-sensitive patterns of neural activity in these data may be consulted for other methodological details (Polyn et al., 2012).

For each studied item, the participant first saw a pre-trial cue (duration 0.7 s) indicating which

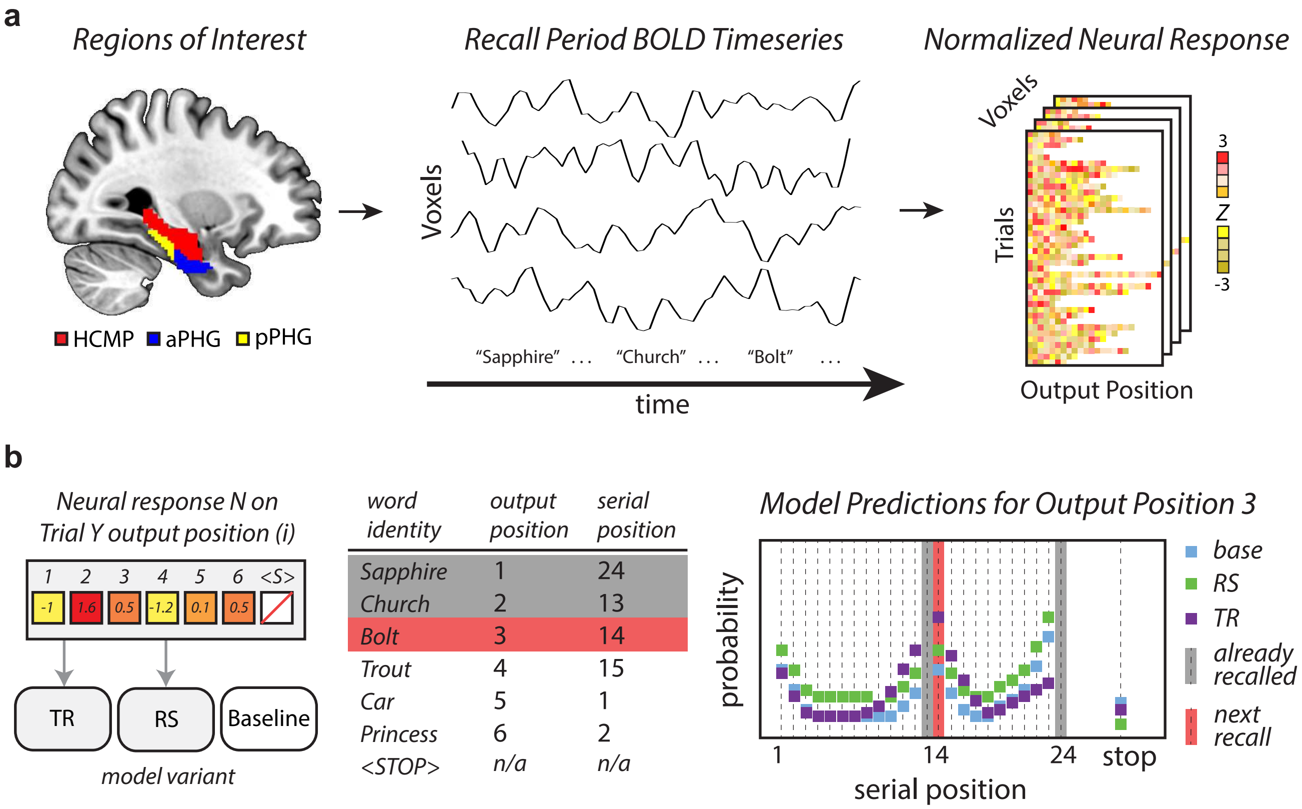

word identity	output position	serial position
Sapphire	1	24
Church	2	13
Bolt	3	14
Trout	4	15
Car	5	1
Princess	6	2
<STOP>	n/a	n/a

Figure 8. Schematic overview of the computational analysis framework. **(a)** BOLD signal from a priori regions of interest within the MTL, including hippocampus (HCMP, red), anterior PHG (aPHG, blue), posterior PHG (pPHG, yellow), and temporal fusiform cortex (anterior and posterior regions not shown) is recorded while subjects recall items from memory. The BOLD timeseries is sampled at the onset of vocalization of a given recall event, and neural responses are standardized within trial. **(b)** For a given neural signal, three models are created. In the temporal reinstatement (TR) and retrieval success (RS) models, this neural signal controls the value of a specific parameter on a recall-by-recall basis. The parameters of the baseline model are not controlled by neural signal. A hypothetical recall sequence and associated neural signal for 7 recall events (including recall termination) demonstrates the predictions of each model. Each model determines a set of probability estimates for a given recall event, corresponding to the likelihood that each studied item is recalled (*serial position*), as well as the likelihood that no more items are recalled (*stop*). Given the increased MTL signal during the second retrieval event, the TR model (purple squares) predicts that nearby items are more likely to be recalled next. The RS model (green squares) predicts a general increase in the likelihood that any studied item will be retrieved, relative to the baseline model (blue squares). The red bar indicates the item that was actually recalled. The likelihood estimates made by each model are aggregated across all recall events to determine the overall likelihood score associated with each model.

judgment to make, followed by a fixation cross (duration 0.3 ± 0.1 s) and the study word (duration 2.5 s). Items were separated by an inter-stimulus interval containing a fixation cross (duration 0.5–5 s), with timing optimized to increase efficiency in estimation of the response to each judgment type (Dale, 1999). A retrieval pre-cue (duration 2 s) followed the final item, indicating whether the current trial involved free recall or source recognition. Finally, a row of asterisks and an auditory tone (duration 0.5 s) indicated the start of the recall period (duration 75 s). During this time, subjects were instructed to recall as many items as they could from the most recent list, in any order. Vocal responses were recorded with a scanner-safe microphone (Resonance Technologies, Inc.), and were scored using *PyParse* (Solway et al., 2010) and *Penn TotalRecall*.

Image Acquisition

Imaging was performed using a 3T Philips Intera Achieva magnet, at the Vanderbilt University Institute of Imaging Science. Functional data were collected using an interleaved gradient echo $T2^*$-weighted pulse sequence with BOLD contrast (TR=2000 msec, TE=30 msec, flip angle=75^o, voxel size=3.0x3.0x3.6 mm, FOV=192 mm). 30 oblique slices, oriented parallel to the AC-PC plane were collected during functional scanning. Whole brain structural scans were acquired using an MP-RAGE sequence (TR=2500 msec, TE=4.38 msec, flip angle=8^o, voxel size=1.0x1.0x1.0mm, FOV=256 mm).

Image Processing

The first four functional images of each session were discarded to allow scanner signal to equilibrate. Preprocessing was carried out using the SPM8 software package, as follows: The remaining functional volumes from each run were realigned to the first functional scan, in order to correct for head motion. The mean of this realigned series was computed and coregistered to the T1 structural image. The T1 image was then segmented (i.e., separated into gray matter, white matter, and cerebrospinal fluid), and normalized to Montreal Neurological Institute stereotactic space using the unified segmentation approach (Ashburner and Friston, 2005). Voxels were resampled to 3-mm isotropic and smoothed spatially, using an 8-mm FWHM Gaussian kernel.

Construction of Regions of Interest

BOLD timeseries were extracted from the MTL, as well as a set of nearby temporal fusiform regions previously shown to play a role in the retrieval of temporal sequences (Lehn et al., 2009; Ekstrom and Bookheimer, 2007). Extra-hippocampal regions of interest (ROIs), including anterior and posterior regions of the parahippocampal gyrus and temporal fusiform cortex, were constructed using the Harvard-Oxford atlas. Hippocampus was defined as all hippocampal subregions (i.e., the subicular complex, dentate gyrus, and cornu ammonis), as well as the entorhinal cortex, from the Jülich Atlas probabilistic maps (Eickhoff et al., 2005; Amunts et al., 2005). A 25% threshold was applied to all probabilistic maps, resulting in an ROI of 2024 voxels within the MTL and surrounding cortical regions. We created an additional set of ROIs that partitioned both MTL cortex (8 ROIs) and hippocampus (6 ROIs) along their anterior-posterior axes. Each ROI was up to 6 mm in length, limited by the anterior-posterior extent of the MTL. ROI placement respected the anatomical boundary between perirhinal cortex and parahippocampal cortex (Insausti et al., 1998).

A Neurally Informed Computational Model of Memory Search

Overview of the general approach

We used a computational model of memory search as part of an analytic framework designed to determine whether neural signal from the MTL contained information that could improve the model's ability to predict the sequence of responses made by participants during the recall task. This model was based on the Context Maintenance and Retrieval (CMR) model of free recall (Polyn et al., 2009a). We created a set of model variants, in order to test specific hypotheses regarding the functional properties of neural signal recorded from different regions of the MTL.

The analysis framework is presented schematically in Figure 8. Figure 8a describes the neural signals incorporated into the model. We recorded BOLD timeseries from voxels within a priori anatomical ROIs, as participants performed a memory-search task. The BOLD signal at the time of each recall event was collected, and normalized across the events in a given trial.

Figure 8b demonstrates how a set of model variants are used to infer what cognitive operations are reflected in BOLD signal changes during memory search. For a given neural signal, two neurally informed model variants were created. The behavior and predictions of each model variant are determined by a set of model parameters, each of which corresponds to a different cognitive mechanism. For each neurally informed model, the degree of engagement of a particular cognitive mechanism was controlled by neural signal sampled at the level of individual recall events.

On each trial of the experiment, participants produced a series of responses, which were coded as recall events. An example recall sequence is presented, in which the participant recalled six items before terminating recall. This was coded as a series of seven events, one for each of the recalled items, and a termination event. For each recall event, the model produced a likelihood score: the model's estimate of the probability of that particular response occurring, given the particular set of recall events leading up to that response. These probability scores were collected in a vector $\mathbf{p}_{event}$. The fitness of a model, given a particular set of parameters, was then determined by:

$$L = -\sum log(\mathbf{p}_{event}). \tag{IV.1}$$

By this equation, a smaller value of L corresponds to a better-fitting model (i.e., one that makes more accurate predictions regarding the recall sequences). For each model variant, an optimization procedure was used to estimate the set of parameters that maximized the likelihood that the model generated the observed behavioral data.

The predictive power of the neurally informed model variants were compared with the predictions of a baseline version of the model (which was not informed by neural data). If BOLD signal from a particular region was informative to a model mechanism, this would improve the ability of the neurally informed model to predict recall sequences, resulting in a significant improvement to the global likelihood score associated with that model.

We additionally created a generative version of the baseline model, which generates synthetic recall sequences for a given set of parameters. In this version of the model, the behavior of the model during recall is stochastically determined by the probability of each possible recall event (i.e., recall of a list item, or termination), rather than the observed recall sequences. The generative model was used to demonstrate the ability of the model to capture important summary statistics characterizing recall behavior.

Basic structure of the model

The CMR model is best described as a simplified neural network, in which two representational layers interact with one another via two sets of associative weighted connections. Each layer contains a set of elements with activation states that can vary between 0 and 1. The first layer contains a feature-based representation of studied material ($\mathbf{f}$), and the second layer contains a contextual representation ($\mathbf{c}$), where $\mathbf{f}$ and $\mathbf{c}$ are column vectors, each containing 50 elements. To simulate the presentation or retrieval of an individual item, activation of $\mathbf{f}$ changes to represent that item. As a simplifying assumption, item representations in $\mathbf{f}$ correspond to a unit vector, with a single element in $\mathbf{f}$ activated. As such, 24 elements in $\mathbf{f}$ correspond to the individual items from the study list. The remaining elements are used to simulate the activation of task-irrelevant information during the inter-stimulus intervals of the study period (24 elements), or during the end-of-list retention interval (1 element). The final element is used to initialize context at the start of each list. The dimensionality of $\mathbf{c}$ is constrained to match that of $\mathbf{f}$. Activation patterns in both $\mathbf{c}$ and $\mathbf{f}$ are constrained to be of unit length.

These layers are connected by two associative matrices, one that allows featural representations to update the current state of context (the item-to-context matrix, $\mathbf{M}^{FC}$), and another that allows context to reactivate item features during memory search (the context-to-item matrix, $\mathbf{M}^{CF}$). Each of these matrices is initialized with a set of pre-experimental associations, corresponding to associations formed prior to the experimental session; learning processes create experimental associations as the list progresses.

The diagonal elements of $\mathbf{M}^{FC}$ allow an item representation $\mathbf{f}$ to influence $\mathbf{c}$, when the item is first studied. A model parameter γ controls the relative strength of pre-experimental and experimental associations; these diagonal elements are initialized at $1-\gamma$, with other elements initialized to zero. Elements of $\mathbf{M}^{CF}$ representing associations between context and individual list items are initialized at a uniform value determined by model parameter α; these pre-experimental associations are meant to represent a participant's knowledge of relationships between the studied items.

Simulating the study period

The study period of each trial was simulated as a sequence of 49 events: 24 study events, which simulated the presentation of a particular item, and 25 disruption events (one preceding each study event, and one following the final study event). The equations below describe how the state of the model changes over the course of these events. We use a subscript $t-1$ to indicate when a particular term represents the influence of a prior state of the model, where t indexes the set of 49 events. We have omitted the t subscript for terms representing the current state of the model.

To simulate presentation of an item during study, encoding processes activate that item's representation $\mathbf{f}_i$, where i indexes the serial position of the item on the list. This information projects through $\mathbf{M}^{FC}$ to influence the contextual representation. An integrative mechanism governs context updating, such that the updated state of the contextual representation is a function of both the incoming information and the prior state of context:

$$\mathbf{c} = \rho \mathbf{c}_{t-1} + \beta \mathbf{c}^{\mathrm{IN}}, \tag{IV.2}$$

where

$$\mathbf{c}^{\mathrm{IN}} = \mathbf{M}^{FC}\mathbf{f}, \tag{IV.3}$$

and is normalized to unit length prior to updating context. Here, β is a model parameter controlling the amount of item information that is integrated into the current state of context, and ρ is a scaling parameter that ensures that $\mathbf{c}$ is of unit length, as follows:

$$\rho = \sqrt{1 + \beta^2[(\mathbf{c}_{t-1} \cdot \mathbf{c}^{\mathrm{IN}})^2 - 1]} - \beta(\mathbf{c}_{t-1} \cdot \mathbf{c}^{\mathrm{IN}}). \tag{IV.4}$$

During encoding, β is set to β_{enc}; below, β will take on other values to simulate contextual updating during inter-item intervals, and during recall.

After context is updated, an episodic learning process creates associative structures binding the current state of **f** to **c**, according to:

$$\mathbf{M}^{FC} = \mathbf{M}^{FC}_{t-1} + \gamma \mathbf{c}\mathbf{f}^{\top} \tag{IV.5}$$

$$\mathbf{M}^{CF} = \mathbf{M}^{CF}_{t-1} + \phi_i \mathbf{f}\mathbf{c}^{\top}, \tag{IV.6}$$

where γ controls the strength of experimental associations. ϕ_i is a scaling factor that increases context-to-item associations for early list positions to capture the primacy effect (the enhanced recall performance associated with the first few list positions). Primacy scaling is determined by the following equation:

$$\phi_i = \phi_s e^{-\phi_d (i-1)} + 1, \tag{IV.7}$$

where ϕ_s and ϕ_d are free parameters, and i indexes serial position of the item.

Preliminary simulations suggested that this primacy gradient did not adequately describe the primacy effect in the behavioral data. As such, we incorporated a secondary primacy mechanism, inspired by prior theoretical work (Laming, 1999). By this mechanism, at the start of the recall period, the model partially reactivates the contextual state associated with the start of the study list. This process follows the contextual updating rule described in Equation IV.2, using model parameter β_s to determine the fidelity of reactivation of start-of-list context. We found that a version of the model with both primacy mechanisms (primacy gradient and start-of-list contextual retrieval) was able to account well for the behavioral variance associated with the primacy effect.

The model also allows the contextual representation to be perturbed by task-irrelevant information during the inter-stimulus intervals (ISIs) and the end-of-list retention interval (RI), as described in prior work (Sederberg et al., 2008). A representation of the task-irrelevant information is activated on **f** and is allowed to update the contextual representation, following Equation IV.2, with the exception that the rate of integration is controlled by either β_{isi} or β_{ri}. We assume that no associative learning takes place during these intervals (i.e., $\mathbf{M}^{FC}$ and $\mathbf{M}^{CF}$ are not updated), and that these task-irrelevant representations do not enter the recall competition described below.

Simulating the recall period

On each trial, the participant made a series of responses, which were coded as a series of recall events, and a termination event (e.g., Figure 8b). Repetitions and recall errors (i.e., intrusions) were rare during this task. In order to simplify the dynamics of the model, we removed recall events corresponding to repetitions of already recalled items (46 events, across 120 recall trials), as well as prior and extra-list intrusions (a total of 37 events).

For each recall event, the context representation, **c**, is projected through the associative weight matrix $\mathbf{M}^{CF}$, determining the relative support (**s**) for each individual item representation in **f**:

$$\mathbf{s} = (\mathbf{M}^{CF}\mathbf{c}). \tag{IV.8}$$

Here, **s** is a vector in which each element corresponds to the support for a given studied item. If a participant were to recall an item that was assigned a zero probability in the recall competition, the likelihood metric used to assess model performance would assign a likelihood of negative infinity to that model. To avoid this possibility, we introduced the assumption that there is always some minimal support for any item (for the present simulations, this was set to 10^{-6}). Once **s** is created, a recall competition is simulated: The probability of the model recalling each of the not-yet-recalled study items (p_i, where i indexes serial position), and the probability of recall termination (p_{stop}), are calculated.

The probability of terminating recall, p_{stop}, is determined by an exponential function based on the ratio of support for items that have not yet been recalled to items that have been recalled, as follows:

$$p_{stop} = \xi_s + e^{-\xi_d S_{nr}/S_r}. \tag{IV.9}$$

Here, ξ_d is a model parameter controlling the rate at which p_{stop} rises with output position, and s_r and s_{nr} are scalar values corresponding to the summed support for the already recalled items, and the not-yet-recalled items, respectively. For the present simulation work, ξ_s was fixed to a value of 10^{-3}, and corresponds to the probability that recall terminates before any items are retrieved. The ξ_d parameter is controlled by neural signal in the retrieval success (RS) version of the model, described below.

We then set the support values for already recalled items to zero, and calculate the probabilities associated with the recall of each of the remaining studied items (p_i), as follows:

$$p_i = (1 - p_{stop}) \frac{\mathbf{s}_i}{\sum_k^N \mathbf{s}_k}, \tag{IV.10}$$

where N is the number of items in the list.

At this point, the element of p corresponding to the item that was actually reported by the participant (or p_{stop}, if the participant terminated recall at this point) is appended to the vector p_{event} (from Eq. IV.1). If this is a termination event, the trial is over, and the model is initialized for the next trial. If this is a recall event, the model simulates recall of that item. First, the featural representation of the item is reactivated on $\mathbf{f}$. The reactivated item representation is then projected through $\mathbf{M}^{FC}$, which retrieves the temporal code associated with that item. This updates the state of $\mathbf{c}$, following Equation IV.2, setting β to β_{rec}. The β_{rec} parameter is controlled by neural signal in the temporal reinstatement (TR) version of the model, described below.

Incorporating BOLD signal into a model

In order to test hypotheses regarding potential links between BOLD activity in the MTL and particular model mechanisms, we constructed a number of model variants in which neural signal influences specific model parameters on a recall-by-recall basis. In these models, a given model parameter θ is updated for each recall event, according to:

$$\theta_{event} = \theta + \nu N_{event}, \tag{IV.11}$$

where N_{event} represents the neural signal recorded for this recall event (i.e., BOLD signal measured at the onset of vocalization), and ν is a neural scaling parameter determining the influence of the neural signal on the model parameter θ. Thus, θ_{event} represents the value of that model parameter for this particular recall event.

We constructed a TR model in which θ corresponds to β_{rec} (which controls contextual integration during retrieval), and the neural signal is scaled by ν_{TR}. We also constructed a RS model in which θ corresponds to ξ_d (which controls the rate p_{stop} increases as items are recalled), and the neural signal is scaled by ν_{RS}. For the TR model, ν_{RS} was fixed to zero; for the RS model, ν_{TR} was fixed to zero. The baseline model can be considered a restricted variant of either of the neurally informed models, in that both ν_{TR} and ν_{RS} were fixed to zero. Finally, we created a joint model, which allowed both ν_{TR} and ν_{RS} to take non-zero values.

Parameter Estimation Techniques

For a given version of the model, we estimated the set of parameters that best allows the model to capture the observed behavioral data, using a particle swarm optimization (PSO) algorithm to search over the parameter space (Eberhart and Kennedy, 1995). This technique creates a set of particles, each of which can be thought of as a point moving through the high-dimensional parameter space, searching for the region of this space that maximizes the fitness of the model. This technique was used to estimate the optimal parameters for the baseline model, and was used three times for each voxel containing neural signal (for the TR, RS, and joint models).

A swarm was constructed by creating 40 uniformly distributed random parameter sets, each of these serving as the initial position for one of the particles. The movement of each particle was determined by the velocity vector **v**, which was added to the position vector **x** to determine the position of the particle on the each iteration of the search. The set of positions visited by each particle was saved as search progressed, allowing the algorithm to keep track of each particle's best-fit position (**b**) and the global best fit over all particle histories (**g**).

Three steps were repeated until the average change in fitness over 50 generations did not change by more than a specified tolerance (10^{-7}). For each iteration of the PSO algorithm, (1) the fitness L of the parameter set associated with each particle was evaluated; (2) the individual and global best fitness values and positions were updated, and (3) the velocities and positions of each particle were updated.

The velocity of each particle, $\mathbf{v}_i$, in the swarm was determined by:

$$\mathbf{v}_i(t+1) = w\mathbf{v}_i(t) + c_1 r_1[\mathbf{b}_i(t) - \mathbf{x}_i(t)] + c_2 r_2[\mathbf{g}(t) - \mathbf{x}_i(t)], \tag{IV.12}$$

where i indexes a given particle, and t indexes the generation of the particle search. The ith particle is represented by its position in a D dimensional search space, where D is determined by the number of parameters to be fit. The value of $\mathbf{b}_i$ is the position of an individual particle that produced the best fitness value over the history of the search, and $\mathbf{g}(t)$ is the best-fitting position in parameter space over all particles. In the current work, the PSO parameters c_1, and c_2 were fixed at 0.5 and 1.25 respectively. The values of r_1 and r_2 were pseudorandom values drawn from the standard uniform distribution on the interval (0,1) during each generation of the PSO algorithm.

The parameter w controls the inertia of the particles in the swarm, and was updated following:

$$w = 0.9 - 0.4(t-1)/(T-1), \tag{IV.13}$$

where t is the current generation, and T is the maximum number of generations, which was set to 1000 in the implemented parameter searches. For all of the parameter estimation searches reported here, the algorithm terminated search prior to reaching T.

Model Comparison Techniques

Once the optimal set of parameters were estimated for the baseline model and a neurally informed model, a likelihood-ratio test (Wilks, 1938) was used to determine whether any improvement in model predictions for the neurally informed model was significant. This produced a test statistic D (also known as deviance, twice the difference of the log-likelihood of the neural and baseline models) for each voxel within *a priori* regions of interest. Significance was calculated by testing D on a χ^2 distribution with one degree of freedom.

Once D was calculated for all voxels, a Monte Carlo resampling procedure (3dClustSim from AFNI; National Institute of Mental Health, Bethesda; http://afni.nimh.nih.gov/afni) was used to identify significant clusters, correcting for multiple comparisons across the entire search region. First, individual voxels surviving an uncorrected threshold of $p < 0.05$ ($D > 3.8415$) were identified, and a resampling procedure indicated that a cluster extent of 31 would ensure a cluster-level $p < 0.05$, corrected for multiple comparison within the predefined anatomical ROI.

Aikake's Information Criterion (AIC) was used to evaluate model fitness across multiple models (Wagenmakers and Farrell, 2004; Burnham and Anderson, 2004). This measure takes model complexity (number of free parameters) into account, allowing us to compare a neurally informed model to the baseline model. Unlike the likelihood-ratio test, this method does not require nested models, and was used to compare the TR, RS, and joint models to one another. For each model, we computed AIC with a correction for finite samples:

$$AIC_c = 2L + 2V + \frac{2V(V+1)}{(n-V-1)}, \tag{IV.14}$$

where L is the maximum likelihood value for the candidate model (from Eq. IV.1), V is the number of free parameters, and n is the number of estimated data points. AIC weights were computed to determine the probability that each model (of K competing models) generated the observed data, under the assumption that one of the models generated the data, as follows:

$$w_i AIC = \frac{exp(-\frac{1}{2}\Delta_i AIC)}{\sum_{k=1}^{K} exp(-\frac{1}{2}\Delta_k AIC)}. \tag{IV.15}$$

Here, $\Delta_i AIC$ is the difference in AIC_c between a given candidate model (specified by i), and the best-fitting model in the set.

In order to determine which of the models was most supported for a given cluster of voxels, we created an average model representative of that cluster. The parameter values $\hat{\hat{\theta}}$ for this representative model were calculated as a weighted average of the parameter values $\hat{\theta}$ for all of the models associated with the voxels in that cluster, following:

$$\hat{\hat{\theta}} = \sum_{i=1}^{N} w_i AIC \hat{\theta}_i, \tag{IV.16}$$

where $\hat{\theta}_i$ is the set of estimated parameters from voxel i in the set of N voxels in the cluster. This approach was used to calculate the relative fitness of the TR, RS, and joint models for a given cluster.

In order to perform model comparisons for a given anatomical ROI, we employed a bootstrap sampling procedure. For each ROI, informative voxels (i.e., those identified by either the TR or the RS analyses) were selected at random with replacement, allowing for the construction of a distribution of AIC weights for each model type, for each ROI. Bootstrap statistics were used to compare these distributions to one another, and to test for linear trends across anatomical ROIs (at $p < 0.05$, Bonferroni corrected for multiple comparisons).

Results

Behavioral characterization of recall sequences

During the memory search period of the free-recall task, participants produced a series of responses; each response is referred to as a recall event. Figure 9 (red lines) summarizes the major behavioral phenomena present in these recall sequences, in terms of how participants initiated recall, transitioned between recall events, and finally terminated search. Figure 9a depicts the probability of initiating recall with each studied item, arranged in their order of presentation. Participants most often initiated recall with the final list position (demonstrating the recency effect), but sometimes started with the first list position (demonstrating the primacy effect), with a small but non-zero probability of initiating recall with some mid-list item. Our analysis of recall transitions focuses on the temporal organization of the response sequences. Figure 9b depicts the probability of transitions

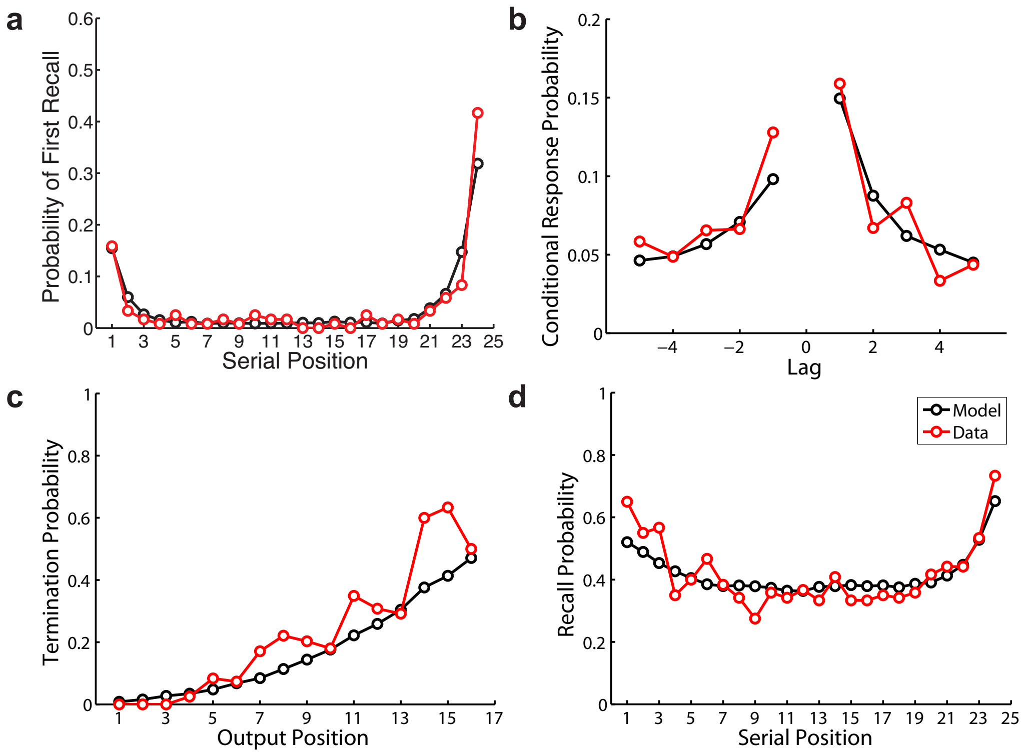

Figure 9. Comparison of summary statistics of behavioral performance (Data; red lines) with predictions of the best-fitting baseline model (Model; black lines). The parameter estimation process found the set of parameters that maximized the model's ability to predict the likelihood of individual recall events; the model was not explicitly fit to these summary statistics. **(a)** Recall initiation, as measured by probability of first recall by serial position. **(b)** Recall transitions, as measured by the probability of transitions in which the two successively recalled items were separated by a particular positional lag. **(c)** Recall termination, as measured by the probability of stopping recall as a function of output position for the first 16 output positions. **(d)** Overall recall performance, as measured by the probability of recalling an item as a function of its serial position.

of different lengths, with length measured as the positional distance in the study list (i.e., the lag) between any two successively recalled items. When a particular item was recalled, there was a strong tendency for the next recalled item to come from a nearby list position, demonstrating the contiguity effect, a nearly ubiquitous phenomenon in free-recall response sequences (Kahana, 1996; Kahana et al., 2008; Kahana, 2012). The peaks for small values of lag are taken as evidence for the temporal organization of the studied material in memory. Temporal organization is taken as a marker of mental time travel, as this behavior indicates that memories formed near in time to the just-recalled item have become more accessible.

At some point, participants failed to recall any more items, and the recall process terminated (Miller et al., 2012). Figure 9c depicts the probability of recall termination as a function of the number of items recalled (i.e., output position). Finally, Figure 9d depicts the probability that a given studied item appeared anywhere in the recall sequence, demonstrating again the primacy and recency effects, as well as the relatively flat probability of recalling a mid-list item. On average, participants recalled 42% of the studied items before the end of the recall period.

Comparison of neurally informed models to a baseline model

In order to determine whether the model provides a good account of the core behavioral phenomena of free recall, we developed a generative version of the model, which produces synthetic recall sequences for a given parameter set. Using the parameter settings for the optimized baseline model, we generated a large number of synthetic recall sequences, creating model-generated versions of the four critical summary statistics described above. Figure 9 (black lines) compares these synthetic recall sequences to the observed recall sequences (red lines). The correspondence between the black and red lines demonstrates a good qualitative fit to the behavioral dynamics of free recall. A quantitative description of the model's fitness is provided in Table 7.

The neurally informed TR model allows signal from a particular MTL voxel to determine the success of the contextual reactivation operation for each recall event. In contrast, the baseline model assumes that the parameter controlling temporal reinstatement (β_{rec}) is stationary over the course of the recall period. The baseline model can capture the average degree of temporal organization in the recall sequences (Figure 9b), but the addition of neural signal can improve the predictive power of the model if it indicates, for a particular recall event, the fidelity with which that temporal code is reactivated. That is, neural signal can potentially allow the model to capture not only the mean level of temporal organization, but also variability in organization, at the level of individual recall events.

We identified two clusters of voxels within the MTL that significantly improved the TR model's predictions relative to the baseline model. Figure 10 presents a deviance (D) map, which indicates

Table 7. Model fitness of representative models.

Model	Cluster	k	Center of Mass (mm)	*n*	*L*
TR	Left MTL	167	-28, -27, -21	11	3581.5
TR	Right pPHG	63	25, -32,-18	11	3580.4
RS	Right aMTL	336	28,-6,-32	11	3570.8
RS	Left MTL	554	-28,-16,-27	11	3571.7
RS	Right pPHG	52	17,-31,-10	11	3578.81
Joint	Left MTL	93	-27,-26,-21	12	3576.91
Baseline	-	-	-	10	3586.7

Note: n reflects the number of free parameters, evaluated using the average neural signal and model parameters within each significant cluster. L is the negative natural logarithm of the maximum likelihood for each model. The extent of each cluster is denoted by k, with coordinates for the center of mass reported in MNI space. TR, temporal reinstatement; RS, retrieval success; pPHG, posterior parahippocampal gyrus; MTL, medial temporal lobe; aMTL, anterior MTL.

the predictive power of the TR model relative to the neurally naive baseline model, on a voxel-by-voxel basis. One cluster consisted of a number of voxels in left MTL cortex extending from entorhinal cortex through posterior parahippocampal gyrus (PHG), as well as posterior temporal fusiform cortex. A second cluster in right MTL extended from the hippocampus through posterior PHG, with the caudal extent of activation reaching posterior temporal fusiform cortex (see Table 8 for more detail). Consistent with the hypothesis that engagement of the parahippocampal cortex during retrieval reflects the reinstatement of contextual information, we observed positive neural scaling factors (ν_{TR}) linking activity in these clusters to the fidelity of temporal reinstatement.

In order to visualize the behavioral consequences of shifts in MTL activity during memory search, we partitioned the set of recall events into periods of high and low neural signal, using a weighted average of the voxels within each MTL cluster. We separately constructed lag-based conditional response probabilities for these two sets of recall events. Figure 10 (right column) shows an increase in the temporal organization of recall events occurring during periods of increased MTL activity.

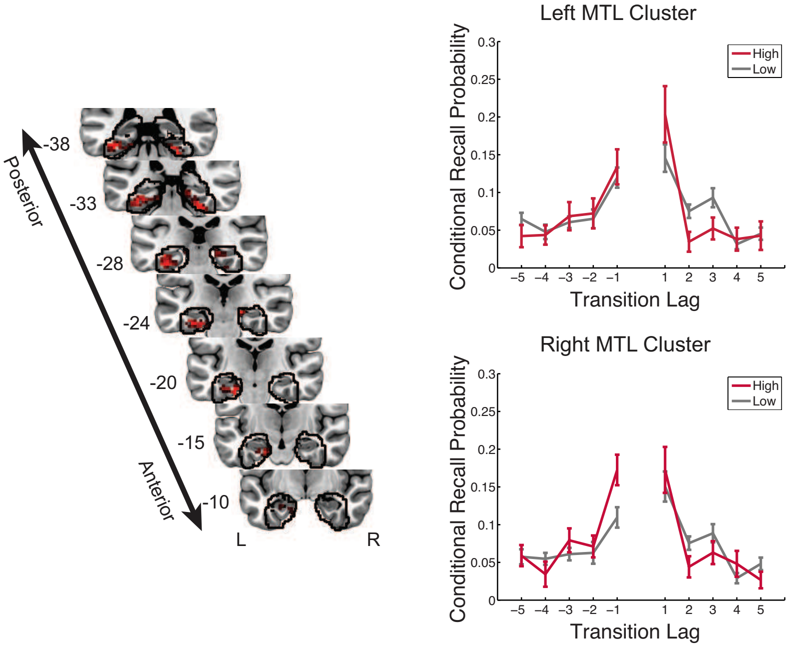

Figure 10. Model evidence for temporal reinstatement processes in the MTL. Left: A deviance map showing clusters of informative voxels ($p < 0.05$, corrected) within anatomically defined regions of interest, outlined in black. Right: Recall events were partitioned on the basis of neural activity in each MTL cluster, and an analysis of temporal organization was carried out separately for each cluster. Periods of high neural activity were associated with increased temporal organization. The y-value indicates the probability (± SEM) that the next recalled item will have a particular lag to the just-recalled item (conditional on the availability of that item for recall). The y-coordinate of coronal sections from the group-average anatomical image is given in MNI space. MTL, medial temporal lobe. R, right. L, left.

Table 8. Peak voxels within a priori regions of interest.

Model	Region (hemisphere)	peak coordinate (mm)	D
Temporal reinstatement	TFC (L)	$-33, -37, -17$	13.30
	ERC (L)	$-18, -19, -29$	13.28
	TFC (R)	$27, -34, -23$	11.57
	HCMP (R)	$18, -25, -11$	9.13
Retrieval success	aPHG (R)	$21, 5, -23$	29.52
	aPHG (L)	$-18, -1, -23$	24.91
	aPHG (R)	$36, -10, -29$	20.21
	HCMP (L)	$-21, -10, -20$	14.93
	HCMP (R)	$18, -28, -14$	11.58

Note: Coordinates are reported in MNI space. TFC, temporal fusiform cortex; ERC, entorhinal cortex; HCMP, hippocampus; aPHG, anterior parahippocampal gyrus. D, deviance from Baseline model. R, right; L, left.

The neurally informed RS model allows signal from a particular MTL voxel to influence the relative likelihood that the model will continue to recall studied items, as opposed to terminating recall. Three clusters of voxels were identified ($p < 0.05$, corrected) that improved the RS model's predictions relative to the baseline model, within *a priori* regions of interest. Two bilateral clusters were comprised mostly of anterior PHG, including perirhinal cortex, the anterior extent of the hippocampus, and anterior parahippocampal cortex. The third cluster spanned right hippocampus and adjacent posterior PHG. The neural signal in these models was associated with a positive neural scaling factor (ν_{RS}; see Table 9); increased neural activity indicated a reduced likelihood that recall will terminate, as shown in Figure 11. These findings are generally consistent with theories in which item information is reactivated in perirhinal cortex during memory retrieval: If perirhinal activity reflects the reactivation of successfully retrieved studied materials, increased perirhinal activity should indicate that the participant will continue to produce recall responses.

Visual inspection of the maps depicted in Figures 10 and 11 suggests that neural signal in certain regions was informative for both models. In order to determine whether, for regions containing neural signal that was informative to both models, these two neurally controlled cognitive

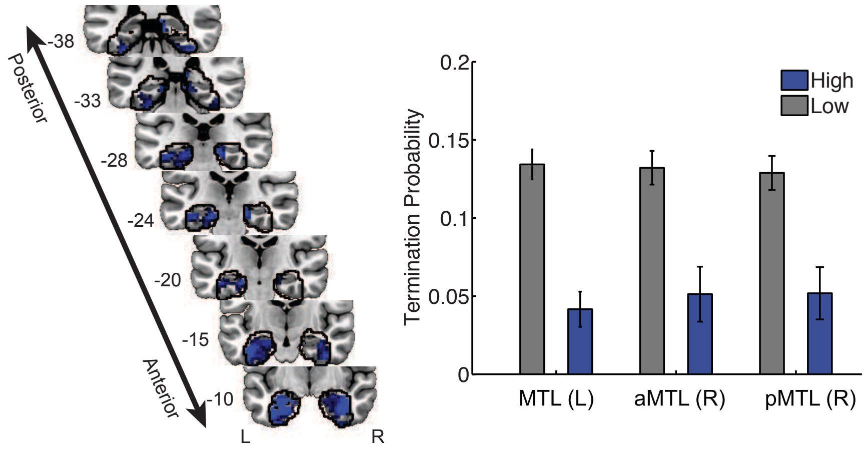

Figure 11. Model evidence for retrieval success processes in the MTL. Left: A deviance map showing clusters of informative voxels ($p < 0.05$, corrected) within anatomically defined regions of interest, outlined in black. Right: Recall events were partitioned on the basis of neural activity in each MTL cluster; periods of high neural activity were associated with a decreased likelihood of recall termination. Y-values correspond to the mean probability (± SEM, averaged across participants) that the recall event in question is the final item in the recall sequence. Y-coordinates of each MTL section are given in MNI space. MTL, medial temporal lobe; aMTL, anterior MTL; pMTL, posterior MTL.

mechanisms explain independent sources of variability in the behavioral data, we constructed a joint neural model. In this joint model, neural signal from a given voxel influenced both the temporal reinstatement and retrieval success mechanisms (with a separate neural scaling parameter for each process). This analysis identified a single cluster of voxels within the left MTL, comprised of hippocampus, posterior PHG, and posterior temporal fusiform cortex, which allowed the joint model to perform better than the baseline model (Figure 12a).

Each of the voxel time courses within this cluster was associated with a positive neural scaling factor for the temporal reinstatement process, and a positive neural scaling parameter for the recall success process. In other words, under this model, increased activity in this region reflects both the high fidelity reactivation of temporal context, as well as a decreased likelihood that recall will terminate. As in our analyses of the TR and RS models, we partitioned the set of recall events into periods of high and low neural signal (Figure 12b), using a weighted average of the voxels within the left MTL cluster. Figure 12c shows a clear increase in the temporal organization of recall events occurring during periods of increased MTL activity. Furthermore, we observed a clear decrease in

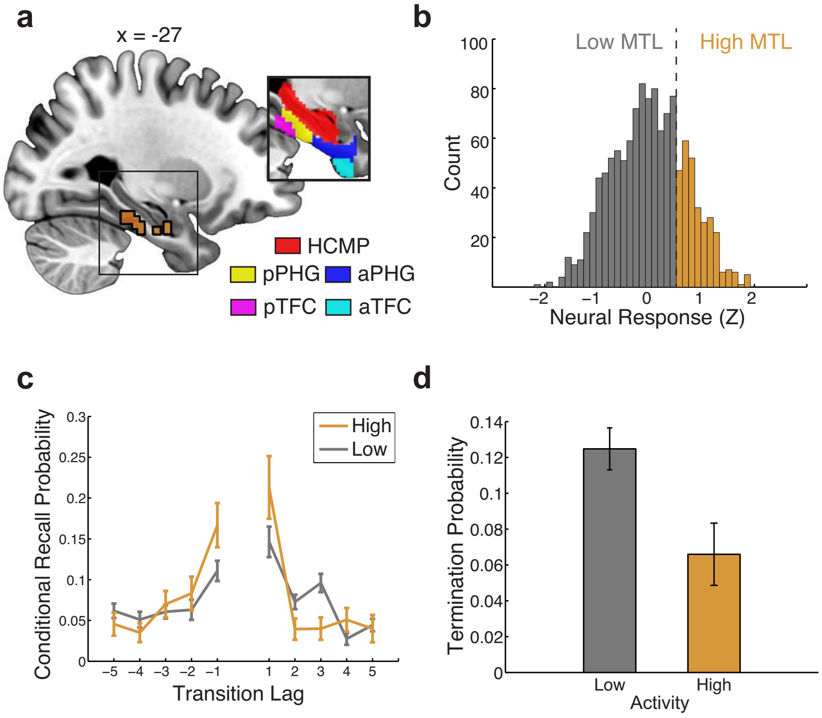

Figure 12. Cortical regions in the left MTL jointly support the temporal reinstatement and retrieval success hypotheses. **(a)** A deviance map indicates a single cluster of voxels where the joint model is significantly better than the neurally naive baseline model, in a functionally defined region of interest, outlined in black (voxels identified as informative to both temporal reinstatement and retrieval success). Inset, apriori anatomical regions of interest. HCMP, hippocampus. PHG, parahippocampal gyrus; aPHG, anterior PHG; pPHG, posterior PHG. TFC, temporal fusiform cortex; aTFC, anterior TFC; pTFC, posterior TFC. X-coordinates are given in MNI space. **(b)** A histogram depicting the distribution of MTL neural responses across all recall events. Neural response is *z*-score normalized within trial and averaged across the voxels in the identified cluster. Responses more than 0.5 standard deviations above the mean response (across all trials) are labeled as high activity recall events. **(c)** Recall events were partitioned according to the level of activation in the cluster; periods of high activity were associated with increased temporal organization. **(d)** Periods of high neural activity were also associated with a decreased likelihood of recall termination.

Table 9. Average model parameters from best fitting models

	Temporal Reinstatement		Retrieval Success			Joint
Parameter	Right pPHG	Left MTL	Right pPHG	Right aMTL	Left MTL	Left MTL
β_{enc}	0.33 (0.0076)	0.35 (0.018)	0.33 (0.0018)	0.33 (0.002)	0.33 (0.004)	0.34 (0.0083)
β_{rec}	0.82 (0.018)	0.81 (0.016)	0.86 (0.0031)	0.86 (0.0018)	0.86 (0.0021)	0.82 (0.017)
ϕ_s	1.69 (0.08)	1.48 (0.13)	1.69 (0.031)	1.81 (0.059)	1.75 (0.054)	1.54 (0.069)
ϕ_d	0.43 (0.0084)	0.42 (0.014)	0.43 (0.0035)	0.44 (0.0072)	0.43 (0.0075)	0.42 (0.0089)
γ	0.23 (0.011)	0.27 (0.018)	0.23 (0.0022)	0.23 (0.0012)	0.23 (0.0017)	0.26 (0.01)
ξ_d	2.37 (0.046)	2.35 (0.047)	2.37 (0.025)	2.50 (0.035)	2.44 (0.048)	2.36 (0.029)
α	0.05 (0.0019)	0.05 (0.0011)	0.05 (0.00023)	0.05 (0.00025)	0.05 (0.0005)	0.05 (0.0011)
ν_{TR}	0.35 (0.014)	0.10 (0.016)	-	-	-	0.09 (0.019)
ν_{RS}	-	-	0.35 (0.043)	0.57 (0.042)	0.50 (0.051)	0.26 (0.046)
β_s	0.28 (0.043)	0.28 (0.054)	0.23 (0.003)	0.22 (0.0064)	0.22 (0.006)	0.26 (0.016)
β_{ri}	0.76 (0.14)	0.75 (0.14)	0.82 (0.0035)	0.82 (0.0047)	0.82 (0.0056)	0.78 (0.039)
β_{ipi}	0.90 (0.0027)	0.90 (0.0044)	0.89 (0.00059)	0.89 (0.00038)	0.89 (0.00086)	0.90 (0.0034)

Note: Mean values from each cluster are shown, with their associated standard deviation in parentheses. pPHG, posterior parahippocampal gyrus; MTL, medial temporal lobe; aMTL, anterior MTL.

the probability of recall termination for the set of recall events with high MTL activity (Figure 12d). A bootstrap analysis confirmed that representative models constructed from this cluster favored the joint model over both the RS and TR models alone ($wAIC = 0.68(\pm 0.009\ \ SEM)$, $p < 0.0001$).

Model support varies along the anterior-posterior axis of the MTL

The maps presented in Figures 10 and 11 suggest the relationship between neural signal and the temporal reinstatement process in the model is stronger in posterior MTL regions, while the relationship between neural signal and retrieval success is stronger in anterior regions. To test whether evidence of a cognitive operation differed along the anterior-posterior axis of the MTL, we carried out a weighted Akaike's Information Criterion (*wAIC*) analysis (Burnham and Anderson, 2004). We computed four wAIC scores corresponding to the four models under consideration (baseline, TR, RS, and joint) for each voxel within anatomical ROIs constructed along the anterior-posterior axis of the MTL (Figure 13a). For each ROI, we used a bootstrap sampling procedure to generate an estimated average wAIC score for each model. This sampling procedure was restricted to neurally informative voxels (i.e., those identified in the deviance maps of Figures 10, 11, and 12), answering the question: If a neural signal in this region is informative for at least one of our neural models, which of the neural models is best supported?

The relative support for each of the three neural models is presented for hippocampal ROIs (Figure 13b) and MTL cortical ROIs (Figure 13c), with the ROIs arranged in terms of their position along the anterior-posterior axis of the region. Within the hippocampus, RS models were most supported in anterior ROIs; evidence for these models significantly increased in the anterior direction, as revealed by linear regression ($\beta = 6.79(\pm 2.28 \ \ SEM), p < 0.0001$). This pattern also held across MTL cortical ROIs: Evidence for RS models significantly increased in the anterior direction ($\beta = 14.32(\pm 0.62 \ \ SEM), p < 0.0001$). Within the hippocampus, a significant linear trend in the opposite direction was observed for the TR model, with increasing support in posterior ROIs ($\beta = -11.09(\pm 3.97 \ \ SEM), p < 0.0001$). This pattern also held across MTL cortical ROIs: Evidence for the TR models significantly increased in the posterior direction ($\beta = -25.19(\pm 1.90 \ \ SEM), p < 0.0001$). Support for the joint model did not vary along the anterior-posterior axis in the hippocampus ($\beta = -13.7(\pm 7.55 \ \ SEM), p = 0.14$), though in MTL cortical ROIs there was a reliable increase in support for this model in the posterior direction ($\beta = -26.77(\pm 3.24 \ \ SEM), p < 0.0001$).

For two of the three posterior hippocampal ROIs, and all of the posterior MTL cortical ROIs, the joint model was strongly favored. While we observed an anatomical gradient to these signals, both processes (i.e., temporal reinstatement and retrieval success) were reflected in neural signal from posterior regions. These posterior MTL cortical ROIs spanned parahippocampal cortex and adjacent temporal fusiform cortex.

MTL signal is informative at the level of individual trials

As mentioned, our baseline model assumes that the parameters associated with temporal reinstatement and item retrieval are stationary over the recall period. This does not mean that the baseline model predicts that the behavioral markers associated with those parameters are stationary over the recall period. This is clearly indicated in Figure 9c: Despite the recall termination parameter ξ_d

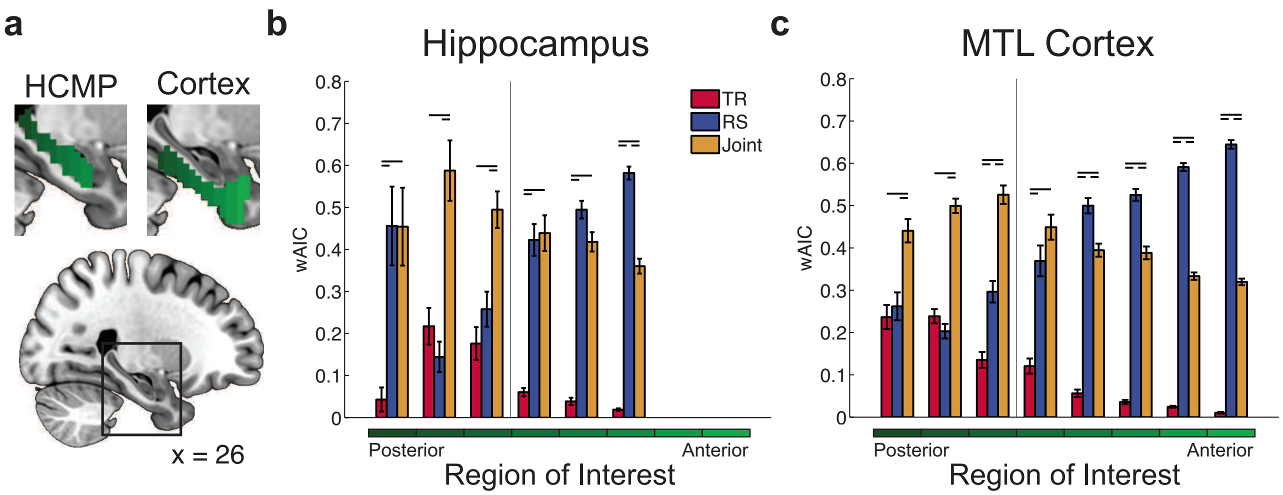

Figure 13. Relative fitness of neural models across MTL subregions. **(a)** Anatomically defined ROIs along the anterior-posterior extent of the hippocampus (HCMP, left panel) and MTL cortex (right panel). **(b)** Average wAIC scores from 6 anatomically defined hippocampal ROIs. **(c)** Model fitness from 8 anatomically defined MTL cortical ROIs. Bars indicate bootstrap estimated average wAIC scores for neurally informative models within that ROI. Error bars reflect bootstrap estimated standard error of the mean. Horizontal dashes denote significant pairwise differences ($p < 0.05$, Bonferroni corrected). The vertical line denotes the anatomical boundary between perirhinal and parahippocampal cortex. TR, temporal reinstatement. RS, retrieval success.

being stationary, the model captures the increasing probability of recall termination as a function of output position (due to the dynamics described in Equation IV.9). Likewise, the baseline model captures a small decline in temporal organization with output position: According to the baseline model, temporal reinstatement is equivalent across these recall events, but the temporal organization associated with early recall events is amplified by the recency effect, the tendency for the first few recall events to come from the final few serial positions of the study list.

It is worth considering whether a neural signal could shift in such a way that it could be artifactually identified as informative to one of the models, despite not reflecting the cognitive operation embodied by the model. For example, if the baseline model did not perfectly capture the decline in temporal organization from early to later output positions, it is possible that a neural signal that generally decreased over the course of the recall period would be identified as neurally informative for the TR model, as it would allow the model to decrease the amount of temporal reinstatement in later output positions, relative to early output positions. Similarly, one can imagine an equivalent scenario for the RS model: A neural signal that generally changes its magnitude between early and late output positions could help the model fit the ever increasing tendency towards recall termination with later output positions. We developed a permutation-based analysis of these neurally informed models to address these concerns.

This permutation analysis was designed to rule out the possibility that our analytic framework identified a neural signal reflecting some general process that changes as a function of output position, but does not indicate temporal reinstatement or item retrieval *per se*. For each representative model associated with a given MTL cluster, we permuted the observed neural signal recorded for a given output position, across trials. Permutations were constrained to occur within-subject, ensuring variability in BOLD response between subjects did not bias the results of this analysis. If the observed neural signal contains information that reflects a general process that changes as a function of output position, permuted signal should be as informative as trial-specific neural data. We observed significantly improved performance in the two representative TR models constructed from left ($p = 0.005$) and right ($p = 0.011$) MTL clusters, relative to models informed by permuted neural signal. The same was true for the three representative RS models, constructed from the right anterior MTL cluster ($p < 0.001$), the left MTL cluster ($p < 0.001$), and the right posterior PHG cluster ($p = 0.009$). These results confirm that trial-level variability in neural signal improved the ability of the neurally informed models predict recall behavior.

Discussion

In order to determine the cognitive functions of MTL subregions during memory search, we developed computational models that tested hypotheses regarding the links between complex cognitive operations and BOLD activity recorded during retrieval. We found evidence that distinct MTL structures are associated with different computational mechanisms predicting successful performance and temporal organization during a free-recall task. Our findings implicate the posterior PHG and hippocampus in reinstating the temporal context of prior episodes. This temporal reinstatement is thought to be an important mechanism supporting the subjective reliving of past experience (Tulving, 1993). In contrast, anterior MTL structures, including perirhinal cortex, were agnostic to the temporal structure of retrieved memories, while generally supporting recall of items from the targeted episode.

The hypothesis that particular MTL subregions control the fidelity of mental time travel was strongly supported by the data: Two clusters of voxels carried signal whose recall-by-recall fluctuations improved the predictive power of the temporal reinstatement model relative to both the retrieval success model and a baseline model. Multiple MTL structures, including right hippocampus, bilateral parahippocampal cortex, and surrounding temporal fusiform cortex contributed to this model. When these regions showed increased activity for a particular recall event, there was an increased likelihood that the next recalled item would come from a nearby point in time (Figure 10). These results are consistent with theories implicating parahippocampal cortex in the maintenance of contextual information (Davachi, 2006; Ranganath and Ritchey, 2012), studies demonstrating recruitment of the parahippocampal cortex and hippocampus during the retrieval of temporal information (Ekstrom and Bookheimer, 2007), and studies implicating MTL structures in the representation of temporal information in a variety of memory tasks (Jenkins and Ranganath, 2010; Manning et al., 2011; Howard et al., 2012; Ezzyat and Davachi, 2014). These findings are in accord with the proposed role of the MTL in providing temporal structure to one's experience (Levy, 1996; Wallenstein et al., 1998; Howard et al., 2005; Eichenbaum, 2013).

It has been proposed that the hippocampus contains associative structures responsible for binding item and contextual information during the formation of episodic memories (McClelland et al., 1995; Howard et al., 2005; Diana et al., 2007; Polyn and Kahana, 2008). During retrieval, patterns of activity present during encoding are reinstated within cortex (Danker and Anderson, 2010). Studies using multi-voxel pattern analysis (MVPA) have shed light on how reinstated patterns of neural activity reflect the attributes of memory (Polyn et al., 2005; Lewis-Peacock and Postle, 2008; Johnson et al., 2009), and hippocampal activity has been implicated in the success of this reinstatement process (Gordon et al., 2014; Staresina et al., 2013; Bosch et al., 2014). The analytic framework presented here raises the possibility of linking neural representations characterized with

MVPA to the cognitive operations of retrieved-context models of memory search. For example, Polyn et al. (2012) identified patterns of neural activity at study sensitive to the encoding task used on a particular item. These task-sensitive neural representations were reinstated during memory search. One can imagine an extension to the current analytic framework in which the fidelity of the neural reinstatement of task information (measured with MVPA) is used to control a model parameter indicating how strongly the source characteristics of a given item are represented in the contextual representation (Polyn et al., 2009a). As in the current work, support for this neural-cognitive linking hypothesis would take the form of improved behavioral predictions. In this case, an informative neural signal would improve the model's ability to predict variability in source organization during memory search, providing information regarding the representation of source attributes in the MTL. This approach may also prove valuable in relating distributed neural representations of semantic structure (Haxby et al., 2001; Kriegeskorte et al., 2008) to the behavioral dynamics of memory search (Socher et al., 2009; Manning et al., 2012; Morton et al., 2013).

The hypothesis that MTL subregions indicate the success of memory search was also strongly supported by the data: Activity in the anterior extent of MTL cortex, including perirhinal cortex, demonstrated the strongest evidence for the retrieval success process during memory search. Fluctuations in these regions during memory search did not indicate whether recalled materials will be temporally organized; however, when activity in these regions declined, participants were more likely to terminate search. This is consistent with prior work implicating perirhinal cortex in the associative retrieval of item details (Kirwan and Stark, 2004; Düzel et al., 2003; Law et al., 2005; Diana et al., 2009). One interpretation of these results is that anterior PHG activation during retrieval reflects the reactivation of item-specific information during memory search. This information could then be projected to executive and attentional systems to determine task relevance, and to linguistic systems for verbal report. Under this interpretation, activity in this region would indicate retrieval success (measured in terms of the verbal reports made by the participant), but the level of engagement would not necessarily indicate the temporal organization of the recalled materials.

We observed neural signal in a left MTL region, spanning hippocampus and adjacent entorhinal and parahippocampal cortices, that was informative for both the retrieval success and temporal reinstatement mechanisms of our computational model. A joint model, in which both of these mechanisms were influenced by neural signal, was favored over the other models, when utilizing signal from these regions (Figure 13). One possibility is that these two cognitive processes produce independent neural signals, and hemodynamic activity in this region simply reflects a superposition of these signals. However, it is also possible that the neural circuitry of the posterior MTL performs a function that is important for both of these cognitive operations. Our findings linking the hippocampus to both computational mechanisms align with theories in which this region plays a domain-general role in the retrieval of associative information (McClelland et al., 1995; Diana et al., 2007). Electrophysiological studies with high temporal resolution support this idea, suggesting that associative information flows from the hippocampus to cortex during memory tasks (Naya and Suzuki, 2011; Staresina et al., 2012a). Future computational studies of MTL function may identify a single mechanism signaled by activity within posterior hippocampus and parahippocampal cortex, arbitrating between these possibilities.

We found that the computational mechanisms defined by the model were differentially engaged along the anterior-posterior axis of the MTL, highlighting the anatomical organization of functional signals within this region. Temporal reinstatement effects showed stronger engagement in the posterior hippocampus and PHG, and recall success effects showed stronger engagement in the anterior hippocampus and PHG (Figure 13). A number of studies have examined how the functional properties of the MTL shift as one moves along this anterior-posterior axis. Neuroimaging studies of cued recall suggest that the representational content of retrieved information is important, with retrieval of visual object and scene information driving perirhinal and parahippocampal cortices, respectively (Staresina et al., 2011, 2012b, 2013). A shift in representational selectivity has also been observed in hippocampus; while posterior hippocampus is selectively engaged by scene information, anterior hippocampus seems to be agnostic to the representational content of studied material (Liang et al., 2012; LaRocque et al., 2013; Huffman and Stark, 2014). It has been suggested that the selective engagement of parahippocampal cortex for scene information indicates a more general role in contextual processing, with scenes engaging mechanisms involved in encoding spatial context (Davachi, 2006). This is consistent with a number of studies relating parahippocampal cortical activity to source context (Davachi et al., 2003), nonspatial contextual attributes (Aminoff et al., 2007), and temporal context (Turk-Browne et al., 2012; Hsieh et al., 2014). Our study provides converging evidence for the idea that posterior regions of MTL (namely, posterior hippocampus and parahippocampal cortex) are involved in contextual processing, and our model raises the possibility that context-sensitive neural signals in this region are shaped by the cognitive mechanisms underlying temporal reinstatement.

The findings provided by our neurally informed computational model of memory search represent a significant advance in the ability to understand the contributions of the MTL to human memory. Directly relating neural signals to computational mechanisms has led to advances in a number of cognitive domains, including visual search (Purcell et al., 2012), reinforcement learning (Daw et al., 2011), object categorization (Nosofsky et al., 2012), and problem solving (Rosenberg-Lee et al., 2009). While a number of recent studies suggest the promise of this approach in the domain of episodic memory (Manning et al., 2011; Polyn et al., 2012; Turner et al., 2013a; Polyn and Sederberg, 2014), our understanding of the cognitive processes engaged in memory search remains tentative. A number of prior studies have used GLM-based approaches to make inferences about the functional contributions of MTL regions during memory search (Long et al., 2010; Shapira-Lichter et al., 2012; Kragel and Polyn, 2015). These inferences rely on the logic of cognitive subtraction, which involves the partitioning of behavioral events into distinct groups, and relies on the assumption that a particular cognitive operation is differentially engaged for the two groups. In and of itself, the GLM does not provide evidence regarding the plausibility of this differential engagement, or even whether the proposed cognitive operation is sufficient to account for the observed behavior. By incorporating well-specified cognitive operations directly into the analytic model, our approach overcomes this limitation. The ability of the model to account for the observed behavioral phenomena (Figure 9) demonstrates the sufficiency of the cognitive operations used in the model. With the basic form of the model validated, improvement in the predictive power of a neurally informed model allows us to draw inferences regarding the cognitive processes associated with the observed neural signal. Using this approach, we have developed, to our knowledge, the first computational model using activation of the MTL to predict the organization of human memory, allowing us to make inferences about the mechanisms that are sufficient to give rise to mental time travel.

The neurally informed computational models presented here link particular regions of the MTL with the cognitive operations that enable an individual to search through memories of their past experience. Neural signal in the posterior MTL indicated the fidelity of mental time travel, consistent with the proposal that this region specifies the spatiotemporal context of a memory. Neural signal within multiple MTL structures, including the perirhinal cortex, reflected succesful item retrieval. Neural signal in the hippocampus was linked to both mental time travel and retrieval success, consistent with the proposal that associative structures in this region support the reactivation of mnemonic representations in cortex. This approach demonstrates how computational models of cognition can be integrated with models of neural activation, providing a unified framework to test specific hypotheses regarding how fluctuations in neural signal map onto the dynamics of thought.

CHAPTER V

Dynamics of large-scale cortical networks reveal the cognitive control of episodic memory[4]

Abstract

Distributed large-scale brain networks are thought to exert cognitive control to flexibly guide episodic memory, but the specific functions of these networks remain unclear. We estimated large-scale network activity using independent component analysis of fMRI data as participants performed a memory search task. A short delay following a study list was either unfilled, encouraging the maintenance of episodic information, or contained disruptive math distraction, encouraging reinstatement of the target episodic context. A computational model was used to formalize hypotheses linking large-scale network activity to cognitive control mechanisms supporting maintenance or contextual reinstatement. In the absence of distraction, dorsal attention network activity signaled contextual reinstatement, but after distraction, a frontoparietal control network was linked to this process, showing functional coupling with other large-scale networks, and with posterior medial temporal lobe. These novel behavioral correlates to large-scale brain activity provide insight into the mechanisms facilitating the cognitive control of human memory.

Introduction

Cognitive neuroscientific models of human memory propose that the medial temporal lobe (MTL) system, and in particular, the hippocampus, is critically important for the formation and retrieval of episodic memories of one's past experience (Moscovitch, 1992; Cohen and Eichenbaum, 1993; McClelland et al., 1995; Diana et al., 2007; Ranganath and Ritchey, 2012). In these theories, the MTL is often described as a repository of associative structures that support the reactivation of neuronal ensembles that represent the episodic past. Neural networks spanning prefrontal, parietal and temporal cortices interact with the hippocampus and other MTL structures to flexibly retrieve

---

[4] James E. Kragel and Sean M. Polyn. Dynamics of large-scale cortical networks reveal the cognitive control of episodic memory. *Submitted for publication*, 2015.

memories in a task-appropriate fashion (Miller, 1991; Moscovitch and Winocur, 1992; Buzsáki, 1996; Polyn and Kahana, 2008; Budson and Solomon, 2011). In the past few decades, we have learned a great deal about the nature of these interactions, but the computational mechanisms that enable large-scale cortical networks to control the human memory system remain unclear. However, computational models of human cognition suggest two core mechanisms that may underlie these interactions: First, an integrative mechanism allowing cortical regions to maintain neural representations in the face of distracting, task-irrelevant activity, and second, a cuing mechanism that allows neural representations in cortex to trigger the retrieval of episodic memories.

In the model of prefrontal function proposed by Miller and Cohen (2001), an integrative mechanism allows prefrontal circuitry to maintain task-relevant information in an active state, allowing prefrontal cortex (PFC) to guide processing in posterior cortical regions in a task-appropriate manner. This mechanism supports working memory, in that it allows information to be maintained even in the presence of distracting, task-irrelevant neural signals (Miller et al., 1996). This functional property of PFC has been most reliably associated with neural activity in dorsolateral PFC (DLPFC) in a large number of neuroimaging studies (Cohen et al., 1997; Postle, 2006; Sakai et al., 2002; Postle, 2005; Clapp et al., 2010). Recently, Feredoes et al. (2011) demonstrated that stimulation of DLPFC during distraction elicits increased activity in posterior cortical regions that represent information in working memory, providing causal evidence for its role in top-down control. These findings support the idea that recurrent neural activity between the prefrontal cortex and posterior regions, such as parietal cortex, is important for guiding one's attention to relevant information, and then holding that information in mind (Corbetta and Shulman, 2002; Hasselmo and Stern, 2006).

A number of theories suggest that frontal and parietal cortical regions are critically involved in the cognitive control of episodic memory retrieval, and suggest particular mechanisms allowing these regions to guide the construction and utilization of retrieval cues in a task-appropriate manner (Moscovitch and Winocur, 2002; Becker and Lim, 2003; Simons and Spiers, 2003; Polyn and Kahana, 2008). In neural network models of episodic memory, such as the Complementary Learning Systems (CLS) model of McClelland et al. (1995), a retrieval cue is a distributed pattern of cortical activity that can be used to prompt the hippocampal memory system to reactivate associated episodic memory traces (Norman and O'Reilly, 2003). This reactivated episodic information specifies the spatiotemporal context of a particular past experience, and is thought to be related to the subjective experience of revisiting the past, sometimes referred to as *mental time travel* (Tulving, 1993). These ideas are supported by neuroscientific studies showing that patterns of cortical activity observed during episodic retrieval match the patterns seen during the original study event (Danker and Anderson, 2010). Neuroimaging studies demonstrating the reactivation of category-specific information (Polyn et al., 2005; Morton et al., 2013), task-specific information (Johnson and Rugg, 2007; Polyn et al., 2012), and perceptual information (Wheeler et al., 2000; Bosch et al., 2014), support the generality of this mechanism. Recently, researchers have shown that event-specific patterns are reactivated during episodic retrieval, in prefrontal, temporal, and parietal cortices (Staresina et al., 2013; Kuhl and Chun, 2014). Furthermore, the reactivation of event-specific patterns of cortical activity has associated with increased hippocampal activation (Ritchey et al., 2013; Bosch et al., 2014; Gordon et al., 2014), consistent with theories positing that hippocampal associative structures are critically involved in episodic retrieval.

There is growing consensus in the neuroimaging literature that cognitive control operations are associated with activity in widespread networks of brain regions spanning frontal, parietal, and temporal cortices, with distinct networks associated with distinct aspects of cognitive control (Corbetta and Shulman, 2002; Fox et al., 2006; Vincent et al., 2006; Dosenbach et al., 2008). These networks reveal themselves in analyses of the covariance structure of neuroimaging data; sub-regions within a network may be anatomically distant, but show highly correlated timecourses of neural activation while a participant is at rest (Vincent et al., 2008), as well as during cognitive task performance (Smith et al., 2009). This has motivated the use of statistical techniques such as independent component analysis (ICA) to identify these networks and relate changes in the activation of a particular network to cognitive demands (e.g., Kragel and Polyn, 2015). The dorsal attention network (DAN), which includes regions in dorsal parietal cortex and the frontal eye fields, has been associated with the goal-directed guidance of attention to visuo-spatial information

(Corbetta and Shulman, 2002). The ventral attention network (VAN), on the other hand, which includes regions in inferior prefrontal and parietal cortex, as well as the dorsal anterior cingulate, is more engaged during stimulus-driven attentional capture. The DAN is often contrasted with the default mode network (DMN), which has been associated with internally directed attention, mind-wandering, and memory retrieval (Buckner et al., 2008). The DMN spans the lateral and medial temporal lobes, the angular gyri, and midline regions in prefrontal and posterior parietal cortex, and shows a great deal of overlap with a putative recollection network implicated in the reactivation of episodic information (Okada et al., 2012).

The nature of the interactions between these large-scale brain networks is an area of active research. It has been proposed that the DAN and DMN act in opposition to one another (Fox et al., 2005), with suppression of the DMN requisite for performance on cognitively demanding tasks (Anticevic et al., 2012). This is consistent with the finding that the DMN is suppressed when participants must maintain information in working memory in the face of distraction (Chadick and Gazzaley, 2011). However, recent studies examining interactions between these large-scale networks suggest that this opposition is not observed during retrieval of information from long-term memory (Fornito et al., 2012; Kragel and Polyn, 2015). During internally directed retrieval, a frontoparietal control network (FPCN) spanning lateral prefrontal cortex and the anterior inferior parietal lobe, has been proposed to serve as an interface between the attentional system reflected in DAN activity with the memory system reflected in DMN activity (Vincent et al., 2008).

The goal of the current work is to more precisely specify the cognitive operations associated with neural activity in these large-scale brain networks. In order to do this, we tracked the activity in these large-scale brain networks as participants performed a memory search task designed to pit the cognitive operations of active maintenance and memory retrieval against one another. Specifically, participants studied a list of words, which was followed by a short delay period. In one set of trials, the delay was unfilled, facilitating control operations supporting the active maintenance of information related to the last few studied items. In the rest of the trials, participants performed a math distraction task during the delay, challenging active maintenance, and encouraging the engagement of control operations triggering episodic memory retrieval. Dynamics of large-scale brain networks were characterized during this delay, both in terms of their response to distracting task performance, and in terms of their interactions with one another, and with an MTL region implicated in episodic retrieval. A neuro-cognitive model of memory search (Kragel et al., 2015) allowed us to test specific hypotheses linking activity in large-scale networks to particular cognitive control operations. This modeling framework specifies the linkage from neural signal, to cognitive operation, to behavioral observation, allowing one to assess the validity of a specific neuro-cognitive linking hypothesis in terms of whether the neural signal improves the ability of the model to predict the behavior of the participant, on a trial-by-trial basis.

Results

Using distraction to challenge the memory system

We used a variant of the free-recall paradigm to examine the effects of distraction on the ability of the human memory system to retrieve recently learned information (Figure 14a). Participants recalled a similar percentage of studied items after performing the distraction task (66.4 ±0.04 SEM) as after an unfilled delay interval (65.5 ±0.04 SEM); this difference was not statistically significant ($t_{19} = 0.73$, $p = 0.47$).

Consistent with prior work (Postman and Phillips, 1965; Glanzer and Cunitz, 1966), the presence of distraction during the delay interval led to a reduction in the memorability of end-of-list items. As shown in Figure 14b, the terminal list item was more likely to be recalled during unfilled, relative to filled, trials ($t_{19} = 4.96$, $p < 0.0001$). The effect of end-of-list distraction can be seen in terms of recall initiation (Fig.14c). On trials with an unfilled delay, recall was initiated with the terminal list item on 20.5 (±0.05 SEM) percent of trials, and with the start-of-list item on 22.1 (±0.05 SEM) percent of trials. When the distraction task was performed during the delay interval, the recency effect was attenuated and the primacy effect was enhanced: Recall was initiated with the terminal list item on 11.9 (±0.03 SEM) percent of trials, and with the start-of-list item on 32.4 (±0.05 SEM) percent of trials. A repeated measures ANOVA revealed a significant interaction between condition

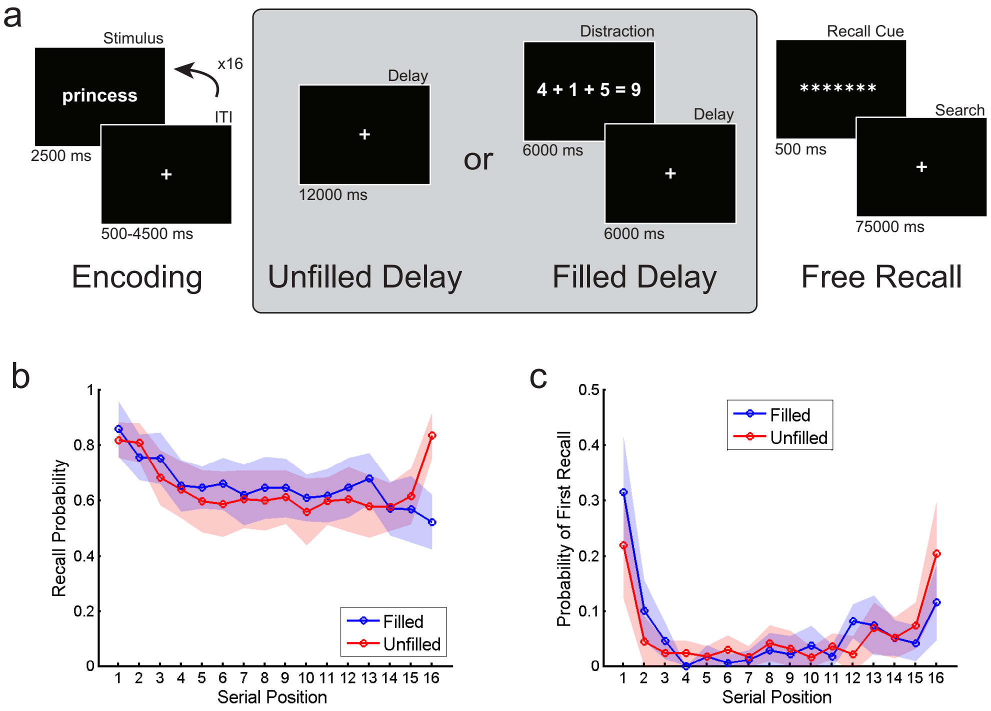

Figure 14. Using free recall to investigate context-based mechanisms. **(a)** Free recall paradigm. **(b)** Mean proportion of items recalled and **(c)** probability of first recall for each delay condition. Shaded regions represent SEM.

(filled vs. unfilled delay) and recall initiation ($F_{1,19} = 5.45$, $p = 0.03$).

Examining the effect of distraction on large-scale brain network activity

We used ICA to identify a set of large-scale brain networks, and to estimate the contributions of these networks to the observed blood oxygenation level-dependent (BOLD) response. In order to determine how the networks identified in this study relate to other large-scale networks identified in the literature, we carried out a spatial correspondence analysis to identify components whose spatial maps were consistent with the spatial maps of large-scale networks identified by Yeo et al. (2011), in a study examining resting-state functional connectivity in 1,000 participants.

This analysis revealed six ICs that demonstrated a high degree of spatial correspondence with intrinsic networks of interest (Figure 15a). A single component, IC9, had a high degree of spatial overlap with the DAN ($r = 0.4448, p < 0.00001$). Another component, IC8, was consistent with the ventral attention network (VAN; $r = 0.2977, p < 0.00001$). Two ICs were spatially consistent with the frontoparietal control network (FPCN): IC21 was predominantly right-lateralized ($r = 0.3368, p < 0.00001$), and IC49 was predominantly left-lateralized ($r = 0.3435, p < 0.00001$). Two networks were spatially consistent with the default mode network (DMN): IC27 ($r = 0.3038, p < 0.00001$), which included posterior cingulate cortex and midline cortical regions, and IC53 ($r = 0.157, p < 0.00001$), which included left angular gyrus and middle frontal gyrus.

Consistent with prior work showing that challenging working memory with distraction engages networks spanning lateral prefrontal cortex (Sakai et al., 2002; Jha et al., 2004), we found a number of ICs with frontoparietal coverage that exhibited consistent changes in activation during the delay period. A linear regression was used to characterize the differential response profile for these ICs between filled and unfilled delay conditions.

The DAN (IC9) was reliably more engaged during the filled delay than the unfilled delay ($t_{19} = 3.31, p = 0.008$), with activation for the unfilled delay less than the implicit baseline of the regression ($t_{19} = -2.57, p = 0.023$). The VAN (IC8), on the other hand, increased in activity during both unfilled and filled delay periods, relative to baseline (unfilled delay: $t_{19} = 4.28, p = 0.0024$; filled delay: $t_{19} = 4.16, p = 0.0011$).

The FPCN (IC21, IC49) components were reliably engaged for both types of delay interval: IC21 (right FPCN), unfilled delay: $t_{19} = 3.15, p = 0.010$; filled delay: $t_{19} = 5.85, p < 0.0001$. IC49 (left FPCN), unfilled delay: $t_{19} = 3.84, p = 0.0033$; filled delay: $t_{19} = 7.65, p < 0.0001$. Furthermore, both FPCN components showed reliably more engagement when the delay was filled, compared to unfilled (IC21: $t_{19} = 3.26, p = 0.0083$; IC49: $t_{19} = 5.14, p = 0.0004$).

Consistent with prior work examining the effect of task-based distraction during memory maintenance, the DMN components (IC27, IC53) showed suppression in the presence of distraction (Wager et al., 2013). IC53 decreased in activation during the filled delay ($t_{19} = -3.58, p = 0.003$), but remained near baseline on unfilled lists ($t_{19} = -0.86, p = 0.40$). IC27 showed decreased engagement during the filled, compared to the unfilled delay period ($t_{19} = -2.79, p = 0.017$). This effect was driven by an increase in activity during unfilled delay ($t_{19} = 2.22, p = 0.046$).

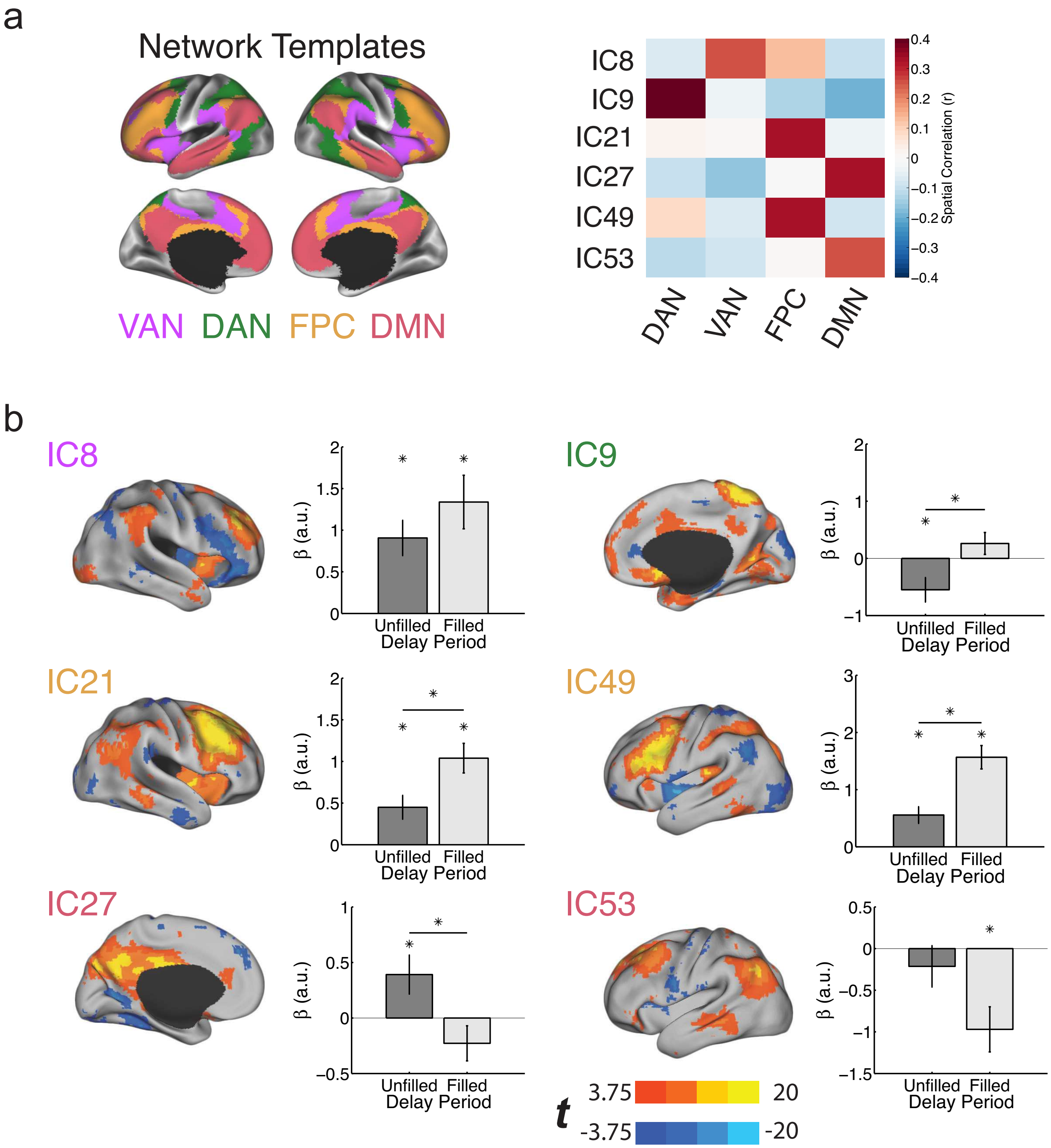

Figure 15. Estimation of large-scale brain networks using ICA. **(a)** Spatial ICA was applied to temporally concatenated group fMRI data, resulting in identification of 61 ICs. A spatial correlation analysis was used to identify ICs corresponding to parcellation maps of the cortical surface (Yeo et al., 2011). Six ICs exhibited positive spatial correlations with networks of interest. DAN, dorsal attention network; VAN ventral attention network; FPCN, frontoparietal control network; DMN default mode network. **(b)** Large-scale networks and their response to distraction. Left, representative t-maps of group-level spatial IC loadings ($p < 0.001$, uncorrected). Right, average β parameters estimating IC activity during the filled and unfilled delay periods. $*$, $p < 0.05$ FDR corrected. a.u., arbitrary units.

Functional connectivity between large-scale networks and the MTL shifts with distraction

These shifts in activation of the large-scale brain networks during the delay could reflect a variety of cognitive control operations related to the maintenance and retrieval of task-relevant mnemonic information. A recent study by Zanto et al. (in press) demonstrates that even with only a single stimulus to be maintained across a short delay, MTL memory systems are engaged if participants anticipate (and encounter) distraction during that delay. Thus, shifts in large-scale network activity may indicate not only the top-down filtering of distracting information, but also the engagement of MTL-based circuitry to support memory performance.

As described above, we observed increased activation of DAN under conditions of distraction, which may reflect the attentional system processing the visually presented distraction stimuli. DMN activity was suppressed during this distraction, but was higher during an unfilled delay, perhaps reflecting attention to internally maintained representations of the studied material. A cingulo-opercular network, which partially overlaps with the VAN examined in the current study, has been proposed regulate the relative activation of the DMN and DAN (Sridharan et al., 2008). Furthermore, the FPCN has been proposed to serve as an interface between DMN and DAN, in tasks where long-term memory structures are important for task performance (Vincent et al., 2008). These ideas motivated us to examine the functional interactions of these networks during the delay interval of the current experiment.

To characterize the contributions of the MTL during the delay period, we constructed a functional ROI that spanned bilateral parahippocampal gyrus and hippocampus. In previous work, this ROI was shown to be involved in the reinstatement of contextual information that guides memory search (Kragel et al., 2015). Examination of the response of this region during the delay period revealed a sustained increase in activation during filled ($t_{19} = 2.35$, $p = 0.029$) but not unfilled ($t_{19} = 1.05$, $p = 0.31$) delay periods (Fig. 16a). To examine whether this MTL activation in the presence of distraction is related to its interactions with putative control networks, we conducted a correlational psychophysiological interaction (cPPI) analysis (Fornito et al., 2012) to examine task-based changes in functional connectivity during the delay period.

Multiple large-scale networks showed reliable delay-dependent interactions with one another, and with the MTL ROI (Fig. 16b). Specifically, the left lateralized FPCN and the VAN showed increased functional coupling to the MTL during the filled, relative to the unfilled delay periods (FPCN: $t_{19} = 5.31$, $p = 0.0004$; VAN $t_{19} = 6.42$, $p = 0.0004$). The left FPCN also exhibited relative increases in functional connectivity to both the VAN ($t_{19} = 3.35$, $p = 0.024$), as well as a subnetwork of the DMN anchored in the PCC ($t_{19} = 2.90$, $p = 0.048$) during the filled delay periods, relative to the unfilled delay periods. These interactions are consistent with prior work implicating a cingulo-opercular network (which overlaps considerably with the VAN) in regulating the relative engagement of the DMN and the DAN (Sridharan et al., 2008), as well as prior work proposing that the FPCN serves as an interface between the attentional systems of the DAN, and the memory systems of the DMN (Vincent et al., 2008).

We carried out a secondary analysis separately contrasting functional connectivity during the filled and unfilled delay periods to baseline estimates of functional connectivity. The functional interactions observed during the unfilled delay were not reliably different from baseline. In the filled delay period, we observed decreased functional coupling between the two subnetworks of the DMN, relative to baseline ($t_{19} = -3.67$, $p = 0.034$). Given that the cPPI analysis accounts for differences in activity associated with performance of the distraction task, as well as any potential sustained responses during the delay period, these shifts in functional connectivity likely reflect task-context-dependent shifts in the interactions of these large-scale networks (Friston et al., 1997).

Linking large-scale brain networks to cognitive operations

The preceding results demonstrate that a brief period of distraction causes recruitment of multiple large-scale brain networks that interact with each other, and with a posterior MTL region. In order to more clearly relate activation in these networks to behavioral performance of participants in this task, we developed a computational model describing a set of interacting cognitive operations sufficient to produce the recall behavior observed in this task (Kragel et al., 2015). The framework associated with the model allows one to formalize specific neuro-cognitive linking hypotheses,

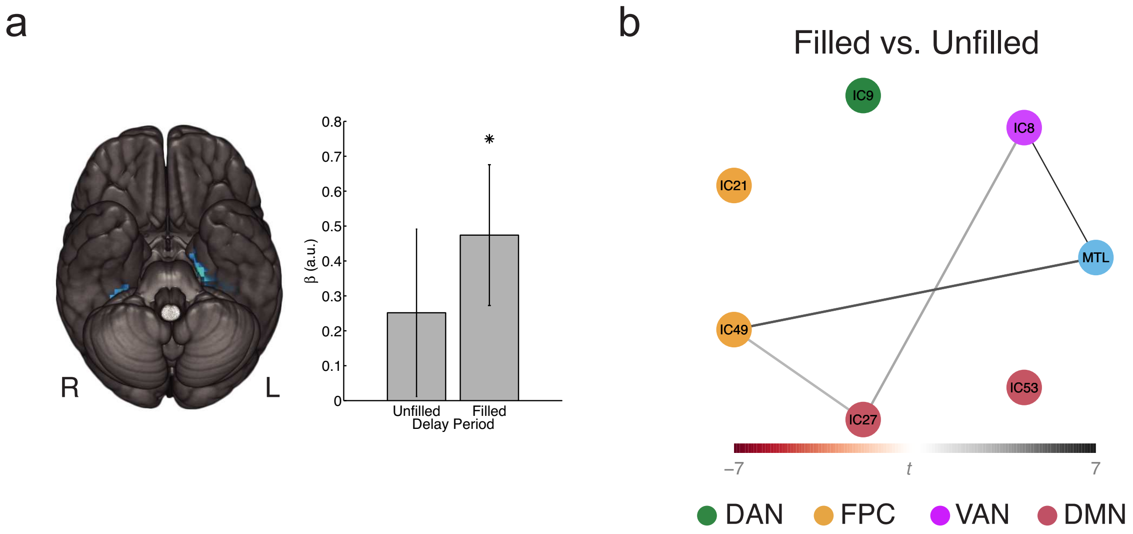

Figure 16. Distraction causes engagement of MTL and shifts in functional connectivity. **(a)** A functional ROI within bilateral MTL exhibits increased activity in the presence of distraction. Mean β estimates of sustained delay-period activity within the MTL are depicted, with error bars depicting standard error. $*$, $p < 0.05$. **(b)** Reorganized functional connectivity in the presence of distraction. Significant differences ($p < 0.05$, FDR corrected) in functional connectivity are denoted by weighted lines. Black lines indicate increased functional connectivity during the filled, relative to the unfilled, delay intervals.

whereby a particular neural signal is used to control a corresponding cognitive operation in the model. If this linkage improves the ability of the model to predict the specific sequence of recalled items produced by participants, this is taken as support for the hypothesis that the neural signal is related to that cognitive operation.

We examined two cognitive mechanisms that could be engaged during the delay period, and whose operation might be reflected in the activation of large-scale brain networks: First, a contextual disruption (CD) process that signals whether mnemonic information is disrupted by distraction, or is successfully maintained across the delay, and second, a contextual retrieval (CR) process that signals whether associative structures are being used to reactivate prior contextual states (a process often called *mental time travel*; Tulving 1993). Engagement of each of these mechanisms during the delay produces a distinct behavioral signature, in terms of how the participant initiates recall: Successful maintenance of mnemonic information through the delay is associated with initial recall of recent (end-of-list) items. Figure 17a shows how the predictions of the model change as distraction becomes more disruptive to the maintained retrieval cue. Successful contextual retrieval is associated with initial recall of the primary (start-of-list) items. Figure 17b shows how model predictions change in terms of the fidelity of this retrieved contextual information.

A baseline version of the model was fit to the behavioral data from the filled-delay and unfilled-delay conditions, and parameter estimates from this model were examined to determine whether there was evidence that the CD and CR mechanisms were more strongly engaged during the filled-delay trials than the unfilled-delay trials. We carried out a differential evolution Markov chain Monte Carlo approach to estimate the posterior distributions of the different model parameters, and used an encompassing prior approach (Wetzels et al., 2010) to sample from these posterior distributions and determine whether the model provided evidence for enhanced engagement of these cognitive operations in the presence of distraction, as quantified by the Bayes factor (BF) statistic. Due to the uniform priors assumed in these analyses, the maximum evidence that can be attained is a Bayes factor of 2.

There was little support for the hypothesis that contextual disruption was increased in the filled-delay condition: Only 27.9% of sampled models were consistent with this prediction ($BF = 0.55$). This may be related to the general difficulty of maintaining an end-of-list contextual state for 12 seconds in the unfilled-delay condition. Despite the lack of evidence for a general increase in CD between the two conditions, it is still possible that this mechanism is differentially engaged on different trials within each condition, and this differential engagement may correspond to trial-by-trial fluctuations in a particular neural signal. On the other hand, there was strong evidence that contextual retrieval was enhanced after distraction: 97.9% of sampled models supported this prediction ($BF = 1.93$).

We developed two families of neurally informed computational models of memory search in order to test whether the recruitment of large-scale cortical networks was related to cognitive processes that determine whether information encoded in either recent (end-of-list), or past (start-of-list), contextual states is accessible during memory retrieval. The CD model family allowed delay-period neural activity to influence whether an internal representation of context was maintained

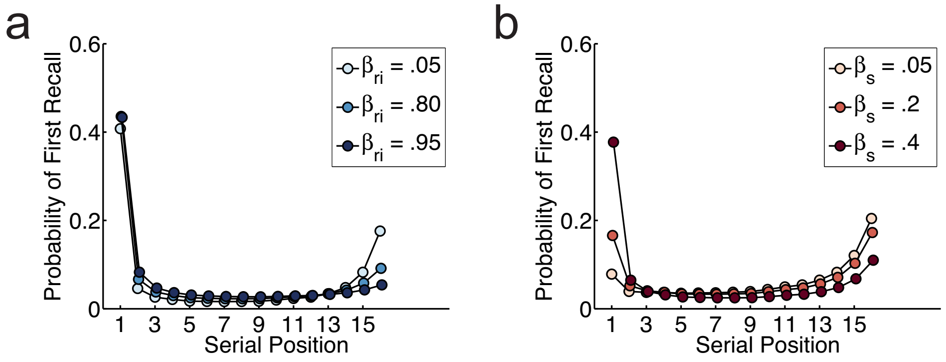

Figure 17. Relating large-scale network activity to cognitive mechanisms. **(a)** Behavioral correlates of contextual disruption (CD). A low value of the β_{ri} parameter indicates that a contextual retrieval cue is successfully maintained in the face of distraction, leading to an enhanced likelihood of initiating recall with an item from the end of the list. In contrast, a high value of β_{ri} indicates that the contextual retrieval cue is disrupted, leading to a more even spread of recall initiation across the list items. **(b)** Behavioral correlates of contextual retrieval (CR). A high value of the β_s parameter indicates the successful retrieval of the context representation associated with the beginning of the study list, leading to an enhanced likelihood of initiating recall with an item from the start of the list. In contrast, a low β_s value indicates failure to retrieve start-list context, leading to a more even spread of recall initiation across the list items.

or disrupted during the delay (Fig. 17a). In this family of models, delay-period network activity recorded on individual trials influenced the contextual disruption parameter, allowing us to test whether activity in a particular network signaled the likely recall of recently learned information. The CR model family was used to determine whether network activity predicts the ability of the memory system to access individual items studied at the beginning of the study episode (Fig. 17b). In this family of models, delay-period network activity recorded on individual trials influenced the contextual retrieval parameter, allowing us to test whether activity in a particular network signaled the likely recall of more temporally distant information. The performance of a given neurally informed model is reported in terms of a deviance statistic (D) which quantifies the improvement in predictive power of the neurally informed model relative to a neurally naive baseline model.

Activation of a single network was linked to the context disruption mechanism: IC9, which is highly spatially consistent with the DAN, was related to context disruption in simulations of both filled-delay and unfilled-delay trials (Fig. 18a). Engagement of this network improved the ability of the CD model to predict recall initiation following both unfilled ($D = 4.03$, $p = 0.044$) and filled

($D = 3.95$, $p = 0.047$) delay periods. This model described a positive relationship between the context disruption parameter, β_{ri}, and observed activation in this network during both delay periods ($\nu_u = 0.042$, $\nu_f = 0.016$). Figure 18c (green bars) shows how activity in this network relates to recall initiation: Increased DAN activity corresponds to a decreased likelihood of initiating recall with an end-of-list item, without a corresponding increase in the likelihood of initiating with a start-of-list item. Activity in a subnetwork of the DMN (IC27) also reflected contextual disruption, but only in the unfilled-delay condition ($D = 4.78$, $p = 0.029$, $\nu_u = 0.977$). Neural signal estimated from the remaining networks of interest did not improve the ability of models within this family to predict recall sequences ($ps > 0.36$).

Activation in the FPCN (IC49) signaled reinstatement of start-of-list contextual information on filled-delay trials (Fig. 18b). Increased recruitment of this network predicted individuals would initiate recall from the beginning of the list ($\nu_f = 0.052$). Likelihood-ratio tests revealed improved fitness of this model, relative to the neurally naive baseline model, in terms of predicting recall sequences during the filled-delay trials ($D = 5.69, p = 0.017$). Figure 18c (orange bars) shows how FPCN activity relates to recall performance; when FPCN activity is high during the delay, there is a slight decrease in the likelihood of initiating recall with an end-of-list item, with a corresponding increase in the likelihood of initiating recall with a start-of-list item. Activity in the previously mentioned DAN also reflected contextual reinstatement, but only in the unfilled-delay condition ($D = 4.96$, $p = 0.026$).

In our analysis of network interactions (Fig. 16b), we found that the FPCN increased its functional coupling to a MTL region of interest that was associated with contextual retrieval in prior work Kragel et al. (2015). This MTL region also showed enhanced engagement during filled-delay periods (Fig. 16a). We tested whether activity in this region was related to the CD and CR model mechanisms in these data. Activity in this region was related to the CR mechanism in the filled-delay trials ($D = 6.20$, $p = 0.013$, $\nu_f = 0.051$) but not in the unfilled-delay trials ($D = 2.97$, $p = 0.085$, $\nu_u = 0.035$). Neural signal from this region was informative for the CD model as well, improving prediction on filled-delay ($D = 6.51$, $p = 0.011$, $\nu_f = 0.1188$) but not unfilled-delay ($D = 3.15$,

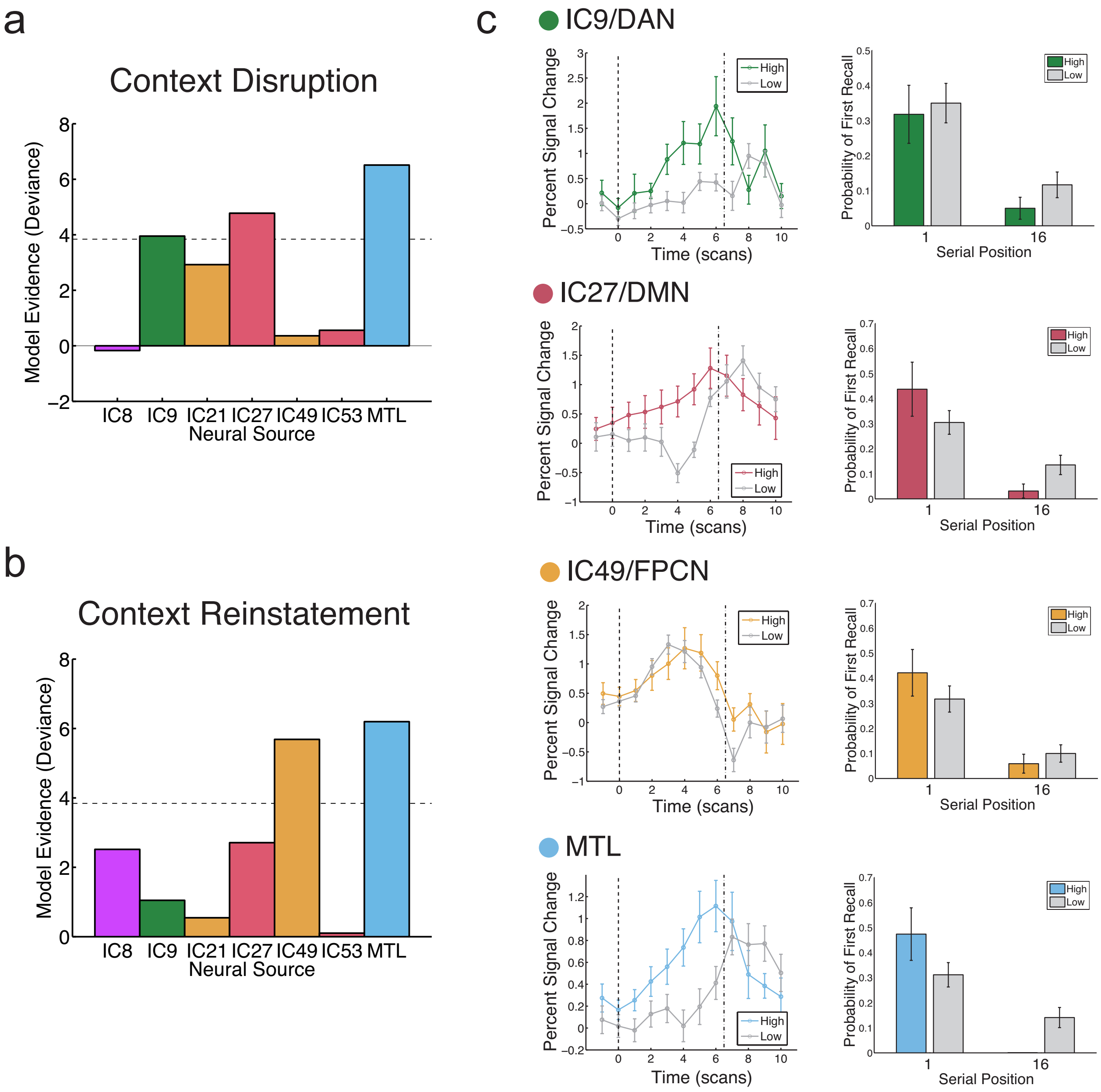

Figure 18. Large-scale brain network and MTL activity reflect distinct computational mechanisms during the filled-delay condition. **(a)** Evidence for neurally informed context disruption models. **(b)** Evidence for context reinstatement models. Deviance statistics above the critical value (denoted in the dashed line) are significant at $p < 0.05$, uncorrected. **(c)** Changes in recall initiation associated with delay-period activation. Left, average activity during the filled delay. The dashed and dotted vertical lines denote the onset of the delay and recall periods, respectively. Right, average probability of recall initiation. Data are partitioned at the 80% quantile. Error bars depict SEM.

$p = 0.076$, $\nu_u = 0.031$) trials.

Figure 18b (bottom panel) demonstrates how neural signal in this region relates to recall initiation on filled-delay trials. When MTL activity was low during the delay period (gray bars), participants sometimes initiated with an item from the beginning of the list, and sometimes with an item from the end of the list. However, when MTL activity was high during the delay (blue bars), the likelihood of initiating recall with start-of-list item increased (consistent with the CR model; Fig. 17b), and the likelihood of initiating with an end-of-list item dropped (consistent with the both CD and CR models; Fig. 17a & b).

While MTL regions are strongly represented in the DMN, our model-based approach dissociated MTL activity from DMN activity. Whereas a number of neuroimaging studies suggest that the DMN supports episodic recollection (Vincent et al., 2006; Okada et al., 2012) and autobiographical memory retrieval (Spreng and Grady, 2009; Svoboda et al., 2006), activity in this network was not informative for the contextual retrieval mechanism in the model (Fig. 18b). Increased DMN activity during the delay reliably indicated a substantially diminished likelihood of initiating recall with an end-of-list item (Fig. 18c, red bars), which was more informative for the CD model than for the CR model. Taken together, these findings are consistent with the idea that the MTL proper mediates contextual retrieval, while activation of the broader cortico-hippocampal DMN reflects whether attention is directed to these internal representations generated by the MTL subsystem (Buckner et al., 2008).

Materials and Methods

Experimental Design

Twenty individuals (14 female) with an average age of 21.64 ± 0.88 years (mean ± SD) provided written, informed consent to participate in the study for monetary compensation, in accordance with the procedures of the Vanderbilt University Institutional Review Board. Participants performed up to 18 trials of a free-recall task, while fMRI data was collected. Each trial consisted of three distinct phases: encoding, delay, and free recall. During the encoding period, participants studied a list of

16 items. Items were presented for 2.5 sec, during which subjects rated the size of the displayed stimulus (i.e., determining whether the stimulus will fit into a shoe box) using an MRI compatible response box. Following the presentation of each stimulus, a fixation cross was displayed during an inter-stimulus interval ranging between 0.5-4.5 s. On each trial, one of two delay period conditions followed the encoding period. For unfilled trials, a fixation cross remained on the screen for 12 s; this delay condition occurred on 50% of trials, pseudo-randomly ordered such that three consecutive lists of the same type did not occur. On filled trials, participants performed six seconds of a self-paced arithmetic task. During this task, mathematical statements (e.g., Figure 14a) were presented in the center of the screen. Participants made a true/false judgment for each mathematical statement, using two buttons on the manual response box. Following the delay, a row of asterisks was displayed on the screen for a duration of 0.5 s, indicating the start of the free-recall period. Subjects were instructed to vocally recall items studied on the most recent list, in any order. Audio recordings of speech were collected using a scanner-safe microphone (Resonance Technologies, Inc.), and were annotated with Penn TotalRecall (http://memory.psych.upenn.edu/TotalRecall).

Image Acquisition

Imaging was performed at the Vanderbilt University Institute of Imaging Science, collected with a 3T Philips Intera Achieva magnet. Functional images were collected using an interleaved gradient echo $T2^*$-weighted pulse sequence with BOLD contrast (TR=2000 msec, TE=30 msec, flip angle=75^o, voxel size=3.0x3.0x3.6 mm, FOV=192 mm). 30 oblique slices, oriented parallel to the AC-PC plane were collected during functional imaging. Whole brain structural scans were acquired using an MP-RAGE sequence (TR=2500 msec, TE=4.38 msec, flip angle=8^o, voxel size=1.0x1.0x1.0mm, FOV=256 mm).

Image Processing

Preprocessing was carried out using the SPM8 (Wellcome Trust Centre for Neuroimaging, University College Longon, England) software package, as follows: The first four functional images of each session were discarded to allow scanner signal to equilibrate. The remaining functional volumes from each run were realigned to the first functional scan, in order to correct for head motion. The mean of this realigned series was computed and coregistered to the T1 structural image. Anatomical segmentation and registration were performed using the VBM8 toolbox, (C. Gaser, Department of Psychiatry, University of Jena, Germany; http://dbm.neuro.uni-jena.de/vbm8). Gray matter, white matter, and cerebrospinal fluid images were spatially aligned using DARTEL (Ashburner, 2007) to create a group-averaged anatomical template. We applied nonlinear transformations to register the group data to Montreal Neurological Institute (MNI) space. The deformations from this procedure were applied to the coregistered functional data, and the resulting output images were resampled to 3-mm isotropic and smoothed with an 8-mm FWHM Gaussian kernel.

Independent Component Analysis

The Group ICA of fMRI toolbox (GIFT, http://icatb.sourceforge.net/, version 2.0d) was used to identify spatially independent, temporally synchronous networks of voxels (Calhoun et al., 2001, 2009). First, temporal concatenation of data from all participants was performed to construct a single dataset that underwent dimensionality reduction using a two-stage principal component analysis procedure (Calhoun et al., 2001). The minimum description length (Li et al., 2007) criteria was used to optimize the number of independent sources within the dataset, which was found to be 61. The Infomax algorithm (Bell and Sejnowski, 1995) was used to generate a timecourse of BOLD signal change and a spatial map for each IC for the concatenated group data, which were back-reconstructed for each individual participant (Calhoun et al., 2001; Meda et al., 2009).

In order to determine significance of spatial distributions with each IC, we standardized back-reconstructed spatial maps of each IC (Beckmann et al., 2005), demonstrating the contribution of each voxel to the overall IC timeseries. An average (i.e., across runs) standardized spatial map was computed for each subject and entered into a one-sample *t*-test. Voxels were considered significant if they exceeded an uncorrected threshold of $p < 0.001$, in conjunction with a cluster extent exceeding 50 voxels.

We implemented a spatial correspondence analysis in order to identify ICs that reflect estimates of functional networks of interest, as opposed to additional sources (e.g., head motion, ventricular pulsation, or additional neural sources). For each IC, we computed Pearson product-moment correlation between the group-averaged spatial map (thresholded at $t < 3.75$) and templates corresponding to 4 cortical networks of interests. These templates were constructed by Yeo et al. (2011) and correspond to binary maps of the DAN, VAN, FPC, and DMN. ICs demonstrating a strong one-to-one correspondence with networks of interest were considered for additional analysis.

Estimation of delay period network activity

Task-relevance of large-scale network activity was tested using a general linear model (GLM) framework. Events were modeled using the canonical hemodynamic response function and its temporal derivative. In the first GLM, separate regressors were used to model the study, delay, recall, and speech periods. Where relevant, filled and unfilled trials were modeled separately. For study trials, subsequently recalled and forgotten items were modeled using unique regressors. Delay-period regressors were constructed with stimulus onsets at the beginning of the delay period, with a duration of 6 s. We constructed two regressors to model recall-period activity for each trial type of interest. A sustained recall regressor of 75 s in duration accounted for block-level effects during memory search. Transient recall-related activity was modeled by constructing a regressor from delta functions occurring at the onset of vocalization. The speech task was modeled with a single regressor, time-locked to the onset of stimulus presentation. Additional nuisance regressors were included to account for motion parameters and differences in mean BOLD signal across sessions. Linear contrasts were used to obtain subject-specific estimates for each effect of interest, which were then entered into a second-level, random-effects analysis. The second GLM was used to estimate delay-period activity at the single trial level, in order to predict recall behavior using cognitive models of memory search. The parameters of this GLM were identical to the first, except separate regressors were used to estimate activity for each delay period of interest.

Network Interaction Analysis

Task-related functional interactions between large-scale networks, as well as signal from independently defined regions of interest within the MTL, were estimated using a correlational psychophysiological interaction (cPPI) analysis (Fornito et al., 2012). Our task-related functional connectivity analysis aimed to identify interactions between distinct cortical networks that change as a function of task-demands (e.g., in response to the disruption of memory processes). While the goal of this analysis is to identify synchronized network dynamics, coordinated activation in separate networks of the brain may arise due to many circumstances, including independent task-based coactivation. To account for such effects, we computed an interaction term using a deconvolution technique (Gitelman et al., 2003). Three separate cPPI analyses were performed, constructing interaction terms from regressors estimating delay-period dependent changes in activity. The first analyses identified task-dependent changes in connectivity due to the unfilled delay, the filled delay, and differences across the two delay periods. In each analysis, we computed the partial correlation between each these interactions terms for each pairwise combination of networks of interest, while accounting for covariation due to task-based activation, previously described motion parameters, and activation in any of the networks of interest. Correlation measures were Fisher z-transformed prior to testing for significance using a one-sample t test, with a threshold of $p < 0.05$, FDR corrected (Benjamini and Hochberg, 1995).

Computational Modeling

In order to test the validity of hypotheses linking activity in large-scale brain networks to particular cognitive operations, we utilized a neurally informed variant of the Context Maintenance and Retrieval model of human memory (Kragel et al., 2015). This approach involved constructing a baseline model, and two neurally informed families of models. The baseline model was fit to behavioral data but was not informed by neural signal. The two neurally informed model variants included a Contextual Disruption (CD) model, in which a given neural signal determined the value of a model parameter controlling how much the model's representation of temporal context was disrupted during the end-of-list distraction period, and a Contextual Reinstatement (CR) model, in which a neural signal determined the fidelity with which the system retrieved the representation of temporal context associated with the beginning of the most recent study list.

An optimization procedure was used to find the set of parameters that allowed each model variant (baseline, CD, CR) to best predict behavioral performance. A likelihood statistic quantified the goodness-of-fit for each model. For each recall event, the model computed a set of scores corresponding to the probability of reporting each studied item, and the probability of recall termination. The log-transformed probability of each recall event was collected, and summed across all recall events in the experiment. This log-likelihood score corresponds to the likelihood that a model gave rise to the observed data, and was used as the basis for the model comparison statistics reported below. Despite being fit to individual recall events, all model variants provided a good fit to the overall behavioral performance as measured by a set of benchmark summary statistics describing recall initiation, transitions between recalled items, recall termination, and overall memorability as a function of serial position on the study list. For more detail regarding the basic model mechanisms, the reader is referred to Kragel et al. (2015). We describe a handful of modifications to the model as implemented in the current simulations.

We allowed a number of model parameters to vary between the two conditions (unfilled delay and filled delay), under the assumption that this experimental manipulation influenced the cognitive processes controlled by these parameters. Distraction task performance was assumed to influence both contextual disruption (controlled by parameter β_{ri}) and the fidelity of contextual reinstatement (controlled by parameter β_s), so these parameters were allowed to take distinct values for each condition. Additionally, in order to capture any condition-level differences in overall recall performance, we allowed the parameter controlling recall termination probability (ξ_d) to vary by condition.

The rule determining the probability of recall termination took a different form than the model examined by Kragel et al. (2015). Here, the probability of stopping recall, p_{stop}, was calculated as a function of output position ($\mathbf{r}$):

$$p_{stop} = \xi_s + e^{\xi_d r}, \tag{V.1}$$

where ξ_d is a free parameter controlling the rate at which the termination probability increases with output position. ξ_s is a parameter that reflects the probability that no items are recalled, and was fixed to a value of 5^{-3} for all simulations.

A probabilistic decision competition was simulated for each recall event, in which the relative support for each item determines the probability of that item being recalled. The relative support for each item **s** is subjected to exponential scaling prior to the recall decision:

$$\mathbf{s} = e^{\frac{2\mathbf{s}}{\tau}}, \tag{V.2}$$

where the free parameter τ describes the ferocity of the competition between items during recall. This decision rule provides some minimum degree of support for all studied items, allowing us to remove a noise parameter (α) from the model.

In order to account for the potential influence of semantic associations on recall behavior, we included an additional free parameter, s, that controlled the strength of pre-experimental associations between items with similar semantic meanings:

$$\mathbf{M}^{CF}_{i,j} = s\mathbf{M}^{sem}_{i,j}, \tag{V.3}$$

where $\mathbf{M}^{sem}_{i,j}$ is a cosine similarity measure of the semantic relatedness of any pair of items i and j. These semantic relatedness scores were computed from the semantic model Word Association Spaces (WAS; Steyvers et al. 2004), in which a vector representation of each word is constructed from a set of free-association norms (Nelson et al., 2004).

Given that in the unfilled delay condition participants would have extra time to encode the final list item, we introduced a parameter λ to enhance the associative strength between the contextual retrieval cue and the final item representation, relative to the other studied items (λ was set to zero in simulations of the filled condition).

$$\mathbf{M}^{CF}(t) = \mathbf{M}^{CF}(t-1) + (\phi(t) + \lambda)\mathbf{f}\mathbf{c}^{\top}, \tag{V.4}$$

where t indexes list position. ϕ is a scaling factor that increases context-to-item associations for early list positions to capture the primacy effect (the enhanced recall performance associated with the first few list positions).

Neurally informed models of free recall

In this work we examined two neurally informed variants of the CMR model. Each neurally informed model was identical to the baseline model, with the sole addition of a neural scaling parameter which allowed neural signal recorded on a particular trial to influence a specific operation in the model.

In the contextual disruption (CD) model, neural signal recorded during the delay period determined how much the contextual representation in the model was disrupted during the delay period. In the baseline model, this was controlled by model parameter β_{ri}, which determines how much distraction-task-related information is integrated into the temporal context representation. Higher values of β_{ri} indicate more disruption to the temporal context representation, as more irrelevant information is integrated into the contextual representation (this operation is described in more detail in Equation 2 of Kragel et al. 2015). In the CD model, neural signal causes β_{ri} to vary from trial to trial:

$$\beta_{ri}(t) = \beta_{ri} + \nu_{ri}N(t), \tag{V.5}$$

where ν_{ri} is a free parameter that scales the estimated neural activity during the delay-period, N, at time t. In order for the models to capture potential differences in the mapping of neural signals onto cognitive processes between the two conditions, we allowed these two free parameters to take on separate values during filled (i.e., $\beta_{ri,f}$ and $\nu_{ri,f}$) and unfilled (i.e., $\beta_{ri,u}$ and $\nu_{ri,u}$) trials.

In the context reinstatement (CR) model, neural signal recorded during the delay period determined the fidelity with which the system retrieved a representation of temporal context from the beginning of the study period. In the baseline model, this was controlled by model parameter β_s, which determines how much of this start-list information is integrated into the temporal context representation (using the same basic machinery described in Equation 2 of Kragel et al. 2015). In the CR model, neural signal causes β_s to vary from trial to trial:

$$\beta_s(t) = \beta_s + \nu_s N(t), \tag{V.6}$$

where ν_s is a free parameter that maps the estimated large-scale network activity, N, onto the context reinstatement parameter, β_s. As in the CD model, these parameters were separately estimated for both list types.

Parameter estimation

For a given version of the model, we estimated the set of parameters that best allowed the model to predict recall behavior, using a particle swarm optimization (PSO) algorithm (Eberhart and Kennedy, 1995). This technique was used to estimate the optimal parameters for the baseline model and for each neurally informed mode family (i.e., CR and CD models). During each application of the PSO algorithm, we constructed each swarm from 50 uniformly distributed random parameter sets, which explored the parameter space for up to 1000 generations or until a stopping criteria (the average change in model fitness over 50 generations) was less than a specified threshold (10^{-7}).

Model comparison and statistical inference

Once the optimal set of parameters was estimated for the baseline model and a neurally informed model, a likelihood ratio test (Wilks, 1938) was used to determine whether any improvement in model predictions for the neurally informed model was significant. This produced a test statistic,

D (also known as deviance, twice the difference of the log-likelihood of the neural and baseline models), for each voxel within a priori regions of interest. Significance was determined by testing D on a χ_1^2 distribution.

In addition to performing inference on the best-fitting parameter set for each model of interest, we used a differential evolution Markov chain Monte Carlo approach to perform Bayesian estimation of model parameters (Turner et al., 2013b). For each model, we ran 20 chains for 500 iterations with a burn-in period of 50 samples per chain, resulting in a total of 9000 samples from the target distribution. The γ parameter was set to a value of $2.38/\sqrt{2d}$, where d was the dimensionality of the parameter space for each model. After ensuring convergence of the chains, 95% highest density intervals (Kruschke, 2010) were constructed for each parameter. Both Savage-Dickey tests (Wagenmakers et al., 2010), and encompassing prior approaches (Wetzels et al., 2010) were used to evaluate model fitness and test hypotheses regarding differences in parameter values between the two delay conditions.

Discussion

In the present work we characterized the response of large-scale brain networks, and regional activation within the MTL, during a delay period following a study episode, which was either unfilled, to encourage maintenance of study items from the end of the study episode, or contained a brief period of distraction task performance, to encourage retrieval of the temporal contextual from the beginning of the study episode. Consistent with other neural investigations of memory in the presence of distraction (Clapp et al., 2010; Wager et al., 2013), we found that distraction elicited enhanced recruitment of the FPCN and a number of other brain networks thought to be involved in cognitive control. Furthermore, we found that activity in posterior MTL (including the hippocampus) showed functional coupling to a subset of these networks after this disruption. Using a model-based approach to cognitive neuroscience (Palmeri, 2014), we related these neural signals to particular cognitive operations, formalized within a simplified neural network model of memory search.

Within this modeling framework, we specified two core computational mechanisms central to cognitive neuroscientific theories of the cognitive control of memory. The first was an integrative mechanism that allows neural circuitry to maintain task-relevant information; in the current model, this maintained information was a context representation targeting the most recent studied materials. A model parameter was introduced to allow a given neural signal to indicate whether this information was successfully maintained through the delay, or whether it was disrupted during performance of a mathematical distraction task. The data supported a model in which activity in the DAN indicates the success or failure of this maintenance operation, regardless of whether participants performed a distraction task during the delay. It has been proposed that the DAN and DMN work in opposition to one another, controlling the relative balance of attention to external or internal information, respectively (Fox et al., 2005; Anticevic et al., 2012). However, recent work brings this stark contrast into question, establishing situations in which DMN can become positively coupled with frontoparietal networks (Fornito et al., 2012; Kragel and Polyn, 2015; Spreng et al., 2010, 2014). We found that a subnetwork of the DMN was also informative regarding contextual disruption, but only during unfilled delay intervals. Prior work implicating the DMN in episodic search tasks (Vincent et al., 2006; Sestieri et al., 2011; Fornito et al., 2012; Kragel and Polyn, 2015) and in the maintenance of internal representations (Buckner et al., 2009; Vilberg and Rugg, 2012) may help us to interpret this result. Maintaining a contextual representation for 12 seconds may be quite demanding even in the absence of external distraction; if increased DMN activity reflected mind wandering during the delay interval, this would presumably be disruptive to a maintained contextual representation (Sahakyan and Kelley, 2002).

The second core cognitive control operation involved the engagement of episodic retrieval processes to reinstate the temporal context of the study list. Prior empirical and theoretical studies suggest that such a contextual reinstatement operation will tend to preferentially support items from the beginning of the targeted study episode (Laming, 1999; Tan and Ward, 2000; Tulving, 2008; Davelaar, 2013). The data supported a model in which the FPCN supports contextual reinstatement, after the memory system was challenged by distraction. From this study alone, we cannot determine whether activity in the FPCN directly reflects the successful retrieval of contextual information, or whether it reflects the engagement of control operations that facilitate the reinstatement of contextual information in posterior regions (e.g., in hippocampus or parahippocampal cortex; Kragel et al. 2015). The latter view is consistent with recent neuroimaging work suggesting that frontoparietal activity supports the maintenance of task-relevant information in posterior regions (Riggall and Postle, 2012), whereas the former view is consistent with a number of studies suggesting that task-relevant information may be maintained in the frontoparietal circuits themselves (Cole et al., 2013; Lee et al., 2013; Waskom et al., 2014; Etzel et al., in press).

The data also supported a model in which DAN activity indicated the engagement of contextual reinstatement in the unfilled-delay trials. In another free-recall experiment, Kragel and Polyn (2015) observed increased functional coupling between the DAN and subnetworks within the DMN during memory search, around the time of successful recall events (and, like here, in the absence of task-relevant visual stimuli). These results suggest that the DAN, usually associated with top-down attention to visuospatial material, may have a direct role in the self-guided retrieval of mnemonic information. One possibility is that in the absence of disruption, the DAN is able to facilitate contextual retrieval, but after distraction the contextual representation is more damaged, and the FPCN must be engaged to mediate contextual retrieval.

Theories of FPCN function suggest that it mediates cognitive control by facilitating communication between cortical modules requisite for the performance of a particular task (Cole et al., 2013; Sneve et al., 2013; Cole et al., 2014), consistent with observations that FPCN exhibits dynamic changes in functional connectivity with various cortical systems over short time scales Monti et al. (2014); Zalesky et al. (2014); Allen et al. (2014); Yu et al. (2015). Our analysis of network interactions during the delay revealed that after distraction, the FPCN shows increased functional coupling with the DMN and a posterior MTL region, which in turn show increased coupling with the VAN. The VAN is highly overlapping with cingulo-opercular networks that have been shown to couple with the DMN during episodic memory tasks (Sestieri et al., 2014a), and contains prefrontal regions implicated in the controlled retrieval of episodic information (Wagner et al., 2001; Badre and Wagner, 2005). As mentioned above, it is possible that these widespread interactions represent the cognitive system's response to the contextual disruption wreaked by the math distraction task, a strategic attempt to reconstruct a contextual cue that will target the desired mnemonic information.

The utilization of cognitive models to interpret neural phenomena represents a growing trend in neuroscientific studies of behavior (e.g., Mitchell et al., 2008; Purcell et al., 2010; Mack et al., 2013; Turner et al., 2013a; Khaligh-Razavi and Kriegeskorte, 2014; Turner et al., in press). These neuro-cognitive models allow one to formulate specific hypotheses linking neural signals to particular cognitive mechanisms, which precisely specify the behavioral consequences of observing that neural signal. This approach can be contrasted with the method of cognitive subtraction (Friston et al., 1996), which, while quite powerful, and of great utility to cognitive neuroscientists, is limited in terms of the nature of the hypotheses that can be tested. In the current work, we examined the relative validity of models linking neural signals to contextual disruption and contextual retrieval operations in a computational model of free recall. The model is a member of a class usually referred to as retrieved-context models, in which a distributed representation of temporal context is constructed during an episode, and is reinstated when that episode is remembered (Howard and Kahana, 2002a; Sederberg et al., 2008; Polyn et al., 2009a). A growing number of studies support the theoretical importance of the temporal reinstatement operation at the heart of the model, including studies of memory misattributions during list learning (Gershman et al., 2013), the semantic organization of memory search (Polyn et al., 2005; Morton et al., 2013), and the temporal organization of remembered items (Manning et al., 2011; Kragel et al., 2015).

Our results reveal the potential cognitive underpinnings of neural activity in several large-scale brain networks, and in the MTL, during a delay interval leading up to a period of memory search. In this neuro-cognitive model, neural signals are associated with cognitive operations, and the validity of these linkages are assessed in terms of the increased ability of the model to predict human behavior. We find that activity in the DAN indicates contextual disruption in the presence of perceptual distraction, but indicates contextual reinstatement in the absence of distraction. After distraction, contextual reinstatement is indicated by activation in the FPCN and MTL, which show functional coupling with the VAN and DMN. These results provide a glimpse into the shifting dynamics and complex interactions of large-scale brain networks in the service of the cognitive control of episodic memory retrieval.

CHAPTER VI

General Discussion

Synopsis

The overarching goal of this work involved identifying the neural correlates of internally-generated memory retrieval, and determining the computational processes mediated by these neural substrates. Prior neural investigations of free recall have associated activity within the MTL with the retrieval of previous encoded information (Gelbard-Sagiv et al., 2008), while activation of prefrontal cortex (Long et al., 2010), as well as frontoparietal systems (Shapira-Lichter et al., 2012) has been suggested to provide a top-down influence on the memory system during search. Despite this body of work, prior studies of the free-recall task have not examined communication between the hippocampus and large-scale cortical networks. In addition, the complexity and unconstrained nature of the free-recall task makes mapping observed neural mechanisms onto specific cognitive operations a challenging task. In contrast, well-characterized computational models of free recall (Howard and Kahana, 2002a; Polyn et al., 2009a) provide a description of computational processes that can explain recall behavior, yet there is minimal direct empirical evidence that the description of these models are reflected in the engagement and communication of neural systems.

In order to investigate the neural and computational mechanisms that allow spontaneous recovery of previously learned information, we examined the neural correlates of free recall. Using a multivariate, data-driven approach to characterize the contributions of large-scale networks during the unconstrained search period, we observed sustained activation of a sub-network of the DMN anchored in posteromedial cortex, encompassing posterior parahippcampal gyrus and the hippocampus. We also demonstrated increased activation of the posterior MTL using univariate based measures, providing evidence that this putative contextual network (see Chapter I for discussion) is engaged during the free recall of verbal material. In addition to the DMN, we associated recall with transient increases in activity with frontoparietal networks, including the DAN. In contrast to models that describe an antagonistic relationship between the DMN and executive control networks (Fox et al., 2005), we characterized increases in functional coupling during both memory search and recall initiation. These findings build upon a growing literature characterizing the neural underpinnings of self-initiated memory search, and identify interactions between disparate neural systems that may be critical to coordinating retrieval.

To more precisely specify the nature of neural processing engaged during free recall, we tested the degree to which the same neural signals that drive retrieval on recognition-based tasks are recruited during the free-recall task. We determined consistent activation within posterior MTL structures associated with the both the free recall of verbal material, as well as the recollection of contextual information from visually presented memory probes; however, the application of multivariate decoding techniques revealed that patterns of neural activity elicited during free-recall did not reliably reflect episodic recollection, as measured in the source recognition paradigm. These results challenge classic models of the free-recall paradigm, which presume that the process of recollection is essential to this task (Mandler, 1980; Yonelinas, 2002). Furthermore, these findings appear at odds with retrieved-context models, that rely on the process of contextual reinstatement in order to account for organizational effects in free recall. While temporal retrieval has been shown to play a role in recognition (Schwartz et al., 2005), episodic reinstatement was observed to vary from trial to trial, only accompanying mnemonic judgments made with high confidence. Multiple lines of neuroimaging (Johnson et al., 2009) and behavioral modeling (Mickes et al., 2009) additionally suggest that recollection is a graded process.

These findings are consistent with the variability in temporal reinstatement reflected in the activation of the posterior MTL, described in neuro-cognitive models of free recall (see Chapters IV and V). Within the retrieved-context framework, MTL structures are critical for predicting the temporal organization of memory search; however, it remains to be demonstrated whether hippocampally driven reinstatement of non-temporal information, such as semantic (Morton et al., 2013), spatial (Miller et al., 2013b), or stimulus-specific (Ritchey et al., 2013; Staresina et al., 2013) features, can account for the additional aspects of organization in memory search (Bower, 1970;

Howard and Kahana, 2002b; Polyn et al., 2009b; Miller et al., 2013a). If neural circuitry within the MTL can account for multiple aspects of recall organization, this would provide evidence for contextual reinstatement mechanisms in the hippocampus as a general determinant of episodic organization (Miller et al., 2013b).

While neural activity in the MTL system can predict temporal (Manning et al., 2011; Kragel et al., 2015) and spatial (Miller et al., 2013b) organization of free recall, interactions between control signals in prefrontal cortex are critical in providing coherent structure to information in memory (Gershberg and Shimamura, 1995; Shimamura et al., 1995; Becker and Lim, 2003). By challenging the memory system with distraction, we demonstrated the validity of neuro-cognitive models in which prefrontal systems, such as the FPCN, can control the manner in which recall is initiated. Activity within the DAN signaled shifts in internal context, consistent with the role of this network in directing shifts in internal attention in multiple cognitive domains (Corbetta and Shulman, 2002; Cabeza et al., 2008; Lückmann et al., 2014). When shifts in internal context disrupt the memory system such that relevant mnemonic information is no longer accessible, prefrontal systems can interact with the MTL to reinstate task-relevant information (Simons and Spiers, 2003). By demonstrating that the a left-lateralized FPCN interacted with the cortico-hippocampal networks (i.e., the DMN) during both memory search and recall initiation, we identified a neural mechanism that enables the human memory system to target task-relevant information in memory.

Future Directions

Using a combination of neuroimaging and modeling techniques, we formally described a set of computational mechanisms that are sufficient to describe the temporal organization of human memory, and are reflected in the engagement of neural structures during performance of the free-recall paradigm. Neurally informed computational models of human memory, such as those detailed in Chapters IV and V, provide an ideal framework to formally test theories of cognitive neuroscience. Consistent with the proposed role of the MTL system in the reactivation of previously learned information (Polyn et al., 2008), the neurally informed models described in Chapter IV demonstrated how activation of structures within the MTL, namely the hippocampus and parahippocampal cortex, signal the retrieval of temporal-contextual information during memory search. Using BOLD signal in these regions to measure the latent process of contextual reinstatement, these models were successful in predicting the temporal organization of recall, providing evidence for this computational mechanism, reflected in the activation of the MTL, as a critical operation in driving recall behavior. The modeling work elaborated in Chapter V extended the role of contextual reinstatement processes by demonstrating it can account for not only the manner in which memory search unfolds, but also the accessibility of recently learned information in memory. By linking activation of the MTL, as well as the FPC networks that interact with the MTL, to the contextual reinstatement mechanism, these studies provide direct evidence for the neural basis of retrieved-context models of human memory (Howard and Kahana, 2002a; Sederberg et al., 2008; Polyn et al., 2009a). These findings raise a number of questions for future research, which will be discussed as they relate to computational models of human memory.

As outlined in Chapter I, the CMR model of free recall (Polyn et al., 2009a) provides computational operations that describe how long-term memories are encoded, stored, and retrieved. A core component of this model is the association formation process that occurs during list learning, which binds a presented item to the episodic context in which it occurs. While neurally informed models have demonstrated links between the hippocampal system and the associative retrieval of contextual information during recall (Kragel et al., 2015), it has not been tested whether neural substrates within the MTL also predict the strength of associations that are formed between items and the contexts they are encountered in during learning. Theoretical models that describe the neuroanatomy of context-based models of human memory describe the hippocampal system as critical to the formation of experimental associations between items and the contexts in which they occur (Howard et al., 2005; Polyn and Kahana, 2008). While extant neuroimaging (Fernández et al., 1998; Wagner et al., 1998; Davachi et al., 2003) and lesion (Scoville and Milner, 1957) studies strongly link the MTL system to episodic encoding, it remains to be determined whether activation of regions such as the hippocampus truly reflect the associative strength of an encoded memory. For example, recent work by Sneve et al. (2015) examining the neural substrates of memory encoding have demonstrated that functional connectivity of the MTL to the DMN, rather than the absolute level of activation during encoding, predicts the durability of an encoded memory. Considering interactions between MTL systems and large-scale cortical networks during learning may prove essential to understanding the formation of associations in episodic memory, as described in the retrieved-context framework.

Evidence from neuroimaging studies of memory encoding suggest that processes outside of the MTL, including the PFC, support subsequent memory (Paller and Wagner, 2002). In addition to providing a description of the neural substrates that reflect association formation during encoding, model-based approaches to understanding subsequent memory effects can provide a more precise description of the processes supported by the PFC in the establishment of individual memories. As described in Chapter I, ventrolateral PFC has been proposed to support encoding through the selection of conceptual item information (Badre and Wagner, 2004), while dorsalateral PFC has been linked to encoding of relational information between items in memory (Blumenfeld et al., 2011). If these prefrontal control operations influence the nature of item-based representations that are available to the memory system, a computational investigation of these signals may provide a specific mechanism supported by the DLPFC that can explain how it supports subsequent recall of learned information, beyond recognition of item information (Staresina and Davachi, 2006). Encoding of relational information during list-learning may allow the representation of an items features to become associated with distinct contexts throughout the study period. Encoding an item in this manner would facilitate its recall due to multiple states of context providing an effective retrieval cue during memory search. Another goal for future work is to develop a parsimonious model of PFC function during both encoding and recall of information. By constraining PFC activity to influence the same cognitive processes during encoding and retrieval, a neurally informed computational model would be ideally suited for this challenge.

While the neuro-cognitive models of human memory described within this work draw direct links between observed engagement of neural structures and specific computational operations, neuroimaging investigations of this nature are inherently correlational in nature. It will be important use stimulation-based techniques in order to establish a causal relationship between brain structures and computational mechanisms. Within the domain of human memory, stimulation of cortico-hippocampal networks has been shown to not only increase the strength of functional connectivity between the hippocampus and cortical modules, but also improve memory performance (Wang et al., 2014). Understanding the computational consequences of stimulation-based changes in neural communication will provide insight into mechanisms that predict how memory performance can be improved. Such advances can potentially lead to the development of targeted methods that may treat memory disorders by strengthening the memory system.

Lesion based studies will also provide a strong source of evidence for structure to function mapping, testing the necessity of a given neural substrate for a specific computational process. While neuropsychological studies of human memory (see Chapter I) demonstrate the necessity of prefrontal cortex and the MTL for specific aspects of memory function (Stuss et al., 1994; Shimamura et al., 1995; Carlesimo et al., 1996; Mangels et al., 1996), understanding the computational consequences due to neurological insults is challenging (cf., Becker and Lim, 2003; Sederberg et al., 2008). One factor that complicates such interpretation is the temporal specificity of the lesion; it can be difficult to determine if encoding, or retrieval based processes are disrupted in clinical populations. As such, techniques such as repetitive TMS that can be applied to temporarily lesion a neural target may prove critical to demonstrating the necessity of PFC and the MTL for specific computational mechanisms. Within the domain of free recall, Innocenti et al. (2012) have demonstrated that disruption of DLPFC is associated with reduction in primacy effects, disruption of the intraparietal lobe during encoded causes deficits to recently learned information. In addition to allowing measures of neural activation to influence cognitive processes within a model, the computational modeling framework developed in Chapter IV serves as an ideal methodology to understand the consequences of focal lesions. The strongest links between neural mechanisms and computational processes can be made when computational models of memory are constrained by not only behavior and on-line measures of brain activation, but also causal deactivation and activation of neural circuitry.

While the precise neural mechanisms that enable the human memory system to flexibly and efficiently retrieve goal-relevant information remain elusive, we identified neural substrates within the MTL that mediate contextual retrieval during the free-recall task, and further characterized how interactions between frontoparietal and cortico-hippocampal networks contribute to the cognitive control of memory. By developing a neurally informed computational model of human memory, we have developed a basis on which to unravel the nuanced mechanisms that enable the mind to access and relive the past.

BIBLIOGRAPHY

Addis, D. R., Wong, A. T., and Schacter, D. L. (2007). Remembering the past and imagining the future: common and distinct neural substrates during event construction and elaboration. *Neuropsychologia*, 45(7):1363–1377.

Allen, E. A., Damaraju, E., Plis, S. M., Erhardt, E. B., Eichele, T., and Calhoun, V. D. (2014). Tracking whole-brain connectivity dynamics in the resting state. *Cerebral Cortex*, 24(3):663–676.

Aminoff, E., Gronau, N., and Bar, M. (2007). The parahippocampal cortex mediates spatial and nonspatial associations. *Cerebral Cortex*, 17(7):1493.

Amunts, K., Kedo, O., Kindler, M., Pieperhoff, P., Mohlberg, H., Shah, N. J., Habel, U., Schneider, F., and Zilles, K. (2005). Cytoarchitectonic mapping of the human amygdala, hippocampal region and entorhinal cortex: intersubject variability and probability maps. *Anatomy and embryology*, 210(5-6):343–352.

Anderson, J. R. and Bower, G. H. (1972). Recognition and retrieval processes in free recall. *Psychological Review*, 79(2):97–123.

Andreasen, N. C., O'Leary, D. S., Cizadlo, T., Arndt, S., Rezai, K., Watkins, G., Ponto, L. L., and Hichwa, R. D. (1995). II. PET Studies of Memory: Novel versus Practiced Free Recall of Word Lists. *NeuroImage*, 2(4):296–305.

Andrews-Hanna, J. R., Reidler, J. S., Huang, C., and Buckner, R. L. (2010a). Evidence for the default network's role in spontaneous cognition. *Journal of Neurophysiology*, 104(1):322–335.

Andrews-Hanna, J. R., Reidler, J. S., Sepulcre, J., Poulin, R., and Buckner, R. L. (2010b). Functional-anatomic fractionation of the brain's default network. *Neuron*, 65(4):550–562.

Anticevic, A., Cole, M. W., Murray, J. D., Corlett, P. R., Wang, X.-J., and Krystal, J. H. (2012). The role of default network deactivation in cognition and disease. *Trends in Cognitive Sciences*, 16(12):584–592.

Ashburner, J. (2007). A fast diffeomorphic image registration algorithm. *NeuroImage*, 38(1):95–113.

Ashburner, J. and Friston, K. J. (2005). Unified segmentation. *NeuroImage*, 26:839–851.

Badre, D. and Wagner, A. D. (2004). Selection, Integration, and Conflict Monitoring: Assessing the Nature and Generality of Prefrontal Cognitive Control Mechanisms. *Neuron*, 41(3):473–487.

Badre, D. and Wagner, A. D. (2005). Frontal lobe mechanisms that resolve proactive interference. *Cerebral Cortex*, 15(12):2003–2012.

Badre, D. and Wagner, A. D. (2007). Left ventrolateral prefrontal cortex and the cognitive control of memory. *Neuropsychologia*, 45(13):2883–2901.

Baldo, J. V., Delis, D., Kramer, J., and Shimamura, A. P. (2002). Memory performance on the California Verbal Learning Test–II: Findings from patients with focal frontal lesions. *Journal of the International Neuropsychological Society*, 8:539–546.

Bar, M., Aminoff, E., and Schacter, D. L. (2008). Scenes unseen: The parahippocampal cortex intrinsically subserves contextual associations, not scenes or places per se. *The Journal of Neuroscience*, 28(34):8539–8544.

Barch, D. M., Sabb, F. W., Carter, C. S., Braver, T. S., Noll, D. C., and Cohen, J. D. (1999). Overt verbal responding during fMRI scanning: Empirical investigations of problems and potential solutions. *NeuroImage*, 10(6):642–657.

Becker, S. and Lim, J. (2003). A computational model of prefrontal control in free recall: Strategic memory use in the california verbal learning task. *Journal of Cognitive Neuroscience*, 15:821–832.

Beckmann, C., Noble, J., and Smith, S. (2000). Artefact detection in FMRI data using independent component analysis. *NeuroImage*, 11(5, Supplement):S614.

Beckmann, C. F., DeLuca, M., Devlin, J. T., and Smith, S. M. (2005). Investigations into resting-state connectivity using independent component analysis. *Philosophical Transactions of the Royal Society of London B: Biological Sciences*, 360(1457):1001–1013.

Bell, A. J. and Sejnowski, T. J. (1995). An information-maximization approach to blind separation and blind deconvolution. *Neural Computation*, 7(6):1129–1159.

Benjamini, Y. and Hochberg, Y. (1995). Controlling the False Discovery Rate: a practical and powerful approach to multiple testing. *Journal of Royal Statistical Society, Series B*, 57:289–300.

Binder, J., Frost, J., Hammeke, T., Bellgowan, P., Springer, J., Kaufman, J., and Possing, E. (2000). Human temporal lobe activation by speech and nonspeech sounds. *Cerebral Cortex*, 10(5):512.

Binder, J. R., Frost, J. A., Hammeke, T. A., Bellgowan, P. S. F., Rao, S. M., and Cox, R. W. (1999). Conceptual processing during the conscious resting state: A functional MRI study. *Journal of Cognitive Neuroscience*, 11(1):80–93.

Birn, R. M., Bandettini, P. A., Cox, R. W., Jesmanowicz, A., and Shaker, R. (1998). Magnetic field changes in the human brain due to swallowing or speaking. *Magnetic Resonance in Medicine*, 40(1):55–60.

Bjork, R. A. and Whitten, W. B. (1974). Recency-sensitive retrieval processes in long-term free recall. *Cognitive Psychology*, 6:173–189.

Blumenfeld, R. and Ranganath, C. (2007). Prefrontal cortex and long-term memory encoding: An integrative review of findings from neuropsychology and neuroimaging. *The Neuroscientist*, 13(3):280.

Blumenfeld, R. S., Parks, C. M., Yonelinas, A. P., and Ranganath, C. (2011). Putting the pieces together: The role of dorsolateral prefrontal cortex in relational memory encoding. *Journal of cognitive neuroscience*, 23(1):257–265.

Blumenfeld, R. S. and Ranganath, C. (2006). Dorsolateral prefrontal cortex promotes Long-Term memory formation through its role in working memory organization. *The Journal of Neuroscience*, 26(3):916–925.

Bosch, S. E., Jehee, J. F. M., Fernández, G., and Doeller, C. F. (2014). Reinstatement of associative memories in early visual cortex is signaled by the hippocampus. *The Journal of Neuroscience*, 34(22):7493–7500.

Bousfield, W. A. (1953). The occurrence of clustering in the recall of randomly arranged associates. *Journal of General Psychology*, 49:229–240.

Bower, G. H. (1970). Organizational factors in memory. *Cognitive Psychology*, 1(1):18–46.

Bower, G. H. (1972). Stimulus-sampling theory of encoding variability. In Melton, A. W. and Martin, E., editors, *Coding Processes in Human Memory*, chapter 5, pages 85–121. John Wiley and Sons, New York.

Brainerd, C. J., Wright, R., Reyna, V. F., and Payne, D. G. (2002). Dual-retrieval processes in free and associative recall. *Journal of Memory and Language*, 46(1):120–152.

Braver, T. S., Barch, D. M., Keys, B. A., Carter, C. S., Cohen, J. D., Kaye, J. A., Janowsky, J. S., Taylor, S. F., Yesavage, J. A., and Mumenthaler, M. S. (2001). Context processing in older adults: Evidence for a theory relating cognitive control to neurobiology in healthy aging. *Journal of Experimental Psychology: General*, 130:746–763.

Bressler, S. L. and Menon, V. (2010). Large-scale brain networks in cognition: emerging methods and principles. *Trends in Cognitive Sciences*, 14(6):277–290.

Brown, M. and Xiang, J. (1998). Recognition memory: neuronal substrates of the judgement of prior occurrence. *Progress in Neurobiology*, 55(2):149–189.

Brown, M. W. and Aggleton, J. P. (2001). Recognition memory: what are the roles of the perirhinal cortex and hippocampus. *Nature Reviews Neuroscience*, 2:51–61.

Buckner, R. L., Andrews-Hanna, J. R., and Schacter, D. L. (2008). The brain's default network. *Annals of the New York Academy of Sciences*, 1124(1):1–38.

Buckner, R. L. and Carroll, D. C. (2007). Self-projection and the brain. *Trends in Cognitive Sciences*, 11(2):49–57.

Buckner, R. L., Sepulcre, J., Talukdar, T., Krienen, F. M., Liu, H., Hedden, T., Andrews-Hanna, J. R., Sperling, R. A., and Johnson, K. A. (2009). Cortical hubs revealed by intrinsic functional connectivity: Mapping, assessment of stability, and relation to alzheimer's disease. *The Journal of Neuroscience*, 29(6):1860–1873.

Budson, A. E. and Solomon, P. R. (2011). *Memory Loss: A Practical Guide for Clinicians*. Elsevier, Philadelphia.

Bullmore, E. and Sporns, O. (2009). Complex brain networks: Graph theoretical analysis of structural and functional systems. *Nature Reviews Neuroscience*, 10(3):186–198.

Burgess, N., Barry, C., and O'Keefe, J. (2007). An oscillatory interference model of grid cell firing. *Hippocampus*, 17(9):801–812.

Burgess, N., Becker, S., King, J., and O'Keefe (2001). Memory for events and their spatial context: models and experiments. *Philosophical Transcripts of the Royal Society London B: Biological Sciences*, 356:1493–1503.

Burgess, N., Maguire, E., and O'Keefe, J. (2002). The human hippocampus and spatial and episodic memory. *Neuron*, 35:625–641.

Burnham, K. P. and Anderson, D. R. (2004). Multimodel inference understanding AIC and BIC in model selection. *Sociological Methods & Research*, 33(2):261–304.

Burwell, R. D., Witter, M. P., and Amaral, D. G. (2004). Perirhinal and postrhinal cortices of the rat: A review of the neuroanatomical literature and comparison with findings from the monkey brain. *Hippocampus*, 5(5):390–408.

Buzsáki, G. (1996). The hippocampo-neocortical dialogue. *Cerebral Cortex*, 6:81–92.

Cabeza, R., Ciaramelli, E., Olson, I., and Moscovitch, M. (2008). The parietal cortex and episodic memory: an attentional account. *Nature Reviews Neuroscience*, 9(8):613–625.

Cabeza, R., Mazuz, Y. S., Stokes, J., Kragel, J. E., Woldorff, M. G., Ciaramelli, E., Olson, I. R., and Moscovitch, M. (2011). Overlapping parietal activity in memory and perception: Evidence for the attention to memory model. *Journal of Cognitive Neuroscience*, 23(11):3209–3217.

Calhoun, V. D., Adali, T., Pearlson, G. D., and Pekar, J. J. (2001). A method for making group inferences from functional MRI data using independent component analysis. *Human Brain Mapping*, 14(3):140–151.

Calhoun, V. D., Liu, J., and Adal, T. (2009). A review of group ICA for fMRI data and ICA for joint inference of imaging, genetic, and ERP data. *NeuroImage*, 45(1, Supplement 1):S163–S172.

Carlesimo, G. A., Marfia, G. A., Loasses, A., and Caltagirone, C. (1996). Recency effect in anterograde amnesia: Evidence for distinct memory stores underlying enhanced retrieval of terminal items in immediate and delayed recall paradigms. *Neuropsychologia*, 34:177–184.

Chadick, J. Z. and Gazzaley, A. (2011). Differential coupling of visual cortex with default network or frontal-parietal network based on goals. *Nature neuroscience*, 14(7):830–832.

Christoffels, I. K., Formisano, E., and Schiller, N. O. (2007). Neural correlates of verbal feedback processing: An fMRI study employing overt speech. *Human Brain Mapping*, 28(9):868–879.

Ciaramelli, E., Grady, C. L., and Moscovitch, M. (2008). Top-down and bottom-up attention to memory: a hypothesis (AtoM) on the role of the posterior parietal cortex in memory retrieval. *Neuropsychologia*, 46(7):1828–1851.

Clapp, W. C., Rubens, M. T., and Gazzaley, A. (2010). Mechanisms of Working Memory Disruption by External Interference. *Cerebral Cortex*, 20(4):859–872.

Clithero, J. A., Smith, D. V., Carter, R. M., and Huettel, S. A. (2011). Within- and cross-participant classifiers reveal different neural coding of information. *NeuroImage*, 56(2):699–708.

Cohen, J. D., Perlstein, W. M., Braver, T. S., Nystrom, L. E., Noll, D. C., Jonides, J., and Smith, E. E. (1997). Temporal dynamics of brain activation during a working memory task. *Nature*, 386:604–608.

Cohen, N. J. and Eichenbaum, H. (1993). *Memory, amnesia, and the hippocampal system*. MIT, Cambridge, MA.

Cole, M. W., Bassett, D. S., Power, J. D., Braver, T. S., and Petersen, S. E. (2014). Intrinsic and task-evoked network architectures of the human brain. *Neuron*, 83(1):238–251.

Cole, M. W., Reynolds, J. R., Power, J. D., Repovs, G., Anticevic, A., and Braver, T. S. (2013). Multi-task connectivity reveals flexible hubs for adaptive task control. *Nature Neuroscience*, 16(9):1348–1355.

Corbetta, M., Patel, G., and Shulman, G. L. (2008). The reorienting system of the human brain: from environment to theory of mind. *Neuron*, 58(3):306–324.

Corbetta, M. and Shulman, G. (2002). Control of goal-directed and stimulus-driven attention in the brain. *Nature reviews. Neuroscience*, 3(3):201–215.

Curtis, C. E. and D'Esposito, M. (2003). Persistent activity in the prefrontal cortex during working memory. *Trends in Cognitive Sciences*, 7(9):415–423.

Cusack, R., Cumming, N., Bor, D., Norris, D., and Lyzenga, J. (2005). Automated post-hoc noise cancellation tool for audio recordings acquired in an MRI scanner. *Human Brain Mapping*, 24(4):299–304.

Dale, A. M. (1999). Optimal experimental design for event-related fmri. *Human Brain Mapping*, 8:109–114.

Danker, J. F. and Anderson, J. R. (2010). The ghosts of brain states past: Remembering reactivates the brain regions engaged during encoding. *Psychological Bulletin*, 136(1):87–102.

Daselaar, S. M., Fleck, M. S., Prince, S. E., and Cabeza, R. (2006). The medial temporal lobe distinguishes old from new independently of consciousness. *J Neurosci*, 26(21):5835–5839.

Davachi, L. (2006). Item, context and relational episodic encoding in humans. *Current Opinion in Neurobiology*, 16(6):693–700.

Davachi, L., Mitchell, J. P., and Wagner, A. D. (2003). Multiple routes to memory: Distinct medial temporal lobe processes build item and source memories. *Proceedings of the National Academy of Sciences*, 100(4):2157–2162.

Davelaar, E. J. (2013). A novelty-induced change in episodic (NICE) context account of primacy effects in free recall. *Psychology*, 4(9):695–703.

Daw, N. D., Gershman, S. J., Seymour, B., Dayan, P., and Dolan, R. J. (2011). Model-based influences on humans' choices and striatal prediction errors. *Neuron*, 69(6):1204–1215.

Diana, R. A., Yonelinas, A. P., and Ranganath, C. (2007). Imaging recollection and familiarity in the medial temporal lobe: a three-component model. *Trends in Cognitive Sciences*, 11(9):379–386.

Diana, R. A., Yonelinas, A. P., and Ranganath, C. (2009). Medial temporal lobe activity during source retrieval reflects information type, not memory strength. *Journal of Cognitive Neuroscience*, 22(8):1808–1818.

Dobbins, I. G., Simons, J. S., and Schacter, D. L. (2004). fMRI evidence for separable and lateralized prefrontal memory monitoring processes. *Journal of Cognitive Neuroscience*, 16(6):908–920.

Donaldson, D. I., Wheeler, M. E., and Petersen, S. E. (2010). Remember the Source: Dissociating Frontal and Parietal Contributions to Episodic Memory. *Journal of Cognitive Neuroscience*, 22(2):377–391.

Dosenbach, N. U., Fair, D. A., Cohen, A. L., Schlaggar, B. L., and Petersen, S. E. (2008). A dual-networks architecture of top-down control. *Trends in cognitive sciences*, 12(3):99–105.

Dosenbach, N. U., Visscher, K. M., Palmer, E. D., Miezin, F. M., Wenger, K. K., Kang, H. C., Burgund, E. D., Grimes, A. L., Schlaggar, B. L., and Petersen, S. E. (2006). A core system for the implementation of task sets. *Neuron*, 50(5):799–812.

Duarte, A., Henson, R. N., Knight, R. T., Emery, T., and Graham, K. S. (2009). Orbito-frontal cortex is necessary for temporal context memory. *Journal of Cognitive Neuroscience*, 22(8):1819–1831.

Duarte, A., Ranganath, C., and Knight, R. T. (2005). Effects of unilateral prefrontal lesions on familiarity, recollection, and source memory. *The Journal of Neuroscience*, 25(36):8333–8337.

Düzel, E., Habib, R., Scott, B., Schoenfeld, A., Lobaugh, N., McIntosh, A. R., Scholz, M., and Heinze, H. J. (2003). A multivariate spatiotemporal analysis of electromagnetic time-frequency data of recognition memory. *NeuroImage*, 18(2):185–197.

Eberhart, R. and Kennedy, J. (1995). A new optimizer using particle swarm theory. In *Proceedings of the Sixth International Symposium on Micro Machine and Human Science, 1995. MHS '95*, pages 39–43.

Egorov, A., Hamam, B., Fransen, E., Hasselmo, M., and Alonso, A. (2002). Graded persistent activity in entorhinal cortex neurons. *Nature*, 420(6912):173–8.

Eichenbaum, H. (2004). Hippocampus: cognitive processes and neural representations that underlie declarative memory. *Neuron*, 44(1):109–120.

Eichenbaum, H. (2013). Memory on time. *Trends in cognitive sciences*, 17(2):81–88.

Eichenbaum, H., Yonelinas, A., and Ranganath, C. (2007). The medial temporal lobe and recognition memory. *Annual Review of Neuroscience*, 30:123–152.

Eickhoff, S. B., Stephan, K. E., Mohlberg, H., Grefkes, C., Fink, G. R., Amunts, K., and Zilles, K. (2005). A new SPM toolbox for combining probabilistic cytoarchitectonic maps and functional imaging data. *NeuroImage*, 25(4):1325–1335.

Ekstrom, A. D. and Bookheimer, S. Y. (2007). Spatial and temporal episodic memory retrieval recruit dissociable functional networks in the human brain. *Learning & Memory (Cold Spring Harbor, N.Y.)*, 14(10):645–654.

Eldridge, L. L., Knowlton, B. J., Furmanski, C. S., Bookheimer, S. Y., and Engel, S. A. (2000). Remembering episodes: a selective role for the hippocampus during retrieval. *Nat Neurosci*, 3(11):1149–1152.

Esterman, M., Chiu, Y.-C., Tamber-Rosenau, B. J., and Yantis, S. (2009). Decoding cognitive control in human parietal cortex. *Proceedings of the National Academy of Sciences*, 106(42):17974–17979.

Estes, W. K. (1959). *Component and pattern models with Markovian interpretations. Studies in Mathematical Learning Theory*. Stanford University Press, Stanford, CA.

Etzel, J. A., Cole, M. W., Zacks, J. M., Kay, K. N., and Braver, T. S. (in press). Reward motivation enhances task coding in frontoparietal cortex. *Cerebral Cortex*.

Ezzyat, Y. and Davachi, L. (2014). Similarity breeds proximity: Pattern similarity within and across contexts is related to later mnemonic judgments of temporal proximity. *Neuron*, 81(5):1179–1189.

Feredoes, E., Heinen, K., Weiskopf, N., Ruff, C., and Driver, J. (2011). Causal evidence for frontal involvement in memory target maintenance by posterior brain areas during distracter interference of visual working memory. *Proceedings of the National Academy of Sciences*, 108(42):17510–17515.

Fernández, G., Weyerts, H., Schrader-Bölsche, M., Tendolkar, I., Smid, H. G. O. M., Tempelmann, C., Hinrichs, H., Scheich, H., Elger, C. E., Mangun, G. R., and Jochen Heinze, H. (1998). Successful verbal encoding into episodic memory engages the posterior hippocampus: A parametrically analyzed functional magnetic resonance imaging study. *The Journal of Neuroscience*, 18(5):1841–1847.

Formisano, E., Esposito, F., Kriegeskorte, N., Tedeschi, G., Di Salle, F., and Goebel, R. (2002). Spatial independent component analysis of functional magnetic resonance imaging time-series: characterization of the cortical components. *Neurocomputing*, 49(1–4):241–254.

Fornito, A., Harrison, B. J., Zalesky, A., and Simons, J. S. (2012). Competitive and cooperative dynamics of large-scale brain functional networks supporting recollection. *Proceedings of the National Academy of Sciences*, 109(31):12788–12793.

Fortin, N. J., Agster, K. L., and Eichenbaum, H. B. (2002). Critical role of the hippocampus in memory for sequences of events. *Nature Neuroscience*.

Fox, M. D., Corbetta, M., Snyder, A. Z., Vincent, J. L., and Raichle, M. E. (2006). Spontaneous neuronal activity distinguishes human dorsal and ventral attention systems. *Proceedings of the National Academy of Sciences of the United States of America*, 103(26):10046–10051.

Fox, M. D., Snyder, A. Z., Vincent, J. L., Corbetta, M., Essen, D. C. V., and Raichle, M. E. (2005). The human brain is intrinsically organized into dynamic, anticorrelated functional networks. *Proceedings of the National Academy of Sciences of the United States of America*, 102(27):9673–9678.

Frank, M. J., Woroch, B., and Curran, T. (2005). Error-related negativity predicts reinforcement learning and conflict biases. *Neuron*, 47(4):495–501.

Friston, K. J., Buechel, C., Fink, G. R., Morris, J., Rolls, E., and Dolan, R. J. (1997). Psychophysiological and Modulatory Interactions in Neuroimaging. *NeuroImage*, 6(3):218–229.

Friston, K. J., Price, C. J., Fletcher, P., Moore, C., Frackowiak, R. S., and Dolan, R. J. (1996). The trouble with cognitive subtraction. *NeuroImage*, 4(2):97–104.

Gelbard-Sagiv, H., Mukamel, R., Harel, M., Malach, R., and Fried, I. (2008). Internally generated reactivation of single neurons in human hippocampus during free recall. *Science*, 3:96–101.

Geller, A. S., Schleifer, I. K., Sederberg, P. B., Jacobs, J., and Kahana, M. J. (2007). PyEPL: A cross-platform experiment-programming library. *Behavior Research Methods*, 39(4):950–958.

Gershberg, F. B. and Shimamura, A. P. (1995). Impaired use of organizational strategies in free recall following frontal lobe damage. *Neuropsychologia*, 33:1305–1333.

Gershman, S. J., Schapiro, A. C., Hupbach, A., and Norman, K. A. (2013). Neural context reinstatement predicts memory misattribution. *The Journal of Neuroscience*, 33(20):8590–8595.

Gitelman, D. R., Penny, W. D., Ashburner, J., and Friston, K. J. (2003). Modeling regional and psychophysiologic interactions in fMRI: the importance of hemodynamic deconvolution. *NeuroImage*, 19(1):200–207.

Glanzer, M. and Cunitz, A. R. (1966). Two storage mechanisms in free recall. *Journal of Verbal Learning and Verbal Behavior*, 5:351–360.

Golland, Y., Bentin, S., Gelbard, H., Benjamini, Y., Heller, R., Nir, Y., Hasson, U., and Malach, R. (2007). Extrinsic and intrinsic systems in the posterior cortex of the human brain revealed during natural sensory stimulation. *Cerebral Cortex*, 17(4):766–777.

Gordon, A. M., Rissman, J., Kiani, R., and Wagner, A. D. (2014). Cortical reinstatement mediates the relationship between content-specific encoding activity and subsequent recollection decisions. *Cerebral Cortex (New York, N.Y.: 1991)*, 24(12):3350–3364.

Greicius, M. D., Krasnow, B., Reiss, A. L., and Menon, V. (2003). Functional connectivity in the resting brain: A network analysis of the default mode hypothesis. *Proceedings of the National Academy of Sciences*, 100(1):253–258.

Guerin, S. A., Robbins, C. A., Gilmore, A. W., and Schacter, D. L. (2012). Interactions between visual attention and episodic retrieval: Dissociable contributions of parietal regions during gist-based false recognition. *Neuron*, 75(6):1122–1134.

Handwerker, D. A., Ollinger, J. M., and D'Esposito, M. (2004). Variation of BOLD hemodynamic responses across subjects and brain regions and their effects on statistical analyses. *NeuroImage*, 21(4):1639–1651.

Haskins, A. L., Yonelinas, A. P., Quamme, J. R., and Ranganath, C. (2008). Perirhinal cortex supports encoding and familiarity-based recognition of novel associations. *Neuron*, 59(4):554–560.

Hasselmo, M. and Stern, C. (2006). Mechanisms underlying working memory for novel information. *Trends in cognitive sciences*, 10(11):487–493.

Hasselmo, M. E., Giocomo, L. M., and Zilli, E. A. (2007). Grid cell firing may arise from interference of theta frequency membrane potential oscillations in single neurons. *Hippocampus*, 17(12):1252–1271.

Hasselmo, M. E. and Wyble, B. P. (1997). Free recall and recognition in a network model of the hippocampus: simulating effects of scopolamine on human memory function. *Behavioural Brain Research*, 89(1–2):1–34.

Haxby, J. V., Gobbini, M. I., Furey, M. L., Ishai, A., Schouten, J. L., and Pietrini, P. (2001). Distributed and overlapping representations of faces and objects in ventral temporal cortex. *Science*, 293:2425–2429.

Haxby, J. V., Guntupalli, J. S., Connolly, A. C., Halchenko, Y. O., Conroy, B. R., Gobbini, M. I., Hanke, M., and Ramadge, P. J. (2011). A common, high-dimensional model of the representational space in human ventral temporal cortex. *Neuron*, 72(2):404–416.

Hayama, H. R., Vilberg, K. L., and Rugg, M. D. (2012). Overlap between the neural correlates of cued recall and source memory: Evidence for a generic recollection network? *Journal of Cognitive Neuroscience*, 24(5):1127–1137.

Hayes, S. M., Buchler, N., Stokes, J., Kragel, J., and Cabeza, R. (2011). Neural correlates of confidence during item recognition and source memory retrieval: Evidence for both dual-process and strength memory theories. *Journal of Cognitive Neuroscience*, 23(12):3959–3971.

Hayes, S. M., Nadel, L., and Ryan, L. (2007). The effect of scene context on episodic object recognition: Parahippocampal cortex mediates memory encoding and retrieval success. *Hippocampus*, 17(9):873–889.

Henson, R. (2006). Forward inference using functional neuroimaging: dissociations versus associations. *Trends in Cognitive Sciences*, 10(2):64–69.

Henson, R., Cansino, S., Herron, J., Robb, W., and Rugg, M. (2003). A familiarity signal in human anterior medial temporal cortex? *Hippocampus*, 13(2):301–304.

Howard, M. W., Fotedar, M. S., Datey, A. V., and Hasselmo, M. E. (2005). The temporal context model in spatial navigation and relational learning: Toward a common explanation of medial temporal lobe function across domains. *Psychological Review*, 112(1):75–116.

Howard, M. W. and Kahana, M. J. (2002a). A distributed representation of temporal context. *Journal of Mathematical Psychology*, 46:269–299.

Howard, M. W. and Kahana, M. J. (2002b). When does semantic similarity help episodic retrieval? *Journal of Memory and Language*, 46:85–98.

Howard, M. W., Viskontas, I. V., Shankar, K. H., and Fried, I. (2012). Ensembles of human MTL neurons "jump back in time" in response to a repeated stimulus. *Hippocampus*, 22(9):1833–1847.

Hower, K. H., Wixted, J., Berryhill, M. E., and Olson, I. R. (2014). Impaired perception of mnemonic oldness, but not mnemonic newness, after parietal lobe damage. *Neuropsychologia*, 56:409–417.

Hsieh, L.-T., Gruber, M. J., Jenkins, L. J., and Ranganath, C. (2014). Hippocampal activity patterns carry information about objects in temporal context. *Neuron*, 81(5):1165–1178.

Huang, J., Carr, T. H., and Cao, Y. (2001). Comparing cortical activations for silent and overt speech using event-related fMRI. *Human Brain Mapping*, 15(1):39–53.

Huffman, D. J. and Stark, C. E. (2014). Multivariate pattern analysis of the human medial temporal lobe revealed representationally categorical cortex and representationally agnostic hippocampus. *Hippocampus*.

Hutchinson, J. B., Uncapher, M. R., and Wagner, A. D. (2015). Increased functional connectivity between dorsal posterior parietal and ventral occipitotemporal cortex during uncertain memory decisions. *Neurobiology of Learning and Memory*, 117:71–83.

Hutchinson, J. B., Uncapher, M. R., Weiner, K. S., Bressler, D. W., Silver, M. A., Preston, A. R., and Wagner, A. D. (2012). Functional heterogeneity in posterior parietal cortex across attention and episodic memory retrieval. *Cerebral Cortex*.

Innocenti, I., Cappa, S. F., Feurra, M., Giovannelli, F., Santarnecchi, E., Bianco, G., Cincotta, M., and Rossi, S. (2012). TMS Interference with Primacy and Recency Mechanisms Reveals Bimodal Episodic Encoding in the Human Brain. *Journal of Cognitive Neuroscience*, 25(1):109–116.

Insausti, R., Juottonen, K., Soininen, H., Insausti, A. M., Partanen, K., Vainio, P., Laakso, M. P., and Pitkänen, A. (1998). MR volumetric analysis of the human entorhinal, perirhinal, and temporopolar cortices. *American Journal of Neuroradiology*, 19(4):659–671.

Jenkins, L. J. and Ranganath, C. (2010). Prefrontal and medial temporal lobe activity at encoding predicts temporal context memory. *Journal of Neuroscience*, 30(46):15558–15565.

Jha, A. P., Fabian, S. A., and Aguirre, G. K. (2004). The role of prefrontal cortex in resolving distractor interference. *Cognitive, Affective, & Behavioral Neuroscience*, 4(4):517–527.

Johnson, J. D., McDuff, S. G., Rugg, M. D., and Norman, K. A. (2009). Recollection, familiarity, and cortical reinstatement: A multivoxel pattern analysis. *Neuron*, 63(5):697–708.

Johnson, J. D. and Rugg, M. D. (2007). Recollection and the reinstatement of encoding-related cortical activity. *Cerebral Cortex*, 17:2507–2515.

Kahana, M. J. (1996). Associative retrieval processes in free recall. *Memory & Cognition*, 24:103–109.

Kahana, M. J. (2012). *Foundations of Human Memory*. Oxford University Press, New York, NY, 1st edition.

Kahana, M. J., Howard, M. W., and Polyn, S. M. (2008). Associative retrieval processes in episodic memory. In Roediger, III, H. L., editor, *Cognitive psychology of memory. Vol. 2 of Learning and memory: A comprehensive reference, 4 vols. (J. Byrne, Ed.)*, pages 467–490. Elsevier, Oxford.

Kahn, I., Andrews-Hanna, J. R., Vincent, J. L., Snyder, A. Z., and Buckner, R. L. (2008). Distinct Cortical Anatomy Linked to Subregions of the Medial Temporal Lobe Revealed by Intrinsic Functional Connectivity. *Journal of Neurophysiology*, 100(1):129–139.

Kahn, I., Davachi, L., and Wagner, A. D. (2004). Functional-neuroanatomic correlates of recollection: implications for models of recognition memory. *Journal of Neuroscience*, 24(17):4172–4180.

Khaligh-Razavi, S.-M. and Kriegeskorte, N. (2014). Deep supervised, but not unsupervised, models may explain it cortical representation. *PLOS Computational Biology*, 10(11):e1003915.

Kirwan, C. B. and Stark, C. E. L. (2004). Medial temporal lobe activation during encoding and retrieval of novel facename pairs. *Hippocampus*, 14(7):919–930.

Kondo, H., Saleem, K. S., and Price, J. L. (2005). Differential connections of the perirhinal and parahippocampal cortex with the orbital and medial prefrontal networks in macaque monkeys. *The Journal of Comparative Neurology*, 493(4):479–509.

Kragel, J. E., Morton, N. W., and Polyn, S. M. (2015). Neural Activity in the Medial Temporal Lobe Reveals the Fidelity of Mental Time Travel. *The Journal of Neuroscience*, 35(7):2914–2926.

Kragel, J. E. and Polyn, S. M. (2015). Functional Interactions Between Large-Scale Networks During Memory Search. *Cerebral Cortex*, 25(3):667–679.

Kriegeskorte, N., Mur, M., Ruff, D. A., Kiani, R., Bodurka, J., Esteky, H., Tanaka, K., and Bandettini, P. A. (2008). Matching categorical object representations in inferior temporal cortex of man and monkey. *Neuron*, 60:1126–1141.

Kruschke, J. K. (2010). What to believe: Bayesian methods for data analysis. *Trends in Cognitive Sciences*, 14(7):293–300.

Kuhl, B. A., Bainbridge, W. A., and Chun, M. M. (2012). Neural reactivation reveals mechanisms for updating memory. *The Journal of Neuroscience*, 32(10):3453–3461.

Kuhl, B. A. and Chun, M. M. (2014). Successful remembering elicits event-specific activity patterns in lateral parietal cortex. *The Journal of Neuroscience*, 34(23):8051–8060.

Laming, D. (1999). Testing the idea of distinct storage mechanisms in memory. *International Journal of Psychology*, 34:419–426.

LaRocque, K. F., Smith, M. E., Carr, V. A., Witthoft, N., Grill-Spector, K., and Wagner, A. D. (2013). Global similarity and pattern separation in the human medial temporal lobe predict subsequent memory. *The Journal of Neuroscience*, 33(13):5466–5474.

Law, J. R., Flanery, M. A., Wirth, S., Yanike, M., Smith, A. C., Frank, L. M., Suzuki, W. A., Brown, E. N., and Stark, C. E. L. (2005). Functional magnetic resonance imaging activity during the gradual acquisition and expression of paired-associate memory. *The Journal of Neuroscience*, 25(24):5720–5729.

Lee, S.-H., Kravitz, D. J., and Baker, C. I. (2013). Goal-dependent dissociation of visual and prefrontal cortices during working memory. *Nature Neuroscience*, 16(8):997–999.

Leech, R., Braga, R., and Sharp, D. J. (2012). Echoes of the brain within the posterior cingulate cortex. *The Journal of Neuroscience*, 32(1):215–222.

Lehn, H., Steffenach, H.-A., Strien, N. M. v., Veltman, D. J., Witter, M. P., and Håberg, A. K. (2009). A specific role of the human hippocampus in recall of temporal sequences. *The Journal of Neuroscience*, 29(11):3475–3484.

Levy, W. B. (1996). A sequence predicting CA3 is a flexible associator that learns and uses context to solve hippocampal-like tasks. *Hippocampus*, 6:579–590.

Lewis-Peacock, J. A. and Postle, B. R. (2008). Temporary activation of long-term memory supports working memory. *Journal of Neuroscience*, 28(35):8765–8771.

Li, Y., Adali, T., and Calhoun, V. D. (2007). Estimating the number of independent components for functional magnetic resonance imaging data. *Human Brain Mapping*, 28:1251–1266.

Liang, J. C., Wagner, A. D., and Preston, A. R. (2012). Content representation in the human medial temporal lobe. *Cerebral Cortex*.

Litman, L., Awipi, T., and Davachi, L. (2009). Category-specificity in the human medial temporal lobe cortex. *Hippocampus*, 19(3):308–319.

Lohnas, L. J., Polyn, S. M., and Kahana, M. J. (in press). Expanding the scope of memory search: Modeling intralist and interlist effects in free recall. *Psychological Review*.

Long, N. M., Öztekin, I., and Badre, D. (2010). Separable prefrontal cortex contributions to free recall. *Journal of Neuroscience*, 30(33):10967–10976.

Lückmann, H. C., Jacobs, H. I. L., and Sack, A. T. (2014). The cross-functional role of frontoparietal regions in cognition: internal attention as the overarching mechanism. *Progress in Neurobiology*, 116:66–86.

Mack, M. L., Preston, A. R., and Love, B. C. (2013). Decoding the brain's algorithm for categorization from its neural implementation. *Current Biology*, 23(20):2023–2027.

Mandler, G. (1980). Recognizing: The judgment of previous occurrence. *Psychological Review*, 87:252–271.

Mangels, J. A., Gershberg, F. B., Shimamura, A. P., and Knight, R. T. (1996). Impaired retrieval from remote memory in patients with frontal lobe damage. *Neuropsychology*, 10(1):32–41.

Manning, J. R., Polyn, S. M., Baltuch, G., Litt, B., and Kahana, M. J. (2011). Oscillatory patterns in temporal lobe reveal context reinstatement during memory search. *Proceedings of the National Academy of Sciences of the United States of America*, 108(31):12893–12897.

Manning, J. R., Sperling, M. R., Sharan, A., Rosenberg, E. A., and Kahana, M. J. (2012). Spontaneously reactivated patterns in frontal and temporal lobe predict semantic clustering during memory search. *Journal of Neuroscience*, 32(26):8871–8878.

Manns, J. R., Howard, M. W., and Eichenbaum, H. (2007). Gradual changes in hippocampal activity support remembering the order of events. *Neuron*, 56(3):530–540.

Mather, M., Cacioppo, J. T., and Kanwisher, N. (2013). How fMRI can inform cognitive theories. *Perspectives on Psychological Science*, 8(1):108–113.

Mayes, A., Montaldi, D., and Migo, E. (2007). Associative memory and the medial temporal lobes. *Trends in cognitive sciences*, 11(3):126–135.

Mazaika, P., Hoeft, F., Glover, G. H., and Reiss, A. L. (2009). Methods and software for fmri analysis for clinical subjects. In *Human Brain Mapping*.

McAndrews, M. P. and Milner, B. (1991). The frontal cortex and memory for temporal order. *Neuropsychologia*, 29(9):849–859.

McCabe, D. P., Roediger, H. L., and Karpicke, J. D. (2010). Automatic processing influences free recall: converging evidence from the process dissociation procedure and remember-know judgments. *Memory & Cognition*, 39(3):389–402.

McClelland, J. L., McNaughton, B. L., and O'Reilly, R. C. (1995). Why there are complementary learning systems in the hippocampus and neocortex: Insights from the successes and failures of connectionist models of learning and memory. *Psychological Review*, 102(3):419–57.

Meda, S. A., Stevens, M. C., Folley, B. S., Calhoun, V. D., and Pearlson, G. D. (2009). Evidence for anomalous network connectivity during working memory encoding in schizophrenia: An ICA based analysis. *PLoS ONE*, 4(11):e7911.

Mickes, L., Seale-Carlisle, T. M., and Wixted, J. T. (2013). Rethinking Familiarity: Remember/-Know Judgments in Free Recall. *Journal of memory and language*, 68(4):333–349.

Mickes, L., Wais, P. E., and Wixted, J. T. (2009). Recollection Is a Continuous Process Implications for Dual-Process Theories of Recognition Memory. *Psychological Science*, 20(4):509–515.

Miller, E. K. and Cohen, J. D. (2001). An integrative theory of prefrontal cortex function. *Annual Review of Neuroscience*, 24:167–202.

Miller, E. K., Erickson, C. A., and Desimone, R. (1996). Neural mechanisms of visual working memory in prefrontal cortex of the macaque. *Journal of Neuroscience*, 16:5154.

Miller, J. F., Lazarus, E. M., Polyn, S. M., and Kahana, M. J. (2013a). Spatial clustering during memory search. *Journal of Experimental Psychology: Learning Memory and Cognition*, 39(3):773–781.

Miller, J. F., Neufang, M., Solway, A., Brandt, A., Trippel, M., Mader, I., Hefft, S., Merkow, M., Polyn, S. M., Jacobs, J., Kahana, M. J., and Schulze-Bonhage, A. (2013b). Neural Activity in Human Hippocampal Formation Reveals the Spatial Context of Retrieved Memories. *Science*, 342(6162):1111–1114.

Miller, J. F., Weidemann, C. T., and Kahana, M. J. (2012). Recall termination in free recall. *Memory & Cognition*, 40(4):540–550.

Miller, R. (1991). *Cortico-hippocampal interplay and the representation of contexts in the brain*. Springer-Verlag.

Milner, B., Corsi, P., and Leonard, G. (1991). Frontal-lobe contribution to recency judgements. *Neuropsychologia*, 29(6):601–618.

Milner, B., Squire, L. R., and Kandel, E. R. (1998). Cognitive neuroscience and the study of memory. *Neuron*, 20(3):445–468.

Mitchell, K. J. and Johnson, M. K. (2009). Source monitoring 15 years later: What have we learned from fMRI about the neural mechanisms of source memory? *Psychological Bulletin*, 135(4):638–677.

Mitchell, T. M., Shinkareva, S. V., Carlson, A., Chang, K. M., Malave, V. L., Mason, R. A., and Just, M. A. (2008). Predicting human brain activity associated with the meanings of nouns. *Science*, 320(5880):1191.

Monti, R. P., Hellyer, P., Sharp, D., Leech, R., Anagnostopoulos, C., and Montana, G. (2014). Estimating time-varying brain connectivity networks from functional MRI time series. *NeuroImage*, 103:427–443.

Morton, N. W., Kahana, M. J., Rosenberg, E. A., Baltuch, G. H., Litt, B., Sharan, A. D., Sperling, M. R., and Polyn, S. M. (2013). Category-specific neural oscillations predict recall organization during memory search. *Cerebral Cortex*, 23(10):2407–2422.

Moscovitch, M. (1992). Memory and Working-with-Memory: A Component Process Model Based on Modules and Central Systems. *Journal of Cognitive Neuroscience*, 4(3):257–267.

Moscovitch, M. and Winocur, G. (1992). The neuropsychology of memory and aging. In Craik, F. I. M. and Salthouse, T. A., editors, *Handbook of Aging and Cognition*, pages 315–372. Earlbaum, Hillsdale, NJ.

Moscovitch, M. and Winocur, G. (2002). The frontal cortex and working with memory. In Stuss, D. T. and Knight, R. T., editors, *Principles of frontal lobe function*, pages 188–209. Oxford University Press, New York.

Mumford, J. A., Turner, B. O., Ashby, F. G., and Poldrack, R. A. (2012). Deconvolving bold activation in event-related designs for multivoxel pattern classification analyses. *NeuroImage*, 59(3):2636–2643.

Murray, L. J. and Ranganath, C. (2007). The dorsolateral prefrontal cortex contributes to successful relational memory encoding. *Journal of Neuroscience*, 27(20):5515.

Naya, Y. and Suzuki, W. A. (2011). Integrating what and when across the primate medial temporal lobe. *Science*, 333(6043):773–776.

Nelson, D. L., McEvoy, C. L., and Schreiber, T. A. (2004). The University of South Florida free association, rhyme, and word fragment norms. *Behavior Research Methods, Instruments and Computers*, 36(3):402–407.

Norman, K. A. and O'Reilly, R. C. (2003). Modeling hippocampal and neocortical contributions to recognition memory: A complementary learning systems approach. *Psychological Review*, 110:611–646.

Norman, K. A., Polyn, S. M., Detre, G. J., and Haxby, J. V. (2006). Beyond mind-reading: Multi-voxel pattern analysis of fMRI data. *Trends in Cognitive Sciences*, 10(9):424–430.

Nosofsky, R. M., Little, D. R., and James, T. W. (2012). Activation in the neural network responsible for categorization and recognition reflects parameter changes. *Proceedings of the National Academy of Sciences*, 109(1):333–338.

Okada, K., Vilberg, K. L., and Rugg, M. D. (2012). Comparison of the neural correlates of retrieval success in tests of cued recall and recognition memory. *Human Brain Mapping*, 33(3):523–533.

Öztekin, I., Long, N. M., and Badre, D. (2010). Optimizing design efficiency of free recall events for fMRI. *Journal of Cognitive Neuroscience*, 22(10):2238–2250.

Paller, K. A. and Wagner, A. D. (2002). Observing the transformation of experience into memory. *Trends in Cognitive Sciences*, 6(2):93–102.

Palmeri, T. J. (2014). An exemplar of model-based cognitive neuroscience. *Trends in Cognitive Sciences*, 18(2):67–69.

Peelen, M. V. and Downing, P. E. (2007). Using multi-voxel pattern analysis of fMRI data to interpret overlapping functional activations. *Trends in Cognitive Sciences*, 11(1):4–5.

Pereira, F., Mitchell, T., and Botvinick, M. (2009). Machine learning classifiers and fMRI: A tutorial overview. *NeuroImage*, 45(1):S199–S209.

Polyn, S. M. and Kahana, M. J. (2008). Memory search and the neural representation of context. *Trends in Cognitive Sciences*, 12:24–30.

Polyn, S. M., Kragel, J. E., Morton, N. W., McCluey, J. D., and Cohen, Z. D. (2012). The neural dynamics of task context in free recall. *Neuropsychologia*, 50(4):447–457.

Polyn, S. M., Morton, N. W., and Kahana, M. J. (2008). Bridging cognitive and neural theories of memory search with the context maintenance and retrieval model. University of Pennsylvania, Society for Neuroscience abstracts. Washington, DC.

Polyn, S. M., Natu, V. S., Cohen, J. D., and Norman, K. A. (2005). Category-specific cortical activity precedes retrieval during memory search. *Science*, 310:1963–1966.

Polyn, S. M., Norman, K. A., and Kahana, M. J. (2009a). A context maintenance and retrieval model of organizational processes in free recall. *Psychological Review*, 116(1):129–156.

Polyn, S. M., Norman, K. A., and Kahana, M. J. (2009b). Task context and organization in free recall. *Neuropsychologia*, 47:2158–2163.

Polyn, S. M. and Sederberg, P. B. (2014). Brain rhythms in mental time travel. *NeuroImage*, 85(2):678–684.

Postle, B. R. (2005). Delay-period activity in prefrontal cortex: one function is sensory gating. *Journal of cognitive neuroscience*, 17(11):1679–1690.

Postle, B. R. (2006). Working memory as an emergent property of the mind and brain. *Neuroscience*, 139(1):23–38.

Postman, L. and Phillips, L. W. (1965). Short-term temporal changes in free recall. *Quarterly Journal of Experimental Psychology*, 17:132–138.

Purcell, B. A., Heitz, R. P., Cohen, J. Y., Schall, J. D., Logan, G. D., and Palmeri, T. J. (2010). Neurally constrained modeling of perceptual decision making. *Psychological Review*, 117(4):1113–1143.

Purcell, B. A., Schall, J. D., Logan, G. D., and Palmeri, T. J. (2012). From salience to saccades: Multiple-alternative gated stochastic accumulator model of visual search. *The Journal of Neuroscience*, 32(10):3433–3446.

Qin, P. and Northoff, G. (2011). How is our self related to midline regions and the default-mode network? *NeuroImage*, 57(3):1221–1233.

Quamme, J. R. (2004). Recall and recognition in mild hypoxia: Using covariance structural modeling to test competing theories of explicit memory. *Neuropsychologia*, 42(5):672.

Raaijmakers, J. G. W. and Shiffrin, R. M. (1980). SAM: A theory of probabilistic search of associative memory. In Bower, G. H., editor, *The psychology of learning and motivation: Advances in research and theory*, volume 14, pages 207–262. Academic Press, New York.

Raaijmakers, J. G. W. and Shiffrin, R. M. (1981). Search of associative memory. *Psychological Review*, 88:93–134.

Raichle, M. E., MacLeod, A. M., Snyder, A. Z., Powers, W. J., Gusnard, D. A., and Shulman, G. L. (2001). A default mode of brain function. *Proceedings of the National Academy of Sciences*, 98(2):676–682.

Ranganath, C. (2010). A unified framework for the functional organization of the medial temporal lobes and the phenomenology of episodic memory. *Hippocampus*, 20(11):1263–1290.

Ranganath, C., Cohen, M. X., Dam, C., and D'Esposito, M. (2004). Inferior temporal, prefrontal, and hippocampal contributions to visual working memory maintenance and associative memory retrieval. *Journal of Neuroscience*, 24(16):3917–3925.

Ranganath, C. and Ritchey, M. (2012). Two cortical systems for memory-guided behaviour. *Nature Reviews Neuroscience*, 13(10):713–726.

Riggall, A. C. and Postle, B. R. (2012). The relationship between working memory storage and elevated activity as measured with functional magnetic resonance imaging. *The Journal of Neuroscience*, 32(38):12990–12998.

Rissman, J., Greely, H. T., and Wagner, A. D. (2010). Detecting individual memories through the neural decoding of memory states and past experience. *Proceedings of the National Academy of Sciences*, 107(21):9849 –9854.

Ritchey, M., Wing, E. A., LaBar, K. S., and Cabeza, R. (2013). Neural similarity between encoding and retrieval is related to memory via hippocampal interactions. *Cerebral Cortex*, 23(12):2818–2828.

Rosenberg-Lee, M., Lovett, M. C., and Anderson, J. R. (2009). Neural correlates of arithmetic calculation strategies. *Cognitive, Affective, & Behavioral Neuroscience*, 9(3):270–285.

Rugg, M. D. (2004). Retrieval Processing in Human Memory: Electrophysiological and fMRI Evidence. In *The Cognitive Neurosciences*, pages 727–737. MIT Press, Cambridge, MA, US.

Sadeh, T., Moran, R., and Goshen-Gottstein, Y. (2014). When items 'pop into mind': variability in temporal-context reinstatement in free-recall. *Psychonomic Bulletin & Review*, pages 1–12.

Sahakyan, L. and Kelley, C. M. (2002). A contextual change account of the directed forgetting effect. *Journal of Experimental Psychology Learning, Memory, and Cognition*, 28(6):1064–1072.

Sakai, K., Rowe, J. B., and Passingham, R. E. (2002). Active maintenance in prefrontal area 46 creates distractor-resistant memory. *Nature Neuroscience*, 5(5):479–484.

Schacter, D. L., Addis, D. R., and Buckner, R. L. (2007). Remembering the past to imagine the future: the prospective brain. *Nature Reviews Neuroscience*, 8(9):657–661.

Schoffelen, J.-M., Oostenveld, R., and Fries, P. (2005). Neuronal coherence as a mechanism of effective corticospinal interaction. *Science*, 308:111–113.

Schon, K., Hasselmo, M. E., Lopresti, M. I., Tricarico, M. D., and Stern, C. E. (2004). Persistence of parahippocampal representation in the absence of stimulus input enhances long-term coding: a functional magnetic resonance imaging study of subsequent memory after a delayed match-to-sample task. *Journal of Neuroscience*, 24:11088–11097.

Schwartz, G., Howard, M. W., Jing, B., and Kahana, M. J. (2005). Shadows of the past: Temporal retrieval effects in recognition memory. *Psychological Science*, 16:898–904.

Scoville, W. B. and Milner, B. (1957). Loss of recent memory after bilateral hippocampal lesions. *Journal of Neurology, Neurosurgery, and Psychiatry*, 20:11–21.

Sederberg, P. B., Howard, M. W., and Kahana, M. J. (2008). A context-based theory of recency and contiguity in free recall. *Psychological Review*, 115(4):893–912.

Seeley, W. W., Menon, V., Schatzberg, A. F., Keller, J., Glover, G. H., Kenna, H., Reiss, A. L., and Greicius, M. D. (2007). Dissociable intrinsic connectivity networks for salience processing and executive control. *The Journal of Neuroscience*, 27(9):2349–2356.

Sestieri, C., Corbetta, M., Romani, G. L., and Shulman, G. L. (2011). Episodic memory retrieval, parietal cortex, and the default mode network: functional and topographic analyses. *The Journal of Neuroscience*, 31(12):4407–4420.

Sestieri, C., Corbetta, M., Spadone, S., Romani, G. L., and Shulman, G. L. (2014a). Domain-general signals in the cingulo-opercular network for visuospatial attention and episodic memory. *Journal of Cognitive Neuroscience*, 26(3):551–568.

Sestieri, C., Tosoni, A., Mignogna, V., McAvoy, M. P., Shulman, G. L., Corbetta, M., and Romani, G. L. (2014b). Memory accumulation mechanisms in human cortex are independent of motor intentions. *The Journal of Neuroscience*, 34(20):6993–7006.

Shannon, B. J. and Buckner, R. L. (2004). Functional-anatomic correlates of memory retrieval that suggest nontraditional processing roles for multiple distinct regions within posterior parietal cortex. *The Journal of Neuroscience*, 24(45):10084–10092.

Shapira-Lichter, I., Oren, N., Jacob, Y., Gruberger, M., and Hendler, T. (2013). Portraying the unique contribution of the default mode network to internally driven mnemonic processes. *Proceedings of the National Academy of Sciences*.

Shapira-Lichter, I., Vakil, E., Glikmann-Johnston, Y., Siman-Tov, T., Caspi, D., Paran, D., and Hendler, T. (2012). Inside out: A neuro-behavioral signature of free recall dynamics. *Neuropsychologia*, 50(9):2245–2256.

Shimamura, A. P., Janowsky, J. S., and Squire, L. R. (1990). Memory for the temporal order of events in patients with frontal lobe lesions and amnesic patients. *Neuropsychologia*, 28(8):803–813.

Shimamura, A. P., Jurica, P. J., Mangels, J. A., Gershberg, F. B., and Knight, R. T. (1995). Susceptibility to memory interference effects following frontal lobe damage: Findings from tests of paired-associate learning. *Journal of Cognitive Neuroscience*, 7(2):144–152.

Shirer, W. R., Ryali, S., Rykhlevskaia, E., Menon, V., and Greicius, M. D. (2012). Decoding subject-driven cognitive states with whole-brain connectivity patterns. *Cerebral Cortex*, 22(1):158–165.

Shulman, G. L., Fiez, J. A., Corbetta, M., Buckner, R. L., Miezin, F. M., Raichle, M. E., and Petersen, S. E. (1997). Common Blood Flow Changes across Visual Tasks: II. Decreases in Cerebral Cortex. *Journal of Cognitive Neuroscience*, 9(5):648–663.

Simons, J. S., Henson, R. N. A., Gilbert, S. J., and Fletcher, P. C. (2007). Separable forms of reality monitoring supported by anterior prefrontal cortex. *Journal of Cognitive Neuroscience*, 20(3):447–457.

Simons, J. S. and Spiers, H. J. (2003). Prefrontal and medial temporal lobe interactions in long-term memory. *Nature Reviews Neuroscience*, 4(8):637–648.

Skinner, E. I. and Fernandes, M. A. (2007). Neural correlates of recollection and familiarity: A review of neuroimaging and patient data. *Neuropsychologia*, 45(10):2163–2179.

Smith, S. M., Fox, P. T., Miller, K. L., Glahn, D. C., Fox, P. M., Mackay, C. E., Filippini, N., Watkins, K. E., Toro, R., Laird, A. R., and Beckmann, C. F. (2009). Correspondence of the brain's functional architecture during activation and rest. *Proceedings of the National Academy of Science USA*, 106(31):13040–13045.

Sneve, M. H., Grydeland, H., Nyberg, L., Bowles, B., Amlien, I. K., Langnes, E., Walhovd, K. B., and Fjell, A. M. (2015). Mechanisms Underlying Encoding of Short-Lived Versus Durable Episodic Memories. *The Journal of Neuroscience*, 35(13):5202–5212.

Sneve, M. H., Magnussen, S., Alnæs, D., Endestad, T., and D'Esposito, M. (2013). Top–Down Modulation from Inferior Frontal Junction to FEFs and Intraparietal Sulcus during Short-term Memory for Visual Features. *Journal of Cognitive Neuroscience*, 25(11):1944–1956.

Socher, R., Gershman, S. J., Perotte, A. J., Sederberg, P. B., Blei, D. M., and Norman, K. A. (2009). A bayesian analysis of dynamics in free recall. In Bengio, Y., Schuurmans, D., Lafferty, J., Williams, C. K. I., and Culotta, A., editors, *Advances in Neural Information Processing Systems*. MIT Press.

Solway, A., Geller, A. S., Sederberg, P. B., and Kahana, M. J. (2010). Pyparse: A semiautomated system for scoring spoken recall data. *Behavior Research Methods*, 42(1):141–147.

Spaniol, J., Davidson, P. S., Kim, A. S., Han, H., Moscovitch, M., and Grady, C. L. (2009). Event-related fMRI studies of episodic encoding and retrieval: Meta-analyses using activation likelihood estimation. *Neuropsychologia*, 47(8–9):1765–1779.

Spreng, R. N., DuPre, E., Selarka, D., Garcia, J., Gojkovic, S., Mildner, J., Luh, W.-M., and Turner, G. R. (2014). Goal-congruent default network activity facilitates cognitive control. *The Journal of Neuroscience*, 34(42):14108–14114.

Spreng, R. N. and Grady, C. L. (2009). Patterns of Brain Activity Supporting Autobiographical Memory, Prospection, and Theory of Mind, and Their Relationship to the Default Mode Network. *Journal of Cognitive Neuroscience*, 22(6):1112–1123.

Spreng, R. N., Stevens, W. D., Chamberlain, J. P., Gilmore, A. W., and Schacter, D. L. (2010). Default network activity, coupled with the frontoparietal control network, supports goal-directed cognition. *NeuroImage*, 53(1):303–317.

Sridharan, D., Levitin, D. J., and Menon, V. (2008). A critical role for the right fronto-insular cortex in switching between central-executive and default-mode networks. *Proceedings of the National Academy of Sciences*, 105(34):12569 –12574.

St. Jacques, P. L., Kragel, P. A., and Rubin, D. C. (2011). Dynamic neural networks supporting memory retrieval. *NeuroImage*, 57(2):608–616.

Staresina, B. P., Cooper, E., and Henson, R. N. (2013). Reversible information flow across the medial temporal lobe: The hippocampus links cortical modules during memory retrieval. *The Journal of Neuroscience*, 33(35):14184–14192.

Staresina, B. P. and Davachi, L. (2006). Differential encoding mechanisms for subsequent associative recognition and free recall. *Journal of Neuroscience*, 26(36):9162.

Staresina, B. P. and Davachi, L. (2010). Object unitization and associative memory formation are supported by distinct brain regions. *The Journal of Neuroscience*, 30(29):9890–9897.

Staresina, B. P., Duncan, K. D., and Davachi, L. (2011). Perirhinal and parahippocampal cortices differentially contribute to later recollection of object- and scene-related event details. *The Journal of Neuroscience*, 31(24):8739–8747.

Staresina, B. P., Fell, J., Do Lam, A. T. A., Axmacher, N., and Henson, R. N. (2012a). Memory signals are temporally dissociated in and across human hippocampus and perirhinal cortex. *Nature Neuroscience*, 15(8):1167–1173.

Staresina, B. P., Henson, R. N. A., Kriegeskorte, N., and Alink, A. (2012b). Episodic reinstatement in the medial temporal lobe. *Journal of Neuroscience*, 32(50):18150–18156.

Stelzer, J., Chen, Y., and Turner, R. (2013). Statistical inference and multiple testing correction in classification-based multi-voxel pattern analysis (MVPA): Random permutations and cluster size control. *NeuroImage*, 65:69–82.

Stern, C. E., Sherman, S. J., Kirchhoff, B. A., and Hasselmo, M. E. (2001). Medial temporal lobe and prefrontal contributions to working memory tasks with novel and familiar stimuli. *Hippocampus*, 11(4):337–346.

Steyvers, M., Shiffrin, R. M., and Nelson, D. L. (2004). Word association spaces for predicting semantic similarity effects in episodic memory. In Healy, A. F., editor, *Cognitive Psychology and its Applications: Festschrift in Honor of Lyle Bourne, Walter Kintsch, and Thomas Landauer.*, pages 237–249. American Psychological Association, Washington, DC.

Stuss, D. T., Alexander, M. P., Palumbo, C. L., Buckle, L., Sayer, L., and Pogue, J. (1994). Organizational Strategies of Patients With Unilateral or Bilateral Frontal Lobe Injury in Word List Learning Tasks. *Neuropsychology*, 8:355–355.

Sui, J., Adali, T., Pearlson, G. D., and Calhoun, V. D. (2009). An ICA-based method for the identification of optimal FMRI features and components using combined group-discriminative techniques. *NeuroImage*, 46(1):73–86.

Suzuki, W. A. (1996). The anatomy, physiology and functions of the perirhinal cortex. *Current Opinion in Neurobiology*, 6(2):179–186.

Svoboda, E., McKinnon, M. C., and Levine, B. (2006). The functional neuroanatomy of autobiographical memory: A meta-analysis. *Neuropsychologia*, 44(12):2189–2208.

Tan, L. and Ward, G. (2000). A recency-based account of the primacy effect in free recall. *Journal of Experimental Psychology Learning, Memory, and Cognition*, 26:1589–1626.

Tendolkar, I., Arnold, J., Petersson, K. M., Weis, S., Brockhaus-Dumke, A., Eijndhoven, P. v., Buitelaar, J., and Fernández, G. (2008). Contributions of the medial temporal lobe to declarative memory retrieval: Manipulating the amount of contextual retrieval. *Learning & Memory*, 15(9):611–617.

Tubridy, S. and Davachi, L. (2011). Medial temporal lobe contributions to episodic sequence encoding. *Cerebral Cortex*, 21(2):272–280.

Tulving, E. (1983). *Elements of Episodic Memory*. Oxford, New York.

Tulving, E. (1993). What is episodic memory? *Current Directions in Psychological Science*, 2(3):67–70.

Tulving, E. (2005). Episodic Memory and Autonoesis: Uniquely Human? In *The missing link in cognition: Origins of self-reflective consciousness*, pages 3–56. Oxford University Press, New York, NY, US.

Tulving, E. (2008). On the law of primacy. In Gluck, M. A., Anderson, J. R., and Kosslyn, S. M., editors, *Memory and Mind: A Festschrift for Gordon H. Bower*, chapter 3, pages 31–48. Taylor & Francis, New York, NY.

Turk-Browne, N. B., Simon, M. G., and Sederberg, P. B. (2012). Scene representations in parahippocampal cortex depend on temporal context. *The Journal of Neuroscience*, 32(21):7202–7207.

Turner, B. M., Forstmann, B. U., Wagenmakers, E.-J., Brown, S. D., Sederberg, P. B., and Steyvers, M. (2013a). A Bayesian framework for simultaneously modeling neural and behavioral data. *NeuroImage*, 72:193–206.

Turner, B. M., Sederberg, P. B., Brown, S. D., and Steyvers, M. (2013b). A Method for Efficiently Sampling From Distributions With Correlated Dimensions. *Psychological methods*, 18(3):368–384.

Turner, B. M., van Maanen, L., and Forstmann, B. U. (in press). Informing cognitive abstractions through neuroimaging: The neural drift diffusion model. *Psychological Review*.

Tzourio-Mazoyer, N., Landeau, B., Papathanassiou, D., Crivello, F., Etard, O., Delcroix, N., Mazoyer, B., and Joliot, M. (2002). Automated anatomical labeling of activations in SPM using a macroscopic anatomical parcellation of the MNI MRI Single-Subject brain. *NeuroImage*, 15(1):273–289.

Usher, M. and McClelland, J. L. (2001). The time course of perceptual choice: The leaky, competing accumulator model. *Psychological Review*, 108(3):550–592.

van de Ven, V., Esposito, F., and Christoffels, I. K. (2009). Neural network of speech monitoring overlaps with overt speech production and comprehension networks: A sequential spatial and temporal ICA study. *NeuroImage*, 47(4):1982–1991.

Van Essen, D. C. (2002). Windows on the brain: the emerging role of atlases and databases in neuroscience. *Current Opinion in Neurobiology*, 12(5):574–579.

Van Essen, D. C., Drury, H. A., Dickson, J., Harwell, J., Hanlon, D., and Anderson, C. H. (2001). An integrated software suite for surface-based analyses of cerebral cortex. *Journal of the American Medical Informatics Association*, 8(5):443 –459.

Vilberg, K. L. and Rugg, M. D. (2008). Memory retrieval and the parietal cortex: a review of evidence from a dual-process perspective. *Neuropsychologia*, 46(7):1787–1799.

Vilberg, K. L. and Rugg, M. D. (2012). The neural correlates of recollection: Transient versus sustained fMRI effects. *The Journal of Neuroscience*, 32(45):15679–15687.

Vincent, J. L., Kahn, I., Snyder, A. Z., Raichle, M. E., and Buckner, R. L. (2008). Evidence for a frontoparietal control system revealed by intrinsic functional connectivity. *Journal of Neurophysiology*, 100(6):3328–3342.

Vincent, J. L., Snyder, A. Z., Fox, M. D., Shannon, B. J., Andrews, J. R., Raichle, M. E., and Buckner, R. L. (2006). Coherent spontaneous activity identifies a hippocampal-parietal memory network. *Journal of Neurophysiology*, 96:3517–3531.

Wagenmakers, E.-J. and Farrell, S. (2004). AIC model selection using akaike weights. *Psychonomic Bulletin & Review*, 11(1):192–196.

Wagenmakers, E.-J., Lodewyckx, T., Kuriyal, H., and Grasman, R. (2010). Bayesian hypothesis testing for psychologists: A tutorial on the Savage–Dickey method. *Cognitive Psychology*, 60(3):158–189.

Wager, T. D., Spicer, J., Insler, R., and Smith, E. E. (2013). The neural bases of distracter-resistant working memory. *Cognitive, Affective, & Behavioral Neuroscience*, 14(1):90–105.

Wagner, A., Shannon, B., Kahn, I., and Buckner, R. (2005). Parietal lobe contributions to episodic memory retrieval. *Trends in Cognitive Science*, 9(9):445–453.

Wagner, A. D., Par-Blagoev, E. J., Clark, J., and Poldrack, R. A. (2001). Recovering meaning: left prefrontal cortex guides controlled semantic retrieval. *Neuron*, 31(2):329–338.

Wagner, A. D., Schacter, D. L., Rotte, M., Koutstaal, W., Maril, A., Dale, A. M., Rosen, B. R., and Buckner, R. L. (1998). Building memories: remembering and forgetting of verbal experiences as predicted by brain activity. *Science*, 281:1188–1191.

Wallenstein, G. V., Eichenbaum, H., and Hasselmo, M. (1998). The hippocampus as an associator of discontiguous events. *Trends in Neurosciences*, 21(8):317–323.

Wang, J. X., Rogers, L. M., Gross, E. Z., Ryals, A. J., Dokucu, M. E., Brandstatt, K. L., Hermiller, M. S., and Voss, J. L. (2014). Targeted enhancement of cortical-hippocampal brain networks and associative memory. *Science*, 345(6200):1054–1057.

Waskom, M. L., Kumaran, D., Gordon, A. M., Rissman, J., and Wagner, A. D. (2014). Frontoparietal representations of task context support the flexible control of goal-directed cognition. *The Journal of Neuroscience*, 34(32):10743–10755.

Wetzels, R., Grasman, R. P. P. P., and Wagenmakers, E.-J. (2010). An encompassing prior generalization of the Savage–Dickey density ratio. *Computational Statistics & Data Analysis*, 54(9):2094–2102.

Wheeler, M. E. and Buckner, R. L. (2004). Functional-anatomic correlates of remembering and knowing. *NeuroImage*, 21(4):1337–1349.

Wheeler, M. E., Petersen, S. E., and Buckner, R. L. (2000). Memory's echo: Vivid remembering reactivates sensory-specific cortex. *Proceedings of the National Academy of Sciences of the United States of America*, 97:11125–11129.

Wilks, S. S. (1938). The large-sample distribution of the likelihood ratio for testing composite hypotheses. *The Annals of Mathematical Statistics*, 9(1):60–62.

Wixted, J. T. and Squire, L. R. (2010). The role of the human hippocampus in familiarity-based and recollection-based recognition memory. *Behavioural Brain Research*, 215(2):197–208.

Wixted, J. T. and Squire, L. R. (2011). The medial temporal lobe and the attributes of memory. *Trends in Cognitive Sciences*, 15(5):210–217.

Yeo, B. T. T., Krienen, F. M., Sepulcre, J., Sabuncu, M. R., Lashkari, D., Hollinshead, M., Roffman, J. L., Smoller, J. W., Zöllei, L., Polimeni, J. R., Fischl, B., Liu, H., and Buckner, R. L. (2011). The organization of the human cerebral cortex estimated by intrinsic functional connectivity. *Journal of Neurophysiology*, 106(3):1125–1165.

Yonelinas, A. P. (2002). The nature of recollection and familiarity: A review of 30 years of research. *Journal of Memory and Language*, 46:441–517.

Yonelinas, A. P., Aly, M., Wang, W.-C., and Koen, J. D. (2010). Recollection and familiarity: Examining controversial assumptions and new directions. *Hippocampus*, 20(11):1178–1194.

Yonelinas, A. P., Otten, L. J., Shaw, K. N., and Rugg, M. D. (2005). Separating the brain regions involved in recollection and familiarity in recognition memory. *Journal of Neuroscience*, 25(11):3002–3008.

Yu, Q., Erhardt, E. B., Sui, J., Du, Y., He, H., Hjelm, D., Cetin, M. S., Rachakonda, S., Miller, R. L., Pearlson, G., and Calhoun, V. D. (2015). Assessing dynamic brain graphs of time-varying connectivity in fMRI data: Application to healthy controls and patients with schizophrenia. *NeuroImage*, 107:345–355.

Zalesky, A., Fornito, A., Cocchi, L., Gollo, L. L., and Breakspear, M. (2014). Time-resolved resting-state brain networks. *Proceedings of the National Academy of Sciences*, 111(28):10341–10346.

Zanto, T. P., Clapp, W. C., Rubens, M. T., Karlsson, J., and Gazzaley, A. (in press). Expectations of Task Demands Dissociate Working Memory and Long-Term Memory Systems. *Cerebral Cortex*.